

# Improvement of the spatial and spectral coherence in high power diode lasers

**Vijayakumar, Deepak**

*Publication date:*
2011

*Document Version*
Publisher's PDF, also known as Version of record

# Improvement of the spatial and spectral coherence in high power diode lasers

Deepak Vijayakumar

Doctoral Thesis
DTU- Fotonik
Department of Photonics Engineering
Technical University of Denmark
December 2010

Doctoral Thesis
Department of Photonics engineering
Technical University of Denmark
4000 Roskilde
Denmark

To my beloved family…

About light, I’m in the dark.

-- Benjamin Franklin

About light, I’m not in the dark.

-- Deepak Vijayakumar

# RESUMÉ

Ph.d. afhandlingen omhandler udvikling af en lang række optiske feedbackteknikker for højeffekt diodelasere som giver forbedring af de rumlige og spektrale kohærensegenskaber. Der er i projektet udviklet nye diodelasersystemer som kan benyttes til industrielle anvendelser inden for materialebearbejdning. En af teknikkerne er baseret på spektral strålekombination (eng: spectral beam combining) og den er i ph.d. projektet benyttet til at forbedre strålekvaliteten af en 980 nm taperet diodelaser samt til at kombinere to taperede diodelasere til én laserstråle med høj rumlig kohærens.

En anden interessant teknik off-axis spectral beam combining er i projektet benyttet til at forbedre strålekvaliteten af en 980 nm diodelaserbar til et niveau som er bedre end kvaliteten af den enkelte emitter i laserbaren. Rekordhøje niveauer af effekttætheden for laserbaren er opnået med dette system. Lasersystemet er i ph.d. projektet med stor succes blevet brugt til at skære i forskellige typer af polymermaterialer.

Kohærent strålekombination for en 980 nm gain guided tapered laserbar er i projektet benyttet ved hjælp af passiv faselåsning baseret på den såkaldte Talbot effekt.

En Talbot kavitet er blevet realiseret med et Bragg gitter til at opnå kohærent laservirkning i et kompakt lasersystem.

Endvidere er et 980 nm lasersystem med smal spektral linjebredde udviklet i projektet. Systemet er baseret på en diodelaserbar i en Littman-Metcalf ekstern kavitet med Bragg gitter. Den spektrale kohærens af diodelaserbaren er forbedret betydeligt i forhold til det oprindelige lasersystem.

# CONTENTS

# CHAPTER 1

# INTRODUCTION

Diode lasers with continuous wave (cw) output power in excess of 0.5 W are termed as high power diode lasers. High power diode laser sources are being considered as an alternative for conventional solid state and gas laser systems in several applications. Their main advantages being highly energy efficient, compact in size, low cost, the possibilities for mass production, high durability and reliability. Power conversion efficiencies up to 85% at low temperatures and 76% at 10°C have been demonstrated with these devices [1] [2]. When the typical power conversion efficiencies of other conventional laser systems are around 10-15% for CO2 lasers, 1-5% for arc lamp pumped Nd:YAG lasers, 1-35% for diode pumped solid state lasers and 1-2% for excimer lasers. Higher conversion efficiencies leads to lower cooling requirements and hence the reduction in the size of the laser unit. High power outputs could also be yielded by designing array or bar geometries. A single diode laser bar emitting 1 kW of optical output power has been demonstrated recently [3]. Moreover, output powers of several kilo watts have been demonstrated by using diode laser stacks [4]. These devices are commercially available today [5]. State of the art diode lasers shows a high life time of several thousand hours with reliable power output characteristics [6] [7] [8]. But when it comes to the applications, many other factors such as the beam quality, spatial and spectral brightness etc. is also considered to be very important. Applications such as solid state laser pumping and fibre laser pumping requires high power, high brightness sources while industrial material processing applications such as graphics marking, cutting, welding etc requires high power outputs with good to moderately good beam qualities depending on the precision requirements [9]. On the other hand, certain applications such as nonlinear frequency conversion, spin exchange optical pumping of noble gases etc requires a high spectral brightness which could not be provided using a regular high power diode laser which emits with a broad spectral line width [10]. Here, nonlinear frequency conversion requires both high spectral and spatial brightness.

High power diode laser sources are also preferred over other high power sources for certain types of material processing [11] due to some other reasons such as they provides a more uniform heating zone due to beam integration, have better beam absorption for metallic materials due to the shorter operation wavelengths, the ability to produce better quality results which are consistent and repeatable compared to Nd:YAG lasers. They are also quite low on maintenance costs. The compactness of the system also makes them portable and facilitate their application in situations like the laser processing of large parts such as building structures where the 'work pieces' cannot be brought to the laser workstation.

Despite the advances made in material science and diode production technologies, several factors related to the performance of the diode lasers still require improvements. Even though reliable diode laser bars with high output power levels are commercially available today, due to the inherent nature of their geometry, they produce a transverse multimode emission which is low in terms of beam quality which makes them unsuitable for many applications. Another major limitation of a free running high power diode laser is the inherent lack of wavelength selectivity in the laser cavity. This results in a broad emission spectrum with a line width of a few nanometres. The wavelength spectra of a diode laser emission can also change with the increase in the injection current and temperature. For AlGaAs lasers, the wavelength typically changes 0.025 nm/mA and up to 0.4 nm/°C.

Numerous external cavity setups have been demonstrated by various research groups in order to solve these issues related to lateral and longitudinal multi mode emission in diode lasers. The main scope of this thesis is in describing certain interesting techniques which could improve the performance of high power diode laser sources and helps tailoring their emissions to meet the requirements of their applications. Broad area diode laser bars, tapered diode laser bars and tapered diode single emitters have been employed in various external cavity configurations such as spectral beam combining, off-axis spectral beam combining, Talbot cavity, Littman Metcalf cavity, volume Bragg grating (VBG) cavity etc. The near infrared wavelengths of interest in the context of this thesis are 980 nm and 1060 nm which are interesting in material processing applications.

An interesting external cavity technique called spectral beam combining was investigated in detail using both gain guided tapered diode laser bar and DBR-tapered diode single emitters. The former external cavity setup was realized based on a reflective plane ruled diffraction grating whereas the latter was based on a volume Bragg grating. Considerable improvement in the slow axis beam quality parameter has been obtained. The 980 nm tapered diode laser bar yielded 9 W of output power with a slow axis $M^2$ value of 5.3. In the other setup, two 1060 nm tapered diode emitters were combined to get 16 W of output power with a slow axis $M^2$ value of 3.3. This is the first time spectral beam combining has been applied to gain guided tapered diode laser bar and DBR-tapered diode single emitters. Another external cavity technique called off-axis spectral beam combining was applied on a 980 nm broad area diode laser bar which improved the slow axis beam quality to a level considerably better than the single emitter beam quality on the laser bar. In the external cavity, the laser bar emitted 9 W of output power with a slow axis $M^2$ value of 6.4. This experiment also resulted in the state of the art spatial brightness of 79 MW/cm$^2$-str, which is the highest ever to be obtained from a broad area diode laser system. Coherent combining of the gain guided tapered diode laser bar was also investigated. The 980 nm tapered diode laser bar was passively phased locked in a Talbot cavity which produced 2.45 W of coherent output power at 15 A of operating current. Efforts for the spectral narrowing of the gain guided tapered diode laser bar was also made using a Littman Metcalf cavity and a volume Bragg grating cavity. 8 W of narrow line width emission with a line width of 40 pm has been obtained from the Littman Metcalf cavity while 5 W of emission with a line width of 0.2 nm has been obtained from the VBG cavity. To my best knowledge, this is the first time ever spectral beam combining, passive phase locking in a Talbot cavity and spectral narrowing has been successfully performed on gain guided tapered diode laser bars. This gives these results its own significance.

**Thesis structure**

This thesis contains seven chapters starting with a brief introduction about the scope of the works described in this thesis. Chapter 2 goes into the basic semiconductor physics behind the operation of diode lasers and differentiates various types of diode laser geometries, materials of interest and their emission

properties. The experimental methods investigated in order to improve the spatial and temporal coherence of diode laser sources is explained next in the chapters 3-5. Chapter 3 gives an insight to a popular beam combining technique termed as spectral beam combining. It describes the experimental setups that have been realized for the improvement of the lateral mode behaviour of diode laser bars and single emitters. Experimental results are also explained in detail. Chapter 4 deals with a relatively new concept of off-axis spectral beam combining which results in a further improvement over the limitations of the conventional spectral beam combining technique. Chapter 5 describes a coherent phase locking technique based on a diffractive phenomenon termed as 'Talbot effect'. This technique has been employed for the improvement of the beam quality of a tapered diode laser bar. Chapter 6 deals with the improvement of the temporal coherence in a laser bar. It explains a couple of techniques for the wavelength stabilization and line width reduction of the output from a gain guided tapered diode laser bar. Chapter 7 discuss the possible applications of the above described diode laser systems and gives a detailed overview of the involvement of diode lasers in certain material processing applications. Chapter 8 concludes this thesis by highlighting the major achievements made during this study with a summary of the experimental results of all the works that has been described and stating the anticipated improvements for the future.

# CHAPTER 2

# HIGH POWER DIODE LASERS

The first successful operation of a laser was performed in May 1960. It was a solid state ruby laser [12]. In the mean time, people were also interested in the concept stimulated emission applied in semiconductors. By 1962, several groups reported on the lasing action in semiconductors [13] [14] [15]. Since its invention in 1962, its performance in terms of output power, spectral qualities, life time etc. has steadily progressed and it has proved worthy enough to be a replacement for many solid state, chemical and gas laser systems. Today, semiconductor lasers also known as diode lasers find its applications in various medical and industrial fields. This chapter of the thesis provides an insight into the basic physics of semiconductors and the principles behind the working of diode lasers.

## 2.1 Absorption and emission in semiconductors

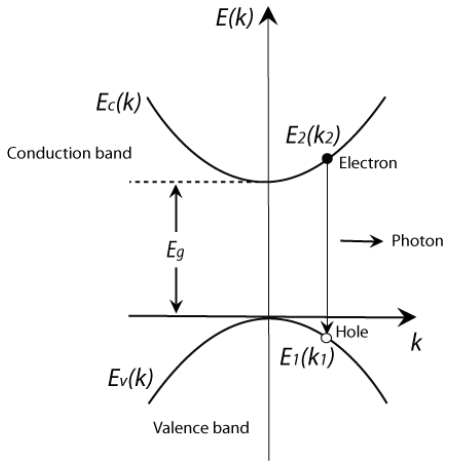


*Fig 2.1. The conduction band and the valance band. Recombination of an electron at E2(k2) and a hole at E1(k1) occurs at k1=k2 and produces a photon of energy $\hbar\omega$.*

The atoms or molecules in a material can absorb energy from external sources and get excited to higher energy states. But the excited state being highly

unstable, the molecules tend to emit the excess energy they possess in the form of light or heat and return to the stable ground states. Energy is both absorbed and emitted in this process. In lasers, such an energy transfer leads to the emission of light.

In solid state and gas lasers, the active medium has sharp energy levels whereas in the semiconductor lasers, the energy levels are broadened into energy bands see Fig. 2.1. A valence band is the highest level of electron energies where the electrons are present at an absolute zero temperature. A conduction band is the range of electron energy which is high enough to free an electron from an atom and to allow it to move freely in the atomic lattice. $E_c(k)$ and $E_v(k)$ represents the electron energies in the conduction band and the valance band respectively. The electron energies of these band structures could be summarized as [16],

$$E_v(k) = -\frac{\hbar^2 k^2}{2m_h} \; and \; E_c(k) = E_g + \frac{\hbar^2 k^2}{2m_e}, \tag{2.1}$$

where $k=2\pi/\lambda$ is the wave number, $\hbar$ is the reduced Planck's constant, $m_e$ and $m_h$ are the effective mass of electrons and holes respectively and $E_g$ is the energy gap between the conduction and the valence band. In the materials used for high power diode lasers, the band gap energy is typically of the order of 0.5-2.5 eV [16].

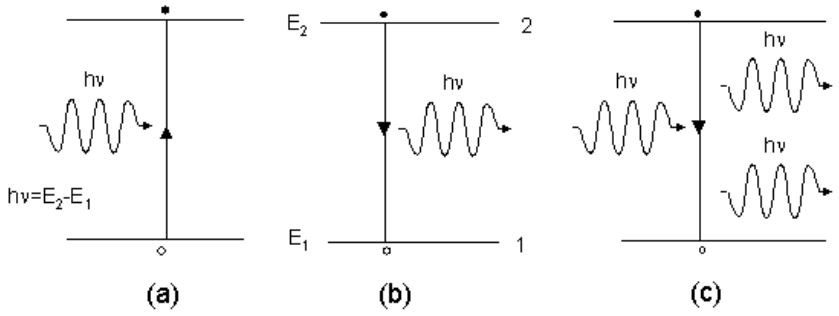


Fig 2.2. *Radiative transitions in semiconductors: (a) Absorption, (b) Spontaneous emission, and (c) Stimulated emission.*

In the absence of an external pump source, in an undoped semiconductor, the concentration of electrons in the valance band is very high and the conduction band is high in the number of holes or absence of electrons. This could be reversed when the material is excited with an external energy source termed as a pump source and it can lead to three different types of radiative transitions in a semiconductor. These are stimulated absorption, spontaneous emission and stimulated emission, see Fig. 2.2. Here, $E_1$ and $E_2$ are the electron energies in the valance band and the conduction band respectively. In Fig. 2.2, the transitions are represented as vertical arrows with the electron energy $\hbar\omega$ pointing upwards for the generation and downwards for the recombination of an electron hole pair. As the momentum of a photon is negligible, a radiative transition between an electron in the conduction band with energy $E_2(k_2)$ and a hole in the valance band with energy $E_1(k_1)$ will only occur at the same wave number $k$, i.e., $k_2 = k_1$. Hence, the energy of the photon involved in the transition is given by

$$E_{ph} = \hbar\omega = E_2 - E_1, \tag{2.2}$$

In the thermal equilibrium at a temperature $T$, the Fermi function $f(E,T)$ gives the probability of finding and electron in an energy state with energy $E$

$$f(E,T) = \frac{1}{\exp\left[\dfrac{E - E_F}{k_B T}\right] + 1}, \tag{2.3}$$

where $k_B$ is the Boltzmann constant and $E_F$ is the Fermi level energy.

Stimulated absorption or simply absorption, the first process depicted in Fig 2.2 occurs when a photon is absorbed and an electro-hole pair is generated. Being a three particle process, the rate of this transition $R_{12}$ is proportional to the particle densities of the non-occupied states $D(E_2)[1-f(E_2,T)]$ in the conduction band at energy $E_2$, the density of the electro occupied states $D(E_1)f(E_1,T)$ in the valance band at $E_1$ and the density of photons $\rho(\hbar\omega)$ with an energy $\hbar\omega=E_2-E_1$ [16].

$$R_{12} = B_{12}\rho(\hbar\omega)D(E_1)f(E_1,T)D(E_2)[1 - f(E_2,T)], \tag{2.4}$$

where $B_{12}$ is proportionality constant for stimulated absorption.

The second process depicted in Fig 2.2 is spontaneous emission which occurs during the recombination of the electron-hole pair. It leads to the emission of a single photon. The emitted photon would be random in phase, direction and time. This is an incoherent emission process which is predominant in devices such as LEDs. The transition rate for spontaneous emission is proportional to the product of electron density at $E_2$ and the hole density at $E_1$. So, the transition rate per volume for spontaneous emission of photons with fixed energy $\hbar\omega=E_2-E_1$ is written as

$$R_{sp} = AD(E_2)\,f(E_2,T)D(E_1)[1-f(E_1,T)], \tag{2.5}$$

where A being the proportionality constant for spontaneous emission and $f(E_1,T)$ and $f(E_2,T)$ are the probability functions..

The third process depicted in Fig.2.2 is stimulated emission. In this case, a photon stimulates the recombination of an electron hole pair which produces a second photon with the same phase and direction as the first photon. This process leads to the emission of coherent radiation and also forms the basic principle behind the operation of lasers. The transition rate $R_{21}$ for stimulated emission can be written as

$$R_{21} = B_{21}\rho(\hbar\omega)D(E_2)\,f(E_2,T)D(E_1)[1-f(E_1,T)], \tag{2.6}$$

where $B_{21}$ is the proportionality constant for stimulated emission.

The proportionality constants in equations (2.4)-(2.6) are known as Einstein's coefficients and they satisfy the condition [16]

$$B_{12} = B_{21} = B, \qquad A = \frac{n^3}{\pi\hbar^3c^3}(\hbar\omega)^2 B, \tag{2.7}$$

where $n$ is the refractive index of the medium. Lasing occurs only when the stimulated emission rate exceeds the rate of absorption in the material. By comparing Equations 2.5, 2.6 and 2.7, the ratio of the rates of stimulated and spontaneous emission can be written as

$$\frac{R_{21}}{R_{sp}} = \frac{B}{A}\rho(\hbar\omega) = \frac{\pi^2\hbar^3c^3}{n^3(\hbar\omega)^2}\rho(\hbar\omega), \tag{2.8}$$

This equation shows that a high photon density is necessary to suppress spontaneous emission. To obtain a high photon density in semiconductor lasers, optical waveguides are implemented to confine the photons in the laser-active region of the device. Furthermore, an optical resonator, mostly a Fabry–Perot resonator, is used to increase the photon density in the resonator cavity. A semiconductor laser can be regarded as an optical oscillator consisting of an optically amplifying medium and a resonator which provides optical feedback to the amplifier.

The basic elements necessary to realize a semiconductor-diode laser are:

- A medium providing optical gain by stimulated emission,
- An optical waveguide which confines the photons in the active region of the device,
- A resonator creating optical feedback, and
- A lateral confinement of injected current, carriers, and photons which is required for operation in a fundamental lateral mode.

## 2.2 Laser diode structures and materials

A typical diode laser consists of a heterostructure made by the epitaxy of an active region sandwiched between a *p* type and an *n* type semiconductor material layer. Figure 2.3 shows the schematic diagram of a double hetero structure and the band structure. When the *p*-*n* junction is forward biased, in the active region, large concentrations of electrons in the conduction band and holes in the valance band are developed. The electrons and holes which are injected into the active region recombine to make the lasing possible. Moreover an optical feedback system is necessary to sustain the laser emission from this structure. Hence a laser cavity is realized within the cleaved surfaces of the structure. The surfaces which are also termed as facets are given proper reflection coatings. Typically, the end facet would have a very high reflective

coating ($R$ > 97%) whereas the front facet is anti-reflection coated ($R$ = 4 - 10%). For the external cavity operation of diode lasers, the front facets are usually provided with very good anti-reflection coatings ($R$ < 0.01-1%) to suppress the free running contributions. The metalized contacts provide external voltage supply which in turn maintains a constant supply of electron and holes for the recombination in the active region. Above a critical value of the external current known as the threshold, the rate of photon emission exceeds the rate of absorption and thus the lasing takes place. Modern diode lasers consist of an active region made of quantum wells rather than bulk materials. This improves the efficiency of the laser as the density of states as a function of energy has distinct steps unlike bulk materials in which it displays a smooth quadratic curve. This keeps the electrons in those particular energy states that are responsible for lasing. In many lasers instead of a single quantum well, multiple quantum wells are used. This is to improve the overlap of the optical mode with the effective gain region.

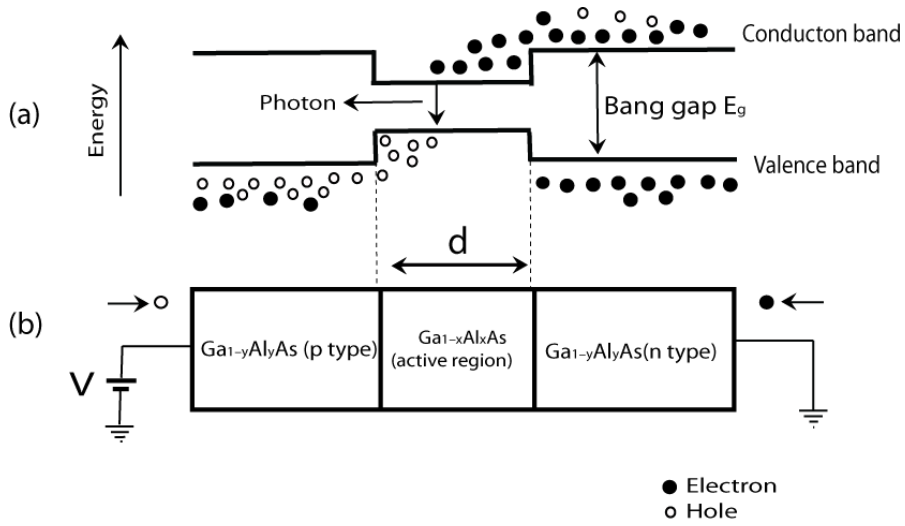


*Fig. 2.3. A double heterostructure. (a) The band structure is shown. The active region has the smallest band gap. (b) Shows the layer structure of a double hetero structure.*

Another important factor to be considered is the power scaling in diode lasers. Many applications such as material processing, display, medical surgeries etc. require higher output powers while there is always limit in the output power a single diode can provide. Power scaling could be done in many

ways for e.g., by simply using broader junctions as in a broad area diode laser or even by using geometries with multiple elements as in a diode laser array or bars. The following subsections deals with it.

### 2.2.1 Broad area lasers (BALs)

Different approaches have been made to increase the optical power output from diode lasers. One of them is simply by increasing the area of the emitting aperture of the diode. In a diode laser, a major factor which limits the power scaling is the catastrophic optical mirror damage (COMD). This happens when the excess heat produced by the high power operation of a diode laser is absorbed by the material which results in the melting of the facets thereby destroying the laser. By widening the injection stripe (as in a BAL), this could also be limited to a great extend. A typical broad area laser has a lateral dimension of 100- 200 microns. The increase in the output power however comes at a price. The emission aperture supports multi mode emission and it leads to the reduction of spatial and temporal coherence of the emission. Moreover, it can cause self induced filamentation [17] due to the carrier induced change in the refractive index of the medium and above a width of 200 microns, the diode structure is also prone to lateral lasing. Broad area lasers that could emit up to 15 W of output power have been demonstrated [18]. However when it comes to power efficiencies, broad area diode lasers offers the best performance with more than 70% efficiencies was demonstrated [19]. This leads to a reduction in the waste heat deposition in the medium and hence one could relax the laser cooling requirements. This could make the entire laser system much simpler.

The multimode emission of broad area diode lasers is responsible for the degradation in the beam quality along the slow axis. Even though for certain applications such as solid state laser pumping in which the beam quality is of less importance, broad area diode lasers could directly be employed, when it comes to applications such as material processing, second harmonic generation, single mode fibre coupling etc, the degrading beam quality with the increase in operating current levels poses serious problems such as reduction in the spatial brightness, reduction in the nonlinear conversion efficiency and an increase in coupling losses in an optical fibre respectively. The lateral far field divergence

increases due to an increasingly dominant multi mode emission structure when the operating power levels are increased. The filamentation leads to a periodic variation of the lateral intensity profile of a broad area diode laser. The highest intensity is not observed along the optical axis. Instead, a bi-lobed off axis intensity distribution could be observed. The broad area laser supports different cavity modes depending on the drive current. These are termed as *broad area modes*. However, the improvement of the beam quality along the slow axis of broad areas has been demonstrated by many research groups using external cavity techniques. Both on-axis and off-axis feedback techniques have been proved useful in this scenario. These techniques involve using a simple external cavity setups [20] [21] and Fourier optical cavities which involves lateral mode selection using a spatial filter [22].

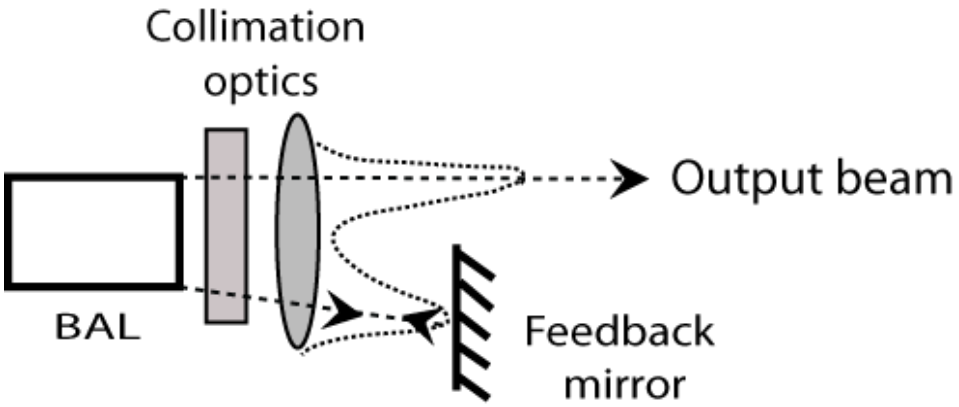


*Fig. 2.4. External cavity BAL based on off-axis partial mirror feedback. The dotted curve represents the bi-lobed far field intensity pattern. Feedback is given to one of the lobes. The other lobe is amplified.*

External cavities employing a spatial filtering element such as a feedback mirror stripe could be used to choose higher order spatial modes for amplification in the laser cavity. By varying the lateral position of the spatial filter in the cavity, one can suppress the lower order spatial modes and selectively amplify higher order modes. This principle has been used to improve the beam quality of a broad area diode laser bar which is explained in detail in chapter 4 of this thesis. A similar technique has been demonstrated here using a commercial BAL. The experimental setup of an off axis mirror feedback setup is shown in figure 2.4. The BAL was collimated along both axes

and a partial or asymmetric feedback was given using a high reflective mirror. As the lateral far field profile of the broad area laser consists of an off-axis bi-lobed intensity profile, the feedback is selectively applied to one of the two lobes. This could amplify the higher order modes in the other lobe and suppress the feedback lobe. A part of the output beam was focused by a 100 mm achromatic lens and directed to a beam scanner to measure the beam widths at different distances from the beam waist. The $M^2$ value of the output beam along the slow axis was measured using the values of the beam widths. The experimental record of the improvement in the slow axis $M^2$ value of the broad area diode laser in the free running mode and in an external cavity mode with a partial mirror feedback is shown in the figure 2.5. In the free running mode the beam parameter was recorded to be 46 and in the external cavity mode the value reduced to 20.

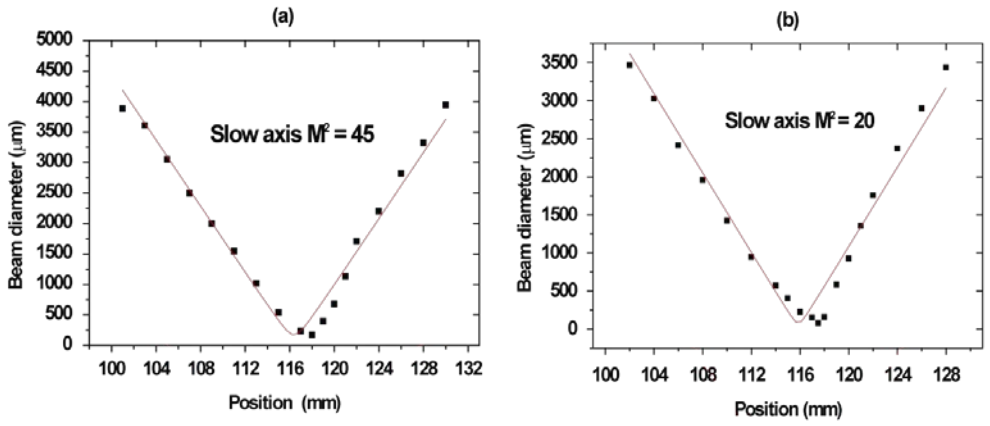


*Fig. 2.5 Slow axis beam caustic of a broad area diode laser (a) free running mode. (b) with a partial mirror feedback. $M^2$ parameters have been measured. Red lines represent the numerical fit and the black dots represent the experimental data. I = 825 mA.*

Regarding the spectral properties of broad area diode lasers, the emission line widths are rather broad of the order or a few nanometres. External cavity setups using a wavelength selective element for e.g., gratings could be used to stabilize the wavelength of operation of BALs and narrow the line width to the order of several picometres. More on this could be found in chapter 6 where different external cavity techniques were employed for the line width reduction of diode laser emissions.

### 2.2.2 Tapered diode lasers

Tapered diode lasers are interesting devices that could combine the capacity to deliver high output powers similar to broad area diode lasers and at the same time provide near diffraction limited beam qualities. The performance of taped diode lasers is much better in terms of modal stability, catastrophic optical mirror damage, filamentation etc. when compared to a broad area diode laser. The key to the superior performance lies in the basic structure of a tapered diode laser. A tapered diode lasers consists of two sections. A ridge waveguide section that acts as a modal filter and produces a single mode emission and a tapered gain region which amplifies the single mode emission to enhance the output power. Emissions with good beam quality is already possible using a single ridge wave guide laser but, such a laser whose stripe width is limited to a few microns can only deliver powers up to 300 mW [23] [24] while, tapered diode lasers can deliver output powers of the order of several watts [25] [26] with a comparable beam quality. In modern tapered diode lasers the ridge waveguide section is index guided and the tapered gain section is gain guided with both sections electrically contacted separately. Figure 2.6 shows the schematic diagram of a tapered diode laser. The length of the ridge section $L_1$ can vary between 100-500 microns and the tapered section $L_2$ could be 1500-2500 microns. The taper angle $\theta$ could vary between 1° (in index guided tapered lasers) to 6°.

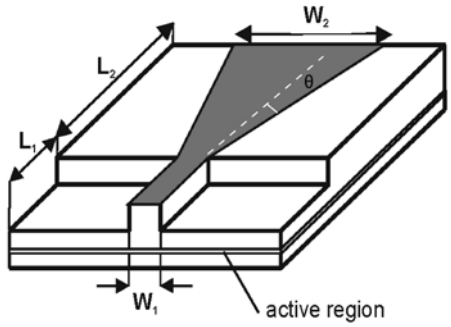


*Fig. 2.6. Schematic diagram of a ridge waveguide tapered geometry of a diode laser.*

$W_1$ and $W_2$ are the lateral widths of the ridge section and the tapered facet respectively. Moreover, tapered devices could also be used as optical

amplifiers by varying the facet reflectivity. A detailed report on the structure of the tapered diode laser, the factors that affects the beam quality such as injection current density, length of the tapered section, output power levels etc, were reported by Kelemen et al [25]. The length of the ridge section is also carefully chosen avoiding saturation effects due to a short ridge and excess power oscillation in a long ridge. Despite these advantages, the emission from a tapered diode laser is also known for its intrinsic astigmatism. This is due to the fact that the light source along the fast axis coincides with the laser front facet whereas the virtual source of the lateral axis is located inside the tapered amplifying medium. Hence to conserve the spatial brightness of a tapered diode laser, it is very important to characterize the astigmatism and to provide proper beam collimation optics along both axes.

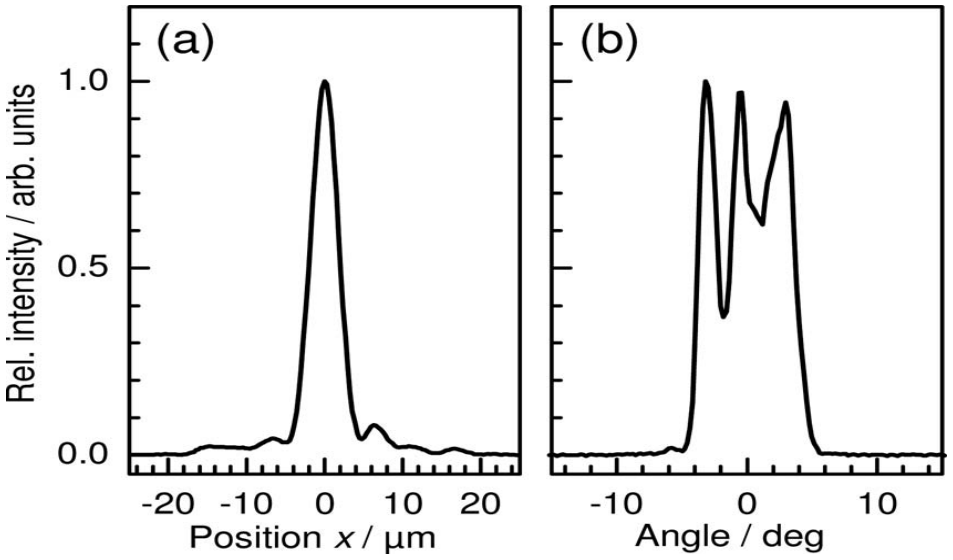


*Fig. 2.7. (a) Near field and (b) far profile of a tapered diode laser at I = 2.3 A and T = 15 °C* [26].

The level of the injection current could also influence the astigmatism. Usually, the astigmatism is observed to be increasing with an increased operating current of the diode due to the fact that the position of the virtual source along the slow axis is pushed further back due to a reduced effective refractive index of the medium which results from an increased carrier density at higher currents. Figure 2.7 shows the intensity profiles of a 650 nm light

output from a tapered diode laser [26]. The near field is near Gaussian while the far field appears non-Gaussian. This is something quite characteristic of tapered diode lasers.

The side lobes in the near field pattern evident from figure 2.7 (a) is the result of power-dependent changes in the shape and position of the virtual point source caused by the carrier and temperature induced refractive index perturbations occurring in the resonant cavity. The major players are filamentation, spatial hole burning, optical pumping and electrical over pumping [27]. At low powers, the carrier density and the gain in the quantum well is uniform. When the power levels increase, the carrier density reduces in the regions with high photon density. This results in the localized reduction of the gain and in turn forms local waveguides which spatially overlaps with the local photon density pattern. This results in the filamentation effect. Optical pumping is another phenomenon that reduces the spatial filtering capability of the ridge wave guide section of the tapered diode laser. The back propagating spherical wave is scattered by the tapered section. This result in the propagation of power in higher order modes towards the ridge wave guide section. The intensity of this scattered light propagating alongside the ridge section increases with drive current. This in turn increases the local carrier density and the region adjacent to the ridge becomes transparent due to this optical pumping effect. This would however reduce the filtering capability of the ridge wave guide section. The unfiltered scattered light from the tapered section would propagate towards the rear facet and reflects back into the tapered section and produce filamentation effects. These side lobes re entering the tapered section gets scattered if their propagation angle is smaller than the taper angle and forms side lobes in the near field pattern.

If the optical pumping effect is suppressed using beam spoilers [28] [29] or by reducing the front facet reflectivity, the carrier density increases rapidly at the edges of the taper as the photon density is low. This leads to a high local gain and eventually leads to a ‘shoulder’ in the intensity profile which would reflect in the near field. This phenomenon is termed as electrical over pumping [30] [31].

Recent advancements in the tapered diode technology have led to the integration of distributed Bragg reflectors (DBR) to the rear facets of tapered diode lasers. DBRs are highly wavelength selective and would help in limiting the line width of the emission of these devices. The wavelength of operation of these devices is related to the period of the DBR structure $d_{Bragg}$, the order of diffraction $m$ and the refractive index of the material $n$ by the equation,

$$d_{Bragg} = \frac{m\lambda}{2n}, \tag{2.9}$$

Recently, over 12 W of output power has been demonstrated at 1060 nm with near diffraction limited beam qualities from DBR tapered diode lasers [32] with a line width as low as 17 pm. These devices have also shown significant potential as pump sources for second harmonic generation creating record power levels at 532 nm using diode lasers [33]. Tests have also revealed that the state of the art tapered devices could provide reliable high power emission up to thousands of hours without failure [32].

### 2.2.3 Diode laser arrays

This geometry consists of different stripes placed next to each other. In this geometry, the proton implantations between the stripes enhance the separation of the current flow from each of them. This leads to a controlled periodic gain profile. The intensity profile on the facets is much more uniform compared to a broad area laser. Hence the risk of catastrophic optical damage is reduced. The self-induced filamentation could also be avoided. In a laser diode array, the width of each stripe is around 5- 10 microns and the separation of each strip is usually same as the strip width. An optical power of several tens of watts could be obtained from a 10 stripes 100 microns array. The closely placed emitters could lead to the coupling between the individual emissions and hence the output consists of an array super mode rather than the characteristic individual emitter modes. Based on the type of optical confinement in the diode laser arrays, the coupling could be evanescent wave coupling or leaky wave coupling.

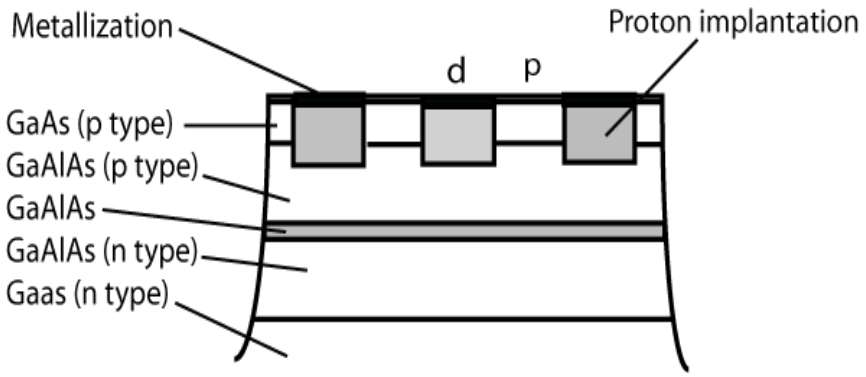


*Fig. 2.8. The schematic diagram of a diode laser array. The stripe width is denoted by d and the spacing between the stripes by p.*

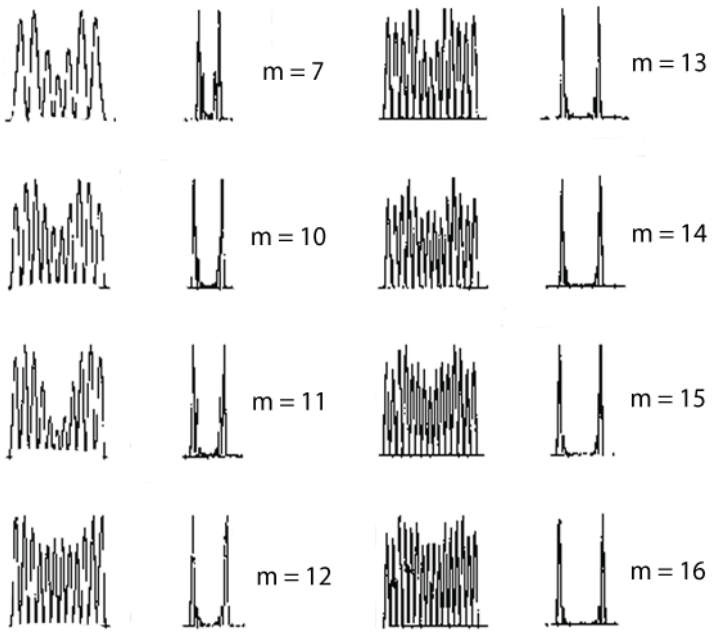


*Fig. 2.9. Near- and far-field patterns of the array modes of a N= 10 stripe gain guided array. Vertical scale is in arbitrary units, horizontal scale unit for the near-fields (left-hand side of the columns) is 10 microns, and horizontal scale unit for the far-fields (right-hand side of the columns) is 2°.* [34]

The far field patterns of a diode laser array could vary depending on the modal gain of the array modes. The fundamental mode with a mode number *m* = 1 is termed as the in phase mode. The higher order modes display an off-axis bi-lobed intensity profile where the different lobes are radiated at an angle with respect to the optical axis. This angular nature helps in the mode discrimination in a laser array using a spatial filter (as discussed in chapter 4). The numerical analysis of a 10 stripe gain guided diode laser array was performed by Verdiell et al [34]. Different near field and far field patterns corresponding to different laser array modes are shown in figure 2.9. At threshold, mode *m* = 10 was observed. With the increase in the drive current, higher order modes such as, *m* = 11, 12 and so on was observed. In this experiment, Verdiell et al observed highest modal gain for *m* = 10. The modes with *m* greater than 10 were observed to be having higher modal gain compared to the lower order modes.

### 2.2.4 Diode laser bars

This geometry consists of a number of emitters placed next to each other in a monolithic structure. The emitters are placed at a sufficient separation so that there is no coupling between their individual emissions. The typical width of diode laser bars is around 5-10 mm. The fill factor or the ratio between the optically active area and the whole area of the diode laser bar is around 30-80%. Diode laser bars are made of broad area laser arrays and tapered diode lasers [35] [36]. Broad area diode laser bars capable of emitting up to a kilo watt of optical output has been demonstrated [3]. The high power emission from a diode laser bar usually has a broad line width of several nanometres. This could be narrowed down by employing an external cavity setup using reflective gratings or volume Bragg gratings.

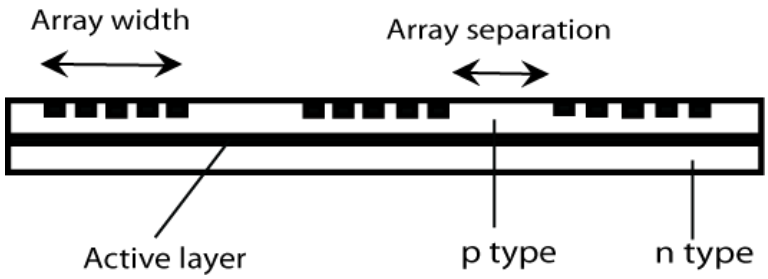


*Fig. 2.10. Cross sectional view of a diode laser bar.*

Broad area diode laser bars finds many applications such as solid state laser pumping, fibre laser pumping, material processing etc. Broad area diode laser bars in VBG cavities provides narrow line width high power emissions that are quite suitable for spin exchange optical pumping. Figure 2.10 shows a cross sectional diagram of a diode laser bar. Often the term ‘laser array’ is used synonymous to a laser bar.

The spatial mode structure of diode laser bars is quite interesting and has been explained in detail with the aid of numerical simulations in [37] [38]. A single lobed intensity profile in the far field is usually desirable for most of the applications. But, the lateral intensity distributions from the individual emitters on the laser bar couples together to form a bi-lobed out of phase intensity profile in the far field. This property has been utilized in controlling the mode structure of their emission in off axis feedback setups [39]. Recently, there has been a lot of interest in the development of laser bars based on tapered diode emitters due to the fact that tapered emitters provides much better beam quality at comparable power levels to broad area emitters. In this thesis, the majority of work has been based on the external cavity operation of tapered diode laser bars and broad area diode laser bars.

### 2.2.5 Diode laser stacks

Diode laser stacks are realized by stacking several diode laser bars on top of each other. However, the stacking of edge emitting laser bars leads to a decrease in the beam quality along the fast axis direction. Better fast axis beam quality could be obtained if these laser bars are as close as possible. Practically this is not possible due to the thickness requirements of the heat sinks in order to achieve effective cooling of the laser bars. This in turn leads to a reduction in the effective spatial brightness of a laser stack. Efforts has been made to tackle this problem using techniques such as polarization coupling, spectral beam combining etc. Laser stacks that could deliver output powers of the order of several kilowatts [40] are commercially available these days. Coupling of the high power output from diode laser stacks using thick multi mode fibres (core diameter ~ 600 microns) are also possible and it proves useful in directed energy applications such as cutting, welding etc.

### 2.2.6 Diode laser materials

Numerous semiconductor materials exhibiting lasing have been investigated since early days. Several important criteria are being followed while selecting the appropriate gain medium. The most important one among those are the reduction of the lattice defects. This quantifies the quality of the interface of two different semiconductor materials. The lattice constants should match better than 0.1% for a good quality interface. The wavelength of interest should also be taken into consideration. The lasing wavelength is closely related to the band gap energy $E_g$ of the material. This could be explained as [41]

$$\lambda = \frac{1.24}{E_g}, \tag{2.10}$$

where λ is the lasing wavelength. The wavelengths of interest in this work are 980 nm and 1060 nm. The broad area laser bar and the tapered diode laser bar used in our works emit around 980 nm while the tapered diode single emitters emit around 1060 nm.

High power diode laser structures consist of single or multiple quantum wells embedded between another material of a higher band gap. The wavelength of emission is determined by the strain in the quantum well which leads to a lattice mismatch between the quantum well and the waveguide. For the emission in the NIR spectrum, Indium gallium arsenide quantum wells embedded in Aluminium gallium arsenide waveguide are typically used. In the broad area diode laser bar used in the experiments described in this thesis, the active region consists of an InGaAs-quantum well embedded in a 1.06 microns thick AlGaAs core region. The optical waveguide was formed by 1 micron thick AlGaAs claddings. After processing, the wafers were thinned and chipped into laser bars with a pitch of 500 microns. The emitter width is 150 microns. The laser was coated with two pairs of a high-reflection $Si/SiO_2$ coating on the back facet with a reflectivity > 97% and a single layer anti-reflection (AR) SiN coating on the front facet with a residual reflectivity < 0.01%.

The tapered diode laser bar which emits around 980 nm is based on a GaAlInAs GaAs laser structure with a large optical cavity. The active region of the laser structure consists of an InGaAs-quantum well embedded in a 1.06

microns thick AlGaAs core region. The quantum well is 7 nm thick. The optical waveguide is formed by 1 micron thick AlGaAs claddings.

The Distributed Bragg Reflector (DBR)–tapered diode lasers used in this work [32] operates around a wavelength of 1060 nm. The structure contains an InGaAs quantum well active region embedded in a 4.8 microns broad AlGaAs core region forming a large optical cavity. The full taper angle is 6°. The DBR–tapered lasers have a total length of 6 mm. The vertical divergence is about 15°. The passive DBR located at the rear end and the active ridge waveguide gain section has both a length of 1 mm. The ridge waveguide width and full taper angle amounts to 5 microns and 6°, respectively. The DBR reflectivity is about 60%.

### 2.3 Fabry-Perot resonator

In an edge emitting diode laser, the resonator is formed between the cleaved surfaces of the diode material. The vertical direction is termed as the “fast axis” and the horizontal direction is termed as the “slow axis”. As there is a difference in the width of the active region in both directions, the beam divergence is also different in two directions. This causes the laser diode to emit an astigmatic beam as shown in the figure 2.11. Hence, such a laser requires separate collimation along both the axes. The axis with the higher divergence is termed as the fast axis and the one with a lower divergence is termed as the slow axis.

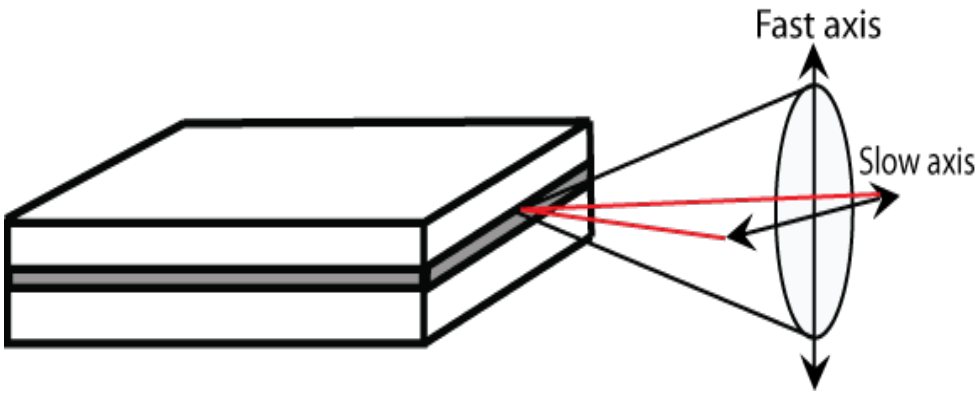


*Fig 2.11. Typical emission characteristics of a Fabry-Perot diode laser.*

## 2.4 Field confinement

The confinement of the optical field in the active region of the diode active region is very important for the operation of the laser. Extend of the field confinement could be explained through a term called confinement factor [16]. It determines the fraction of the optical energy which is confined within the active region. If *J(y)* is the optical intensity along the horizontal direction and *d* is the thickness of the active region, then the confinement factor is termed as

$$\Gamma = \frac{\int_{-d/2}^{+d/2} J(y)dy}{\int_{-\infty}^{+\infty} J(y)dy}, \tag{2.11}$$

There are two ways of realizing optical confinement in a diode laser structure, through index guiding and gain guiding. These techniques are briefly explained in the following subsections.

### 2.4.1 Index guiding

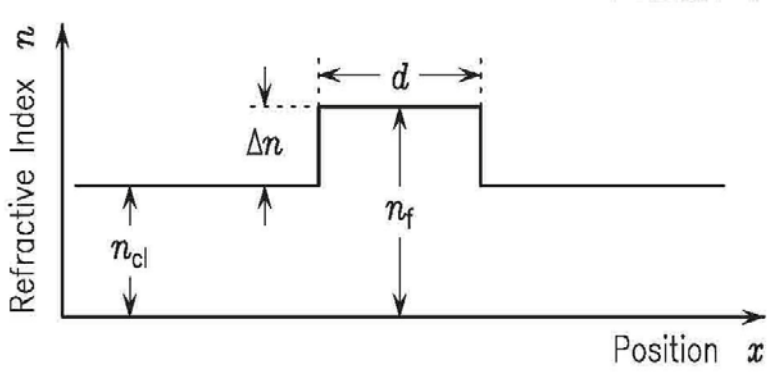


*Fig 2.12. Index guiding*

The basic idea of index guiding (fig. 2.12) relies on achieving an index change between the wave guiding material and the cladding material. The waveguide is formed using a higher refractive index material of refractive index $n_f$ and the cladding layer using a lower refractive index material of refractive index $n_{Cl}$. Thus the optical field could be confined to the active region. With an optimal

index step and core thickness, a near Gaussian fundamental mode could be made to propagate. This technique is termed as index guiding as the mode confinement is achieved by utilizing the refractive index discontinuity in the medium. However the refractive index experienced by an optical wave travelling in this medium $n_{eff}$ would be different from $n_f$ and $n_{Cl}$ and $n_{Cl} \leq n_{eff} \leq n_f$.

### 2.4.2 Gain guiding

In a gain guided diode laser structure (fig 2.13), the carrier injection is done using a narrow metal contact stripe. The effective refractive index $n_{eff}$ is uniform throughout the material in the absence of current injection. The width of the gain region is controlled by properly selecting the width $W$ of the metal strip.

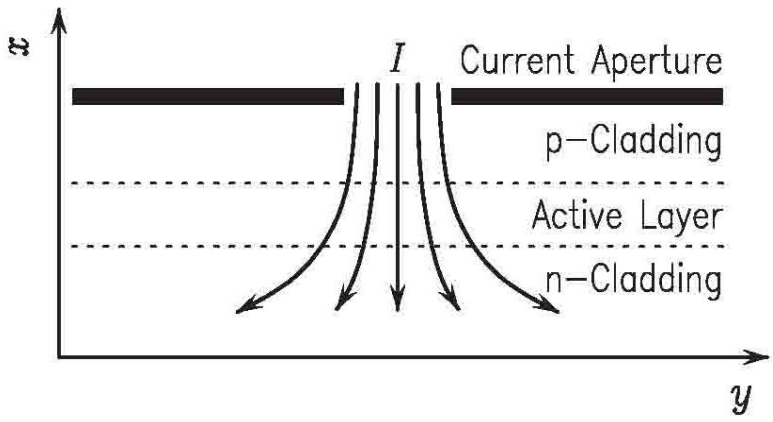


*Fig 2.13. Gain guiding*

With a narrow strip, a narrow gain region could be obtained and thus a good optical confinement. But when the injection current increases, the free carrier plasma effect comes into play and it changes the refractive index of the material. This change is proportional to the injected carrier concentration $N_C$ and is given by the equation [41]

$$\Delta n_C = \frac{e^2}{2m_C \omega^2 \varepsilon_0 n} N_C , \qquad (2.12)$$

where $e$ is the electron charge, $m_C$ is the electron effective mass, $\omega$ is the angular frequency of light, $\varepsilon_0$ is the permittivity in vacuum, and $n$ is the refractive index in the absence of carrier injection.

This change in the refractive index results in the reduction of the optical confinement and is termed as the "anti-guiding effect". It leads to the broadening of the optical field towards the edges of the active region. The Joule heating that occurs as a result of the carrier injection in the diode laser could also result a change in the refractive index of the medium. This temperature induced refractive index change $\Delta n_T$ could be quantified as [42]

$$\Delta n_T \approx 5\times10^{-4}\Delta T\,, \tag{2.13}$$

where $\Delta T$ is the change in the temperature in Kelvin. These two effects play a crucial role in determining the optical confinement in a laser diode.

Gain guiding has an inherent disadvantage that the lateral mode structure is controlled by the gain profile in the active region. However the gain profile is controlled by the carrier density which changes with the strength of pumping. The change in the carrier density also leads to carrier induced refractive index reduction in the waveguide. Thus it becomes difficult to control the mode structure in a purely gain guided laser. But some degree of index guiding could also be induced in a gain guided laser structure so that the laser operates with a combined effect of both gain and index guiding. The index step in such a laser structure $\Delta\mu$ determines whether the device exhibits an index guiding or gain guiding characteristics. The gain guided devices suffer from carrier induced index anti-guiding. The effective index reduction caused by the carriers in the medium is ~0.005. However, when $\Delta\mu$ increases, a transition from gain guiding towards index guiding could be observed. A stable lateral mode propagation could be achieved from such devices if operated in a regime with the value of the index difference, $\Delta\mu$ ~ 0.01 [42] which is much higher compared to the carrier induced index reduction. Such devices are termed as weakly index guided diode lasers, for e.g., a ridge wave guide diode lasers and rib waveguide diode lasers. In strongly index guided structures such as a buried heterostructure device, the active region is buried within a high band gap layers

on all sides. The lateral index step as high as 0.2 determines the characteristics of the lasing and confines the mode to the active region.

## 2.5 Coherence properties of diode lasers

The term “coherence” is derived from the Latin verb *cohaerere* which means, to join together. A light wave is considered to be coherent if two joint parts of the wave exhibit interference. In laser physics, one distinguishes between two different aspects of coherence, namely temporal and spatial coherence.

### 2.5.1 Spatial coherence

Spatial coherence denotes the distance between two points of the wave, over which they still maintains a phase relationship so that they interfere with one another. Spatial coherence governs the focus-ability of the laser beam. i.e., how small the laser beam could be focused. As the focus-ability of the laser beam is the key factor that determines the spatial brightness of the beam which is important in many practical applications of a laser beam, it is essential to have a high degree of spatial coherence to achieve a high spatial brightness from a laser beam. The focus-ability of a laser beam is related to the beam quality parameter of the beam (BPP). The experimental measurement of the BPP is quite important and has been performed during most of the experiments that are described in this thesis. If we consider the propagation of a Gaussian beam through space, The beam width *w(z)* at any position *z* could be explained by the equation,

$$w(z) = w_0 \sqrt{1 + \left( \frac{z}{z_R} \right)^2} \,, \tag{2.14}$$

where $Z_R$ is the Raleigh range which is the distance from the beam waist position at which the beam width is increased by a factor of $\sqrt{2}$ and $w_0$ is the beam waist. Figure 2.14 shows the propagation of a laser beam in *z* direction through space. The divergence of the beam in the far field is a measure of how fast the beam diverges while propagating away from the beam waist given by the angle $\theta$ as explained by equation 2.15.

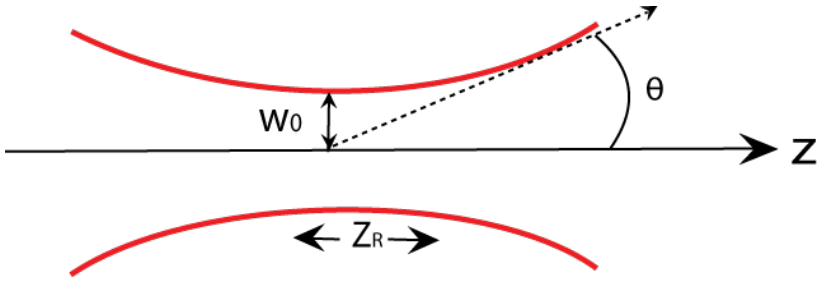


*Fig. 2.14. Propagation of a laser beam through space.*

$$\theta = \frac{\lambda}{\pi w_0}, \tag{2.15}$$

A Gaussian beam is the most fundamental solution of the wave equation in the paraxial approximation and the beam parameter product of it can be explained as

$$BPP = \theta . w_0 = \frac{\lambda}{\pi}, \tag{2.17}$$

As in the case of practical laser beams where the beam profile is non-Gaussian, the BPP describes how much the beam deviates from a theoretical Gaussian mode of propagation. Hence the divergence of a real laser beam $\theta_r$ is described as

$$\theta r = M^2 \frac{\lambda}{\pi w_0}, \tag{2.18}$$

Thus the dependence of the BPP on the divergence of the laser beam is evident. The spatial brightness of a laser beam *B* which could be defined as the power per unit area per unit solid angle [16] is also dependent on the divergence of the laser beam as

$$B = \frac{P_{av}}{\lambda^2 M_x^2 M_y^2}, \tag{2.19}$$

where $P_{av}$ is the average output power of the laser beam, $\lambda$ is the wavelength of emission, $M^2_x$ and $M^2_y$ is the $M^2$ values of the slow and the fast axes respectively. In the case of a Gaussian beam, $M^2_x$ and $M^2_y$ is equal to unity. But in the case of diode lasers, due to the low mode selectivity of the Fabry- Perot resonator, it results in both longitudinal and transverse multi mode emission which is non Gaussian. Hence, the beam quality factor determined by $M^2_x$ and $M^2_y$ would limit the spatial brightness. In general for broad area emitters, the $M^2$ value along the slow axis of the beam is much higher compared to the diffraction limited value (~ 30 times or more). This is due to the broad emitter width that supports multi mode emission which is low in terms of spatial coherence. In many applications of the diode lasers such as solid state laser pumping, graphics marking etc., it is desirable to have a high spatial brightness. Majority of the work which comes under the scope of this thesis has been dedicated towards different techniques that are investigated in order to enhance the spatial coherence property of diode lasers by improving the beam propagation factor.

There are several methods for measuring the $M^2$ value of a laser beam. In case of Gaussian beams, the $1/e^2$ values for the beam waist and the far field divergence could be used in equation 3.4 to calculate the $M^2$ value. Another option is to fit a Siegman hyperbolic curve [43] based on equation 2.14 on to the experimentally observed caustic of the laser beam. This method complies with ISO11146. In case of non- Gaussian beams, measuring $1/e^2$ widths may lead to larger error factors in the $M^2$ value. Hence, the measurements are made using the second moments of the beam width. Thus in case of non-Gaussian beams, equation 3.1 could be modified as,

$$w(z) = w_0 \sqrt{1 + \left( \frac{M^2 \lambda z}{\pi {w_0}^2} \right)^2}, \tag{2.20}$$

where $M^2$ is the beam propagation parameter. In practical terms while measuring the $M^2$ value of a real laser beam, within the Rayleigh range of the laser beam, as many measurement points are noted and outside the Rayleigh range, a few more measurement points are noted and these values are used for the hyperbola fitting.

### 2.5.2 Temporal coherence

Temporal coherence, on the other hand, describes the ability of a wave to interfere with a time-shifted copy of itself. The time during which the phase of the wave changes by a significant amount (reducing the interference) is referred to as *coherence time*. The propagation length during this time is called *coherence length*. The larger the range of frequencies in any given wave, the faster the phase correlation is lost. The line width and coherence length are linked via an inverse proportionality, with a numerical factor depending on the spectral profile of the laser. In case of a Gaussian spectral distribution, the coherence length $l_C$ is given by

$$l_C = \frac{2\ln(2)\,c}{\pi\Delta\nu}\,, \tag{2.21}$$

with $c$ the speed of light and $\Delta\nu$ the line width of the spectrum at full width half maximum. Thus the coherence length is inversely proportional to the line width of the laser emission.

In certain wavelength specific applications of diode lasers such as spin exchange optical pumping [44] [45], pumping alkali vapour lasers [46], non linear frequency conversion [47] [48] etc., it is very important to have a narrow line width of emission to increasing the pumping efficiency and conversion efficiency. In other words, the temporal coherence is also very important when it comes to certain applications. An effort that has been made for the line width reduction and thereby the improvement of the temporal coherence of diode lasers has also been focused in this thesis. By building an external cavity feedback setup using beam shaping optics and wavelength selective elements such as a grating, the longitudinal and transverse mode structure of the diode lasers could be influenced. Such a system is termed as an external cavity diode laser or EDCL in short. The chapters 3-7 gives the detailed description of the different external cavity methods employed for the improvement of the spatial and temporal coherence properties of diode laser sources.

# CHAPTER 3

# SPECTRAL BEAM COMBINING

## 3.1 Motivation

Several external cavity techniques have been employed by various research groups for the improvement of the beam quality of broad diode laser bars. One such technique termed as spectral beam combining is described in this section of the thesis. Recently, there is a lot of interest in tapered diode lasers due to their ability to provide high output powers with good beam qualities. For the first time ever to my best knowledge, this technique has been applied on a gain guided tapered diode laser bar to improve the beam quality of the whole bar to a level equivalent to the single emitter beam quality. Even though the tapered diode emitters could provide nearly diffraction limited beams, when it comes to a tapered diode laser bar, due to the inherent divergent nature of the bar geometry, the slow axis beam quality declines. In this experiment, we could limit the slow axis $M^2$ value of the entire bar to 5.3 which is comparable to that of a single emitter beam quality in the bar. The laser bar yielded 9 W of optical power. In another experiment, the spectral beam combining of two high power tapered diode emitters are described which lead to an output power of 16 W with the slow axis $M^2$ value 3.3 of the combined beam comparable to that of the single emitters. To my knowledge, it is the first time spectral beam combining has been applied to single tapered emitters.

## 3.2 Basic principle

Diode laser bars could provide output powers in the order of several tens of watts. But the spatial brightness of the laser bars are often limited by the high divergence which is characteristic to the bar geometry. The importance of having high spatial brightness has been discussed in the former chapter. Spectral beam combining or SBC [49] is a technique that has been extensively used for improving the beam quality of diode laser arrays, bars and fibre lasers [50]. If one could limit the divergence of the whole bar to that of a single

emitter on the bar and at the same time preserve the output power level, the spatial brightness would significantly increase. This is the principle basic principle of spectral beam combining.

The idea behind SBC is hence to spatially superimpose the light beams from different emitters on the laser bar so that the effective beam divergence of the laser bar is comparable to that of a single emitter on the laser bar. This technique allows the spatial superimposition of the beams along the slow axis and hence improves the beam quality along the slow axis and has in principle, no effect at all to the beam quality of the laser bar along the fast axis. Figure 3.1 shows the schematic diagram of a typical SBC setup of a diode laser array. The light from the laser bar is collimated in the slow axis using a cylindrical lens. The cylindrical lens used in such a setup could also be termed as a Fourier lens as the light beams from different emitters on the laser bar superimposes one over the other on the Fourier plane of the collimating lens. A wavelength selective element such as a reflection grating is placed on the Fourier plane of the lens so that the light is superimposed on the grating surface. The Fourier lens converts the spatial separation of the individual emitters on the laser bar into a separation in the angle of incidence on the grating.

The diffracted light from the grating is fed back into the laser using a plane output coupler. The output coupler being plane would only feedback the light beams that are incident perpendicular on it. Hence, due to different angle of incidence for the light beams from different emitters, the external cavity would select a unique wavelength for each emitter and the plane output coupler forces co-directional propagation of the light beams. Thus the beam divergence of the entire laser bar could be limited to that of a single emitter on the bar while maintaining almost a similar output power level. Losses inherent to an SBC setup are mainly the ones induced by the grating. The light diffracted in to zero order is lost. Hence, a grating with very high diffraction efficiency (above 90%) in the first order is usually preferred for SBC setups. Spectral beam combining has been successfully demonstrated using reflective as well as transmitting gratings [3]. The use of transmission gratings has enabled higher power operations of lasers in the SBC cavity with combining efficiencies as high as 95% [51]. This technique is quite similar to the wavelength multiplexing in communication.

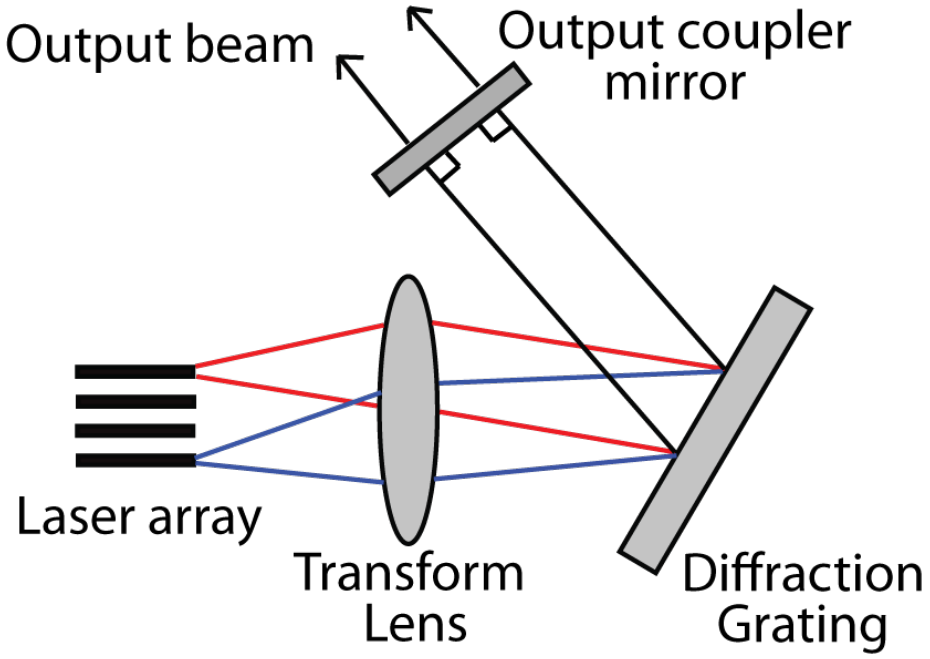


*Fig. 3.1. Spectral beam combining of a laser bar. The transform lens makes the Fourier transform of the light from different emitters which in turn is diffracted by the grating. Light beams perpendicular to the output coupler is fed back into the laser.*

However, this technique improves the spatial brightness of the laser bar at the expense of its spectral brightness. As the external cavity selects different wavelength of operation for each individual emitter on the bar, the output beam is usually spread over a certain range. The wavelength spread of the output beam $\Delta\lambda$ is related to the focal length of the Fourier lens $f$, the spatial extend of the laser bar $d$, and the dispersion of the grating $d\alpha/d\lambda$ by the equation [49]

$$d = f \frac{d\alpha}{d\lambda} \Delta\lambda , \tag{3.1}$$

The grating dispersion is given by

$$\frac{d\alpha}{d\lambda} = \frac{1}{\alpha \cos\alpha_0} , \tag{3.2}$$

where $\alpha$ is the grating period and $\alpha_0$ is the angle of incidence relative to the grating normal for the central emitter in the bar. Even though spectral beam

combining is a popular technique used for improving the beam quality of diode laser bars, the effective beam quality is often limited to a value that is comparable to that of the individual emitter on the bar. Hence, it would be most ideal to apply this technique on laser bars that consists of emitters with high beam quality such as a tapered diode laser bar or a slab coupled optical wave guide laser (SCOWL) bar [52].

Several research groups have made numerous efforts to improve the beam quality of different types of diode laser bars using spectral beam combining. Recently, Gopinath et al., [53] achieved 20 W of output power with a slow axis $M^2$ value of 10 by combining a 25 element broad area laser array using spectral beam combining. Spectral beam combining of a SCOWL arrays [54] provided 30 W of output power with an $M^2$ of 2. Jechow et al [55] obtained 10 W with a slow axis $M^2$ value less than 14 using a standard 25 emitter broad-area stripe laser bar. SBC using volume Bragg gratings have also been of interest recently. They show case a high spectral density and combining efficiency [56].

These works cited above mainly deals with broad area diode laser bars and nothing has been reported on tapered diode laser bars so far despite them being more interesting in terms of beam quality. The following sub-section deals with an experiment intended for the improvement of the beam quality of a tapered diode laser bar.

### 3.3 Spectral beam combining of a tapered diode laser bar

Tapered diode laser bars are interesting devices that could deliver output powers in the order of tens of watts [57]. The individual emitters on a tapered diode laser bar have a very good beam quality compared to that of a broad area diode laser bar. This is due to the structure of the device that supports a single longitudinal mode in the ridge section and amplifies it to higher power levels in the tapered section.

The tapered laser bar provided by Fraunhofer IAF, Germany is based on a (GaAlInAs) (GaAs) laser structure. A detailed description of the materials used in given in the section 2.2.6. The schematic diagram of a single tapered diode on the bar is shown in the figure 3.2. Tapered laser oscillators were

fabricated from epitaxial layer structures. The lateral structure consists of a ridge wave guide section with a length of $L_1$ = 0.5 mm combined with a tapered section with a length of $L_2$ = 2 mm. The tapered angle amounts to 6°. After processing the wafers were thinned and chipped into tapered laser arrays with a width of 6 mm. Since the 2.5 mm long emitters are separated by a pitch of 500 microns, a tapered laser bar consists of 12 single emitters. The ridge-sided facet was covered with a highly-reflecting mirror coating of residual reflectivity, $R$ > 97 %, whereas the front facet was covered with an anti-reflection coating with a rest reflectivity of about 1 %.

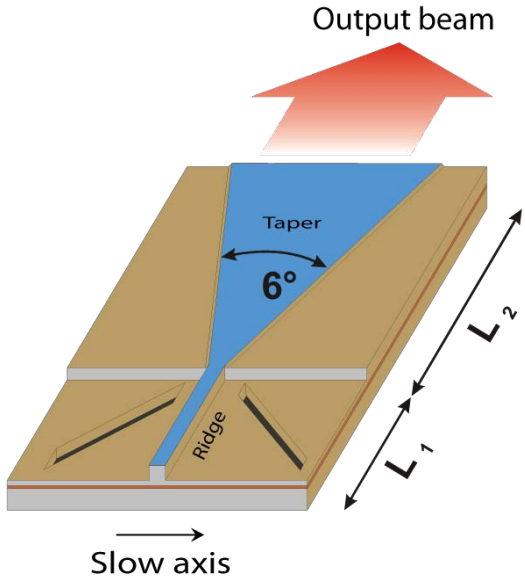


*Fig. 3.2. Schematic view of a tapered diode laser with a ridge section length $L_1$ and a taper section length $L_2$.*

After facet coating, the tapered laser bars were mounted directly p-side down on to copper mounts. Pumping of the laser medium is achieved by current injection via gold bond wires. The $M^2$ values of individual emitters along the slow axis on this tapered bar has been measured to be around 2.5 - 4.6 at 30 A of operating current. The output light has been collimated using a 910 µm focal length, 0.8 numerical aperture *LIMO* cylindrical micro lens attached to the heat sink. In the absence of the external cavity, the laser bar produced 14.5 W at 30 A of operating current. The temperature has been controlled by a thermo electric controller and the laser has been maintained at a temperature of 20°C.

Figure 3.3 shows the near field photograph of the emitters obtained by focusing the light using a 100 mm achromatic lens. A slight smile was observed especially on two emitters at the end.

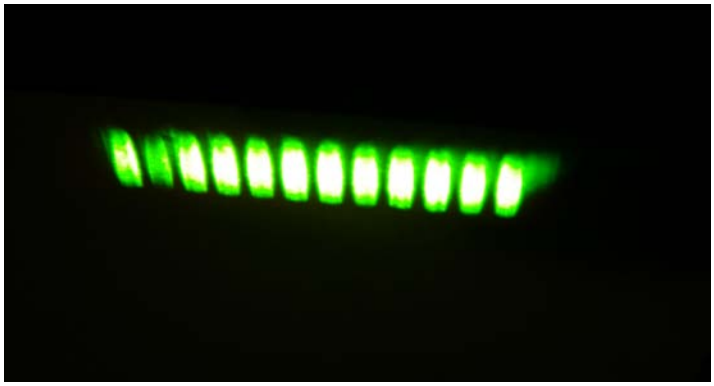

*Fig. 3.3. Near field photograph of the tapered diode laser bar at I= 10A.*

### 3.3.1 Experimental setup

The external cavity setup for spectral beam combining consists of the 12 emitter tapered laser bar, fast axis collimation lens, a 100 mm Fourier transform cylindrical lens $L_1$, a gold plated reflective grating with 1200 lines/mm and a first order diffraction efficiency measured to be 85% at 980 nm, a 100 mm fast axis focusing cylindrical lens $L_2$ and a plane output coupler with a reflectivity of 10% and an AR coated back side. The lens $L_2$ improves the stability of the setup by focusing the beam on the output coupler along the fast axis and thereby increasing the amount of feedback. The zero order beam is used to record the wavelength versus near-field position of the individual emitters. This is done by focusing the light using a 100 mm focal length achromatic lens and by coupling the focused light is into an optical spectrum analyzer (*Advantest Q8347*). Figure 3.4 shows the sketch of the experimental setup.

The light from different emitters on the laser bar superimposes spatially on the surface of the reflective grating and gets diffracted. The first order diffraction is focused on to the output coupler and fed back to the laser. The beam is incident on the grating with an angle of approximately 16º. The plane output coupler enforces the parallel propagation of the light beams from different emitters as the light is incident perpendicular to it. The incident angles

of the light from different emitters on the grating are different. Hence, the external cavity selects a particular wavelength for each emitter. The cavity enforces co-axial beams propagation with different but controlled wavelengths for each array element. The zero order reflection from the grating used to image the near-field of the emitters to record the wavelength versus near-field position of the individual emitters gave a better insight to the spectral behaviour of each emitter under the external cavity operation.

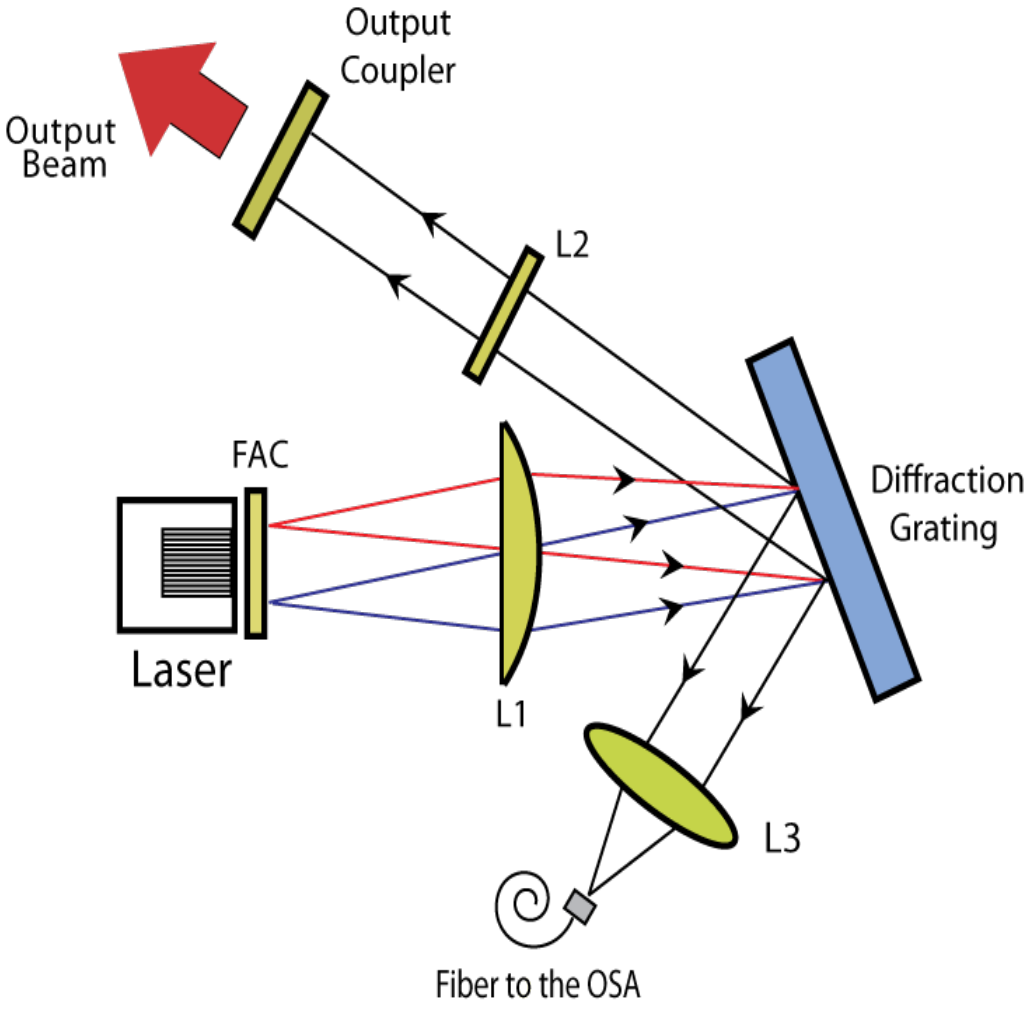


*Fig. 3.4. Experimental setup of the spectral beam combining of the tapered diode laser bar. $L_1$ is a 100 mm focal length cylindrical slow axis collimation lens and $L_2$ is a 100 mm focal length cylindrical fast axis focusing lens. L3 ( f= 100 mm) couples the zero order beam to an OSA.*

### 3.3.2 Output power and beam quality

The light current characteristics of the tapered diode laser bar have been plotted both under free running and the spectral beam combining mode. Figure 3.5 shows the comparison of the output powers in both mode and the variation of the beam quality of the laser in the SBC mode at different operating currents. At 30 A of operating current, the laser bar clocked over 9 W of output power and at 35 A the power went up as high as 11 W. The laser threshold was measured to be 5 A. The light current characteristics of the combined beam gives a slope efficiency of 0.37 W/A.

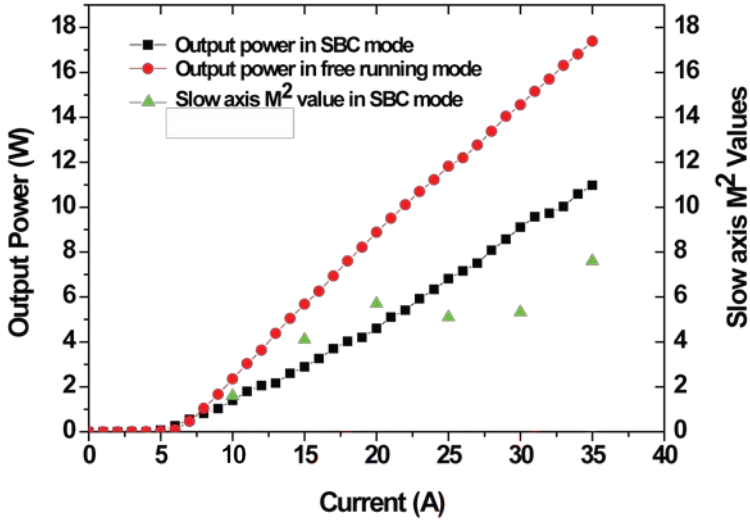


*Fig. 3.5. Variation in the output power and beam quality of the tapered diode laser bar with respect to input current.*

The system exhibits a spectral beam combining efficiency of 63% compared to a free running laser bar. The efficiency is partly limited by the first order diffraction efficiency of the grating which is 85%. Even at high currents, the curve doesn't show any signs of thermal roll over. The beam quality of the output beam has also been measured. The slow axis $M^2$ value was measured to be 5.3 at 30 A and 7.6 at 35 A. These values are comparable to that obtained from a single tapered emitter on the same bar at respective current levels. The

slight mismatch should be due to the smile of the laser bar which leads to an imperfect overlap of the beams. All measurements were made at $1/e^2$ level.

Figure 3.6 (a) shows the profile of the output beam at the focus of a 100 mm achromatic lens and (b) shows the far-field profile of the output beam at 30 A. The focus of the beam is near-Gaussian while the far-field is non-Gaussian which is typical for the far-field of tapered diode lasers [58].

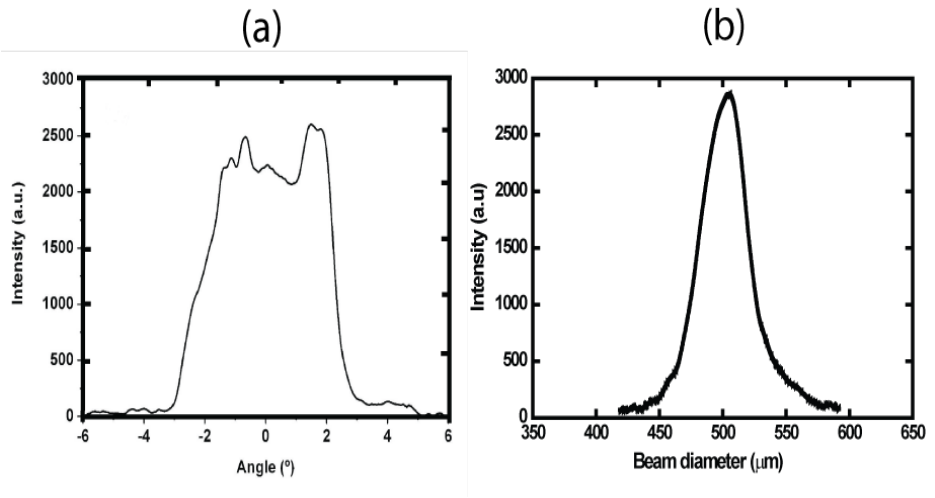


*Fig. 3.6. (a) Profile of the output beam at the focus of a 100 mm achromatic lens. (b) Far field profile of the output beam.*

### 3.3.3 Spectrum and tuning:

The external cavity has been designed for supporting an emission with a wavelength spread of 4 nm between individual emitters as defined by equation 3.1. The actual wavelength spacing was measured to be 4 ± 0.005 nm which matches the numerical value. The total wavelength span of 12 emitters is approximately 44 nm. Figure 3.7 shows the spectrum of the combined output beam at an operating current of 30 A. Intensity variations among the emitters are due to the variation in the power coupled into the OSA fibre.

The spectral tuning of the output beam was limited to approximately 3-4 nm towards both directions due to the limited gain band-width of the laser. Beyond that, the feedback from the output coupler was not strong enough to force the emitters to operate at the wavelength determined by the external

cavity. As a result, side peaks started to appear and the number of main peaks that correspond to emitters on the laser bar reduced. The line width of the individual emitters in the combined mode was observed to be considerably narrower compared to that of the free running laser bar. In the free running mode the line width of the emitters varied between 0.5- 1 nm where as in the SBC mode, it reduced to 30-100 pm.

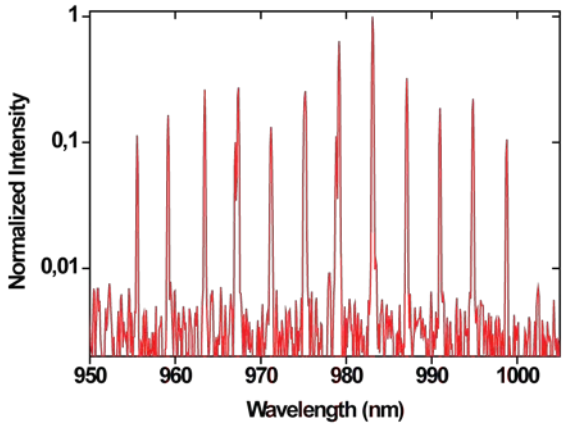


*Fig. 3.7. Wavelength spectrum of the output beam at 30A. The laser temperature was maintained at 20°C.*

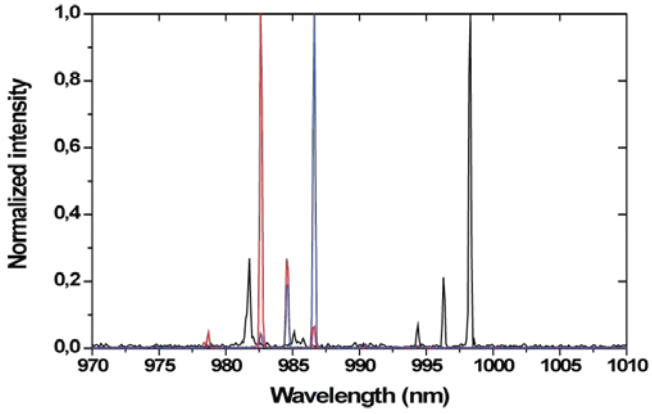


*Fig. 3.8. Wavelength spectrum of the smiley emitters on the tapered diode laser bar. I = 30 A, T = 20 °C. The side peaks are clearly visible in the spectra of these smiley emitters.*

Inspection of the near field images formed from the zero order beam reflection by the grating revealed that, nine out of the twelve emitters were perfectly locked while three emitters on one side showed single side peaks due to imperfect locking. Figure 3.8 gives an insight to the imperfect locking of the smiley emitters. A few side peaks are clearly observable which could possibly due to the smile of the laser bar.

### 3.3.4 Discussion

Spectral beam combining of tapered diode laser bars are of great interest due to the fact that the individual emitters on the bar are capable of delivering high output powers with a good beam quality. Even though fewer works have been recorded on providing external feedback to tapered bars, the recent achievements in this area are promising. Recently, Paboeuf et al., [59] coherently combined an array of ten index guided tapered laser diodes in a Talbot cavity and achieved 1.7 W of output power. As gain guided tapered diode laser bars could deliver even higher output powers, this work has its own significance and to my best knowledge, it is the first attempt to incoherently combine the emitters on a gain guided tapered diode laser bar.

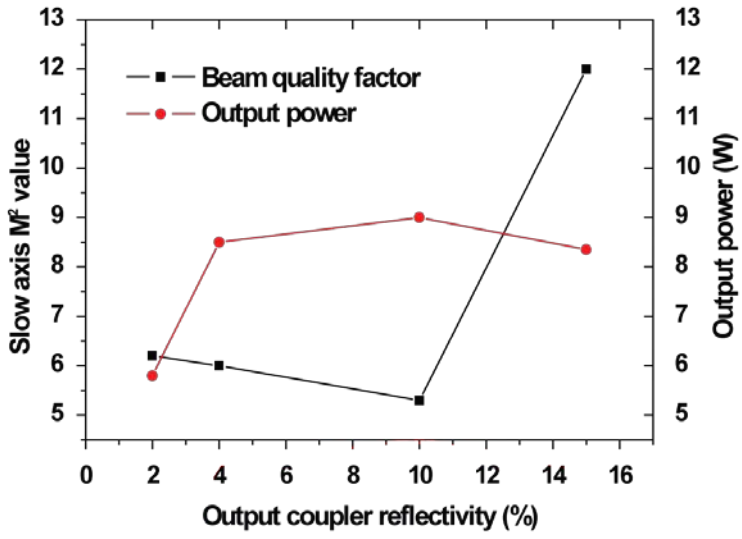


*Fig. 3.9. Variation in the slow axis beam quality and output power of the combined beam with the change in the reflectivity of the output coupler. I = 30 A.*

The experiments were repeated using output couplers of different reflectivity in order to optimize the feedback strength of the setup. With the output couplers of reflectivity below 10%, it was not possible to lock all the emitters on the laser bar especially the ones at the edge of the bar that suffer from the smile. Figure 3.9 shows the variation in the output power and the beam quality with respect to output coupler reflectivity. The one with 10% reflectivity proved to be the best in terms of both beam quality and power.

To summarize the results, 9 W of output power has been achieved from a 12 emitter gain guided tapered diode laser bar with a slow axis beam propagation factor of 5.3 at 30 A of operating current. The beam combining efficiency was measured to be 63%. Results related to this experiment have been reported in article **1** in the appendix.

### 3.4 Spectral beam combining of individual DBR-tapered diode lasers

Another important aspect of spectral beam combining is the power scalability. Two or more lasers running at moderate output power levels could be combined by an external wavelength selective element using this technique so that the combined emission clocks a higher output power level. This solves the problems associated with excess heat generation when lasers are operated at higher power levels. Power scaling is simply done by increasing the number of the individual lasers. Spectral beam combining does not require precise control of the wavelength and the phase of the gain elements compared to coherent beam combining techniques. This sub-section deal with the spectral beam combining of two DBR-tapered diode lasers which results in an output power levels of several watts with good beam quality.

The DBR tapered diode lasers used in this work consists of a distributed Bragg reflector coupled to the back facet of the laser to enhance the spectral selectivity of the laser. These devices have separated electrical contacts of RW section and tapered section, which were implemented to control output power, beam quality, and spectral behaviour independently. A brief description of the diode layer structure is given in the section 2.2.6. The emission wavelength of the material is 1058 nm. The reflectivity of the front facet was 0.5% and the rear facet has a reflectivity $5\times10^{-4}$ which was chosen to prevent unwanted feedback of higher order lateral modes propagating mainly outside the ridge.

This helps in the further improvement of the beam quality of the laser. Further information regarding the material structure, development and characterization of these devices could be found in [32].

Several works has been reported on the SBC of fibre lasers using volume Bragg gratings. Sevian et al [60] reported 750 W of cw power with near diffraction beam quality combining five different fibre lasers. 522 W of output power with a combining efficiency of 93% has been demonstrated with fibre lasers combined using a surface grating [61]. Over 2 kW of power was shown using fibre lasers with a combining efficiency of 61% [62]. Considering lower power operations, Sheng-bao et al [63] combined two low power solid state laser pumped fibre lasers and achieved 0.64 W with a combining efficiency of 69.6%.

### 3.4.1 Experimental setup

The setup consists of two DBR–tapered diode lasers, collimation optics and a reflective volume Bragg grating (VBG). The laser was mounted p-side up on a CuW heat spreader which itself is mounted on a conduction cooled package (CCP) mount allowing for efficient cooling. As the lasers are quite sensitive to temperature variations, active temperature control was necessary using thermo electric coolers. The fast axis of both lasers were collimated using aspheric lenses with a numerical aperture of 0.68 and a focal length of 3.1 mm and the slow axis using cylindrical lens of focal length 15 mm. The intrinsic astigmatism associated with the tapered geometry could thus be compensated. The reflective volume Bragg grating exhibits diffraction efficiencies close to unity when the Bragg condition is satisfied and close to zero at multiple points offset from this condition. The VBG used in this setup has dimensions of (3.4×10×10) $mm^3$ has an average diffraction efficiency of 99.2% at 1062 nm and a spectral selectivity of 0.3 nm (FWHM). The schematic diagram of the experimental setup is being show in figure 3.10.

In this setup, one of the lasers is operating in a transmission mode. i.e., the laser beam incident on the VBG is transmitted through it. The second laser is operated in the diffractive mode. This laser is diffracted by the VBG. By carefully adjusting the wavelengths of emission and the angle of incidence of the diffractive laser beam on the VBG, collinear propagation of both the

transmitted beam and diffracted beam could be achieved. This results in an output beam with a beam quality comparable to that of the individual emitters used and with a combined output power of both lasers.

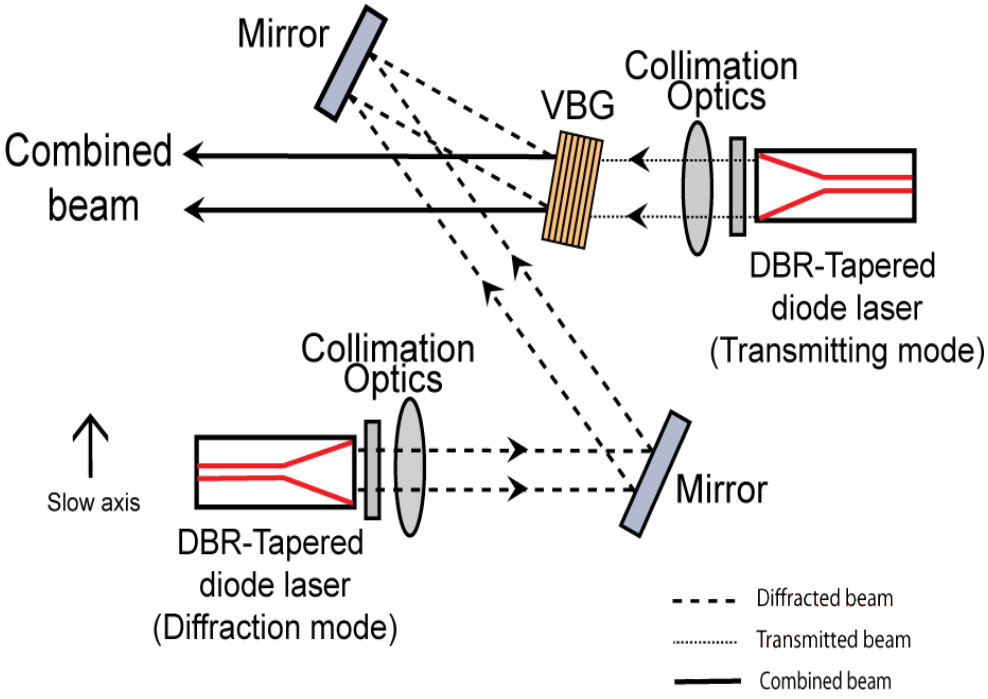


*Fig. 3.10. Schematic of the spectral beam combining setup of two DBR-tapered diode lasers The beam transmitting the grating is indicated by dashes, the diffracted beam by dots. The arrows display the direction propagation of the beams.*

### 3.4.2 Output power and beam quality

The experimental setup has been characterized in terms of output power and beam quality. Figure 3.11 shows the light current characteristics of the individual lasers. The ridge sections of both lasers were maintained at an operating current of 300 mA. In the free running mode, both the transmitting lasers emitted 9.11 W of output power and the diffraction laser emitted 8.05 W at a tapered section current of 14 A. The difference in the output is mainly due to the different operating temperatures for the selection of suitable wavelengths. The transmitting laser was operated at 15.47 °C while the diffracting laser at 23.0 °C. The combined output at the same current level was measured to be 16.08 W. This results in a spectral beam combining efficiency of 93.7%.

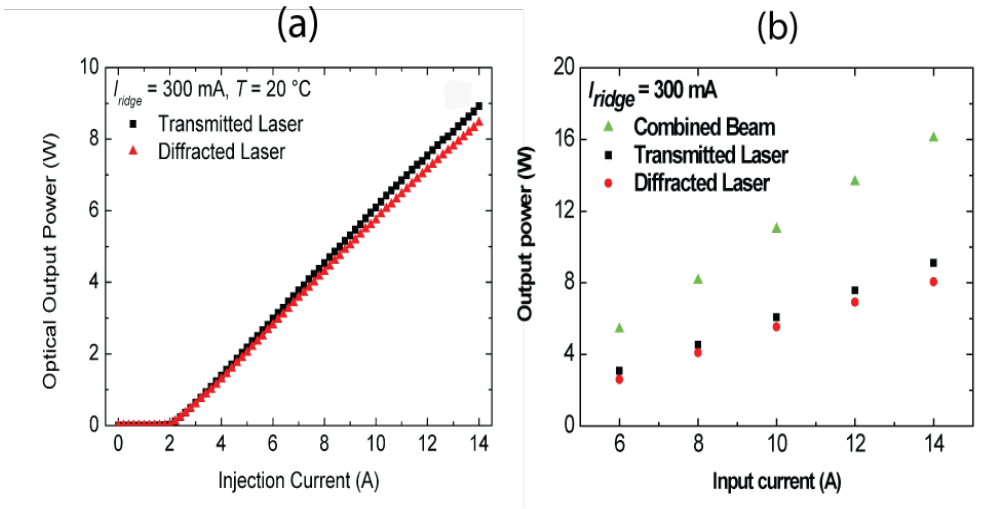


*Fig. 3.11. (a)Light current characteristics of the individual lasers. (b)The SBC output powers at various taper currents. The ridge current was maintained at 300 mA.*

The spectral beam combining efficiency varies slightly with the operating current levels. The lower efficiencies in high-power regimes are usually connected with a slight degradation of laser parameters rather than deteriorating grating parameters [64]. The figure 3.12 shows the variation in the beam combining efficiency with respect to the change in operating (taper) current. The beam propagation parameter of the combined output beam was measured to be 1.8 (fast axis) and 3.3 (slow axis). These values are comparable to those obtained from the individual lasers at the same current under free running mode. Figure 3.13 shows the variation in the beam diameter of the combined output beam with respect to the distance along the axis of the beam propagation at 14 A of taper current. The $1/e^2$ values of the beam width have been measured in both cases. A perfect overlap of the beams from both emitters was assured by the lack of any double peaks in the caustic. This ensures good spectral beam combining.

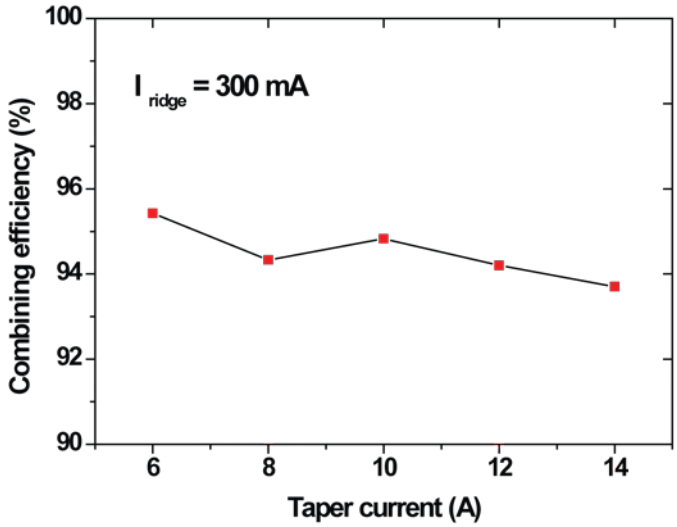


*Fig. 3.12. SBC efficiency versus taper current.*

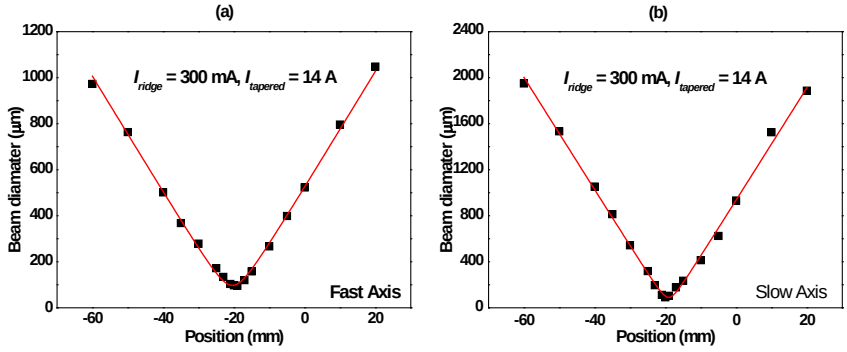


*Fig. 3.13. Caustic of the combined beam at injection currents of 300 mA to the ridge section and 14 A to the tapered section for both lasers.(a) Black dots represent experimental data and red lines represent numerical fit.*

### 3.4.3 Spectral behaviour

During the experiment, optimal beam combining was achieved by properly tuning the wavelength of emission of the lasers and by adjusting the incidence angle of the beams on the grating. The spectral tuning could be done in two

ways. By adjusting the injection current or by adjusting the laser temperatures. In the former case, a red shift of 0.02 nm/A was measured and in the latter, a red shift of 0.09 nm/°C was observed.

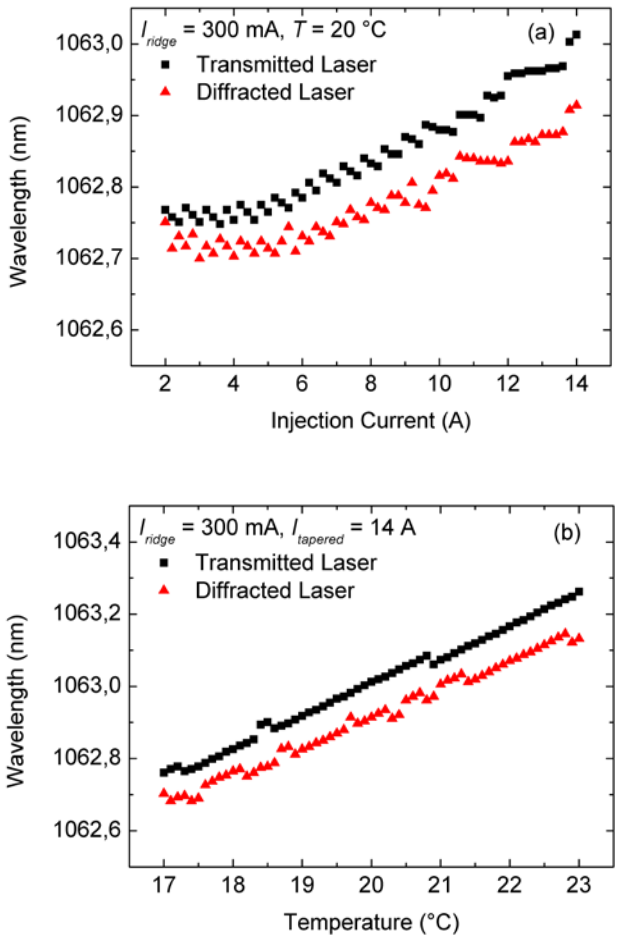


*Fig. 3.14. (a) Wavelength versus injection current of DBR-tapered diode lasers at 300 mA to the ridge section and operating temperatures of 20 °C. (b) Wavelength versus temperature of the same lasers at 14 A to the tapered section.*

Figure 3.14 shows the spectral tuning of the lasers in detail. The temperature tuning results in a wavelength separation of 0.5 nm between the lasers. The wavelength spectrum of the combined output beam is displayed in figure 3.15.

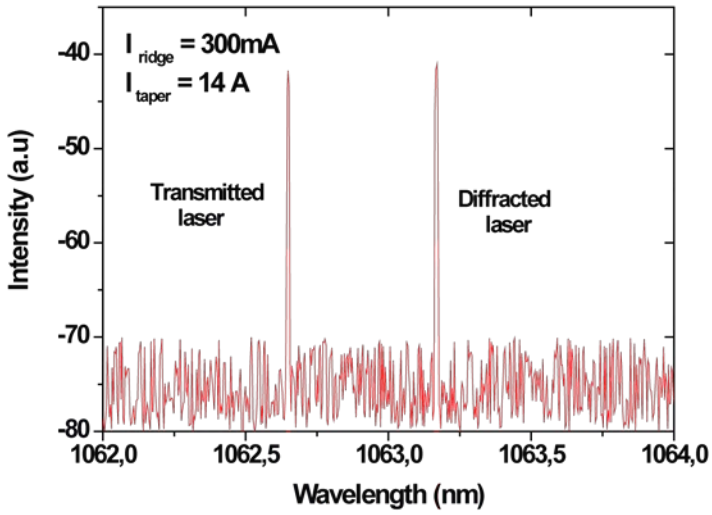


*Fig. 3.15. Optical spectra of the combined laser output at 14 A to the tapered section.*

### 3.4.4 Discussion:

This work demonstrates power scaling using multiple DBR-tapered lasers. A combined output power of 16 W has been achieved using two emitters. This technique has been demonstrated previously using multiple fibre lasers as cited in the literature [60] [61] [62] [63]. But compared to fibre lasers, diode lasers are capable of emitting lower output powers but with much higher conversion efficiencies. Regarding the size of the system, diode lasers also offers a much more compact light source compared to a fibre based light source. Hence, the incoherent beam combining using individual DBR-tapered diode lasers are quite significant and it opens up future possibilities for simple, power efficient and compact light sources which could deliver multiple tens of output power with good beam qualities.

Comparing the spectral beam combining of single emitters with that of diode laser arrays or bars, the latter has a clear advantage of being able to deliver higher output powers. Such systems are also much more compact

compared to those with single emitters. But challenges such as the ‘smile’ associated with the laser bar could limit the beam quality of the bar from being very close to that of the single emitter beam quality of the same bar. Moreover, when it comes to the beam combining of single emitters, one has more flexibility in terms of the optical alignment of the diode axes and hence it is easier to adjust certain laser parameters which in case of laser bars are somewhat rigid. Another important advantage in using single emitters is that the lasers could be controlled individually and even if one emitter fails, it is quite easy to replace it with a new one which is impossible in the case of a laser bar. Thus the SBC of individual good beam quality emitters could lead to high power good beam quality emissions which have numerous potential applications. Results related to this experiment have been reported in article **2** in the appendix.

# CHAPTER 4

# OFF-AXIS SPECTRAL BEAM COMBINING

## 4.1 Motivation

As discussed in the earlier section, spectral beam combining is an efficient technique for improving the beam quality of laser bars. However, the improvement is limited by the inherent beam quality of a single emitter on the bar. Hence, a new technique has been investigated which is a combination of spectral beam is combining as discussed in chapter 3 and lateral mode selection technique discussed in section 2.2.1. This new technique called off-axis spectral beam combining (OASBC) allows further improvement of the beam quality of a laser bar beyond the single emitter beam quality. OASBC has been applied to a broad area diode laser bar which results in a slow axis beam quality which is 5-6 times better compared to a free running single emitter on the bar. This work also resulted in a record spatial brightness level ever to be achieved from a broad area diode laser bar.

## 4.2 Transverse mode selection

High power broad area diode laser bars are reliable, compact and cheap candidates for applications such as cladding pumping of fibre amplifiers [65], graphics marking [9] etc. These devices display very high wall plug efficiencies even up to 76% [2]. Despite the high output power levels, their spatial brightness is considerably low due to a high divergence along the slow axis direction. Several techniques have been investigated by different research groups in order to improve the spatial brightness of the broad area laser bars by improving the slow axis beam quality. One such approach applied on a broad area laser array is using an external cavity providing off-axis feedback to all the emitters in the array [66]. The use of mode apertures, phase masks [67] and phase conjugation [68] has already been reported. The broad area laser bar in general, shows a bi- lobed far field profile [37] [67] [69] [70] **[**71**]** due to coupling of the emission in to an out of phase super mode. Hence, a single

lobed out of phase output mode could be achieved by designing an external cavity feedback system with an angular selectivity. Several approaches have been made using broad area lasers and bars in such off-axis external cavities by different groups. Wolff et al [22] made a theoretical and experimental study of the lateral mode selection of a broad area diode laser in a Fourier optical external cavity to show that transverse modes can be selectively excited up to pump currents more than 200% above the laser threshold. Chi et al [72] improved the $M^2$ value of a 1000 microns wide BAL by a factor of 107 using self injection locking. Jechow et al [55] used a broad area stripe laser bar in an "off-axis" external resonator arrangement, to obtain 10 W of output power with a slow axis $M^2$ value less than 3. In these works, the out of phase mode in the far field of the broad area lasers or arrays have been stabilized using the angular selective external cavity. Thus a single lobed improved beam quality operation of the broad area laser/ array has been achieved.

Even though spectral beam combining [49] which has been explained in the previous chapter could also be applied for improving the beam quality of a broad area laser bar, it is often limited by the fact that the best possible beam quality one could expect from SBC is comparable to the beam quality of a single emitter on that particular laser bar. Hence, in the case of a broad area laser bar consisting of broad area elements with inherently poor beam quality, SBC would not prove to be much of a help. However, for applications that involve coupling the emission for a laser bar into a multi mode fibre, the improvement in the beam quality to a level comparable to that of a single emitter would be good enough. In case one requires any further improvement in the beam quality, off-axis spectral beam combining becomes very interesting. This technique combines the advantages of spectral beam combining and the lateral mode selection techniques and in turn leads to a resultant beam quality in laser bars which is several times better than the beam quality of the individual emitters. Vijayakumar et al [39] improved the beam quality of a broad area diode laser bar 5-6 times compared to the free running single emitter. Jensen et al [73] used OASBC on a segmented broad area diode laser and made an improvement in the slow axis beam quality of a factor of 3.4 compared to the single emitter.

### 4.3 Off-axis spectral beam combining of a broad area diode laser bar

A brief description of the 150 microns wide 19 emitter 980 nm broad area diode laser bar has been given in section 2.2.6. The device has been provided by Fraunhofer ILT, Germany. This device is anti-reflection coated (R<0.01%) on the front facet in order to prevent the lasing within the diode structure. Thus it prevents parasitic self lasing while operated in an external cavity mode. The beam qualities of the individual emitters were measured. The beam propagation factors along the slow axis were found to be around 30- 35. For the entire laser bar the slow axis $M^2$ value was measured to be approximately 1580. The fast axis was nearly diffraction limited. At all current levels, only 12 out of 19 emitters were found to be emitting. The fast axis of the laser bar has been collimated using a 910 microns focal length 0.8 numerical aperture *LIMO* micro lens attached to the heat sink of the laser. In the free running mode, the laser produced 3 W of optical output power at 30 A of operating current. Such a low output power is attributed to the high quality anti reflection coating used on the front facet of the laser. A similar laser bar with a standard anti-reflection coating, which has a residual reflectivity of approximately 5%, used for comparison gave an optical output power of 22 W at 30 A of operating current. Figure 5.1 shows the near field image of the laser bar obtained by focusing the output light using a 100 mm achromatic lens.

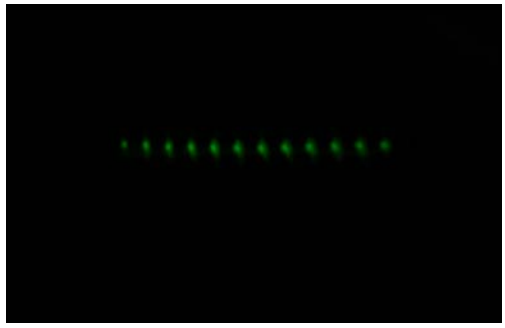

*Fig. 5.1. Near field image of the broad area diode laser bar at I =10A.*

#### 4.3.1 Experimental setup

The experimental setup for the off-axis spectral beam combining (OASBC) consists of the fast axis collimated laser bar, a 100 mm slow axis collimating cylindrical lens, a 1200 lines/mm gold plated reflection grating with 95%

diffraction efficiency in the first order around 980 nm, a D shaped sharp edged highly reflective mirror, a spatial filter, and a 10% reflective plane output coupler. The figure 5.2 shows the schematic of the experimental setup. This configuration is very similar to a standard spectral beam combining setup as shown in figure 4.3 except it consists of a high reflective element and a spatial filter. The high reflective D shaped mirror mounted on a custom mirror mount provides the angular selectivity in the feedback in this cavity. A part of the output beam is sent to a beam profiler to measure the beam quality. All the lenses are AR coated around the operation wavelength.

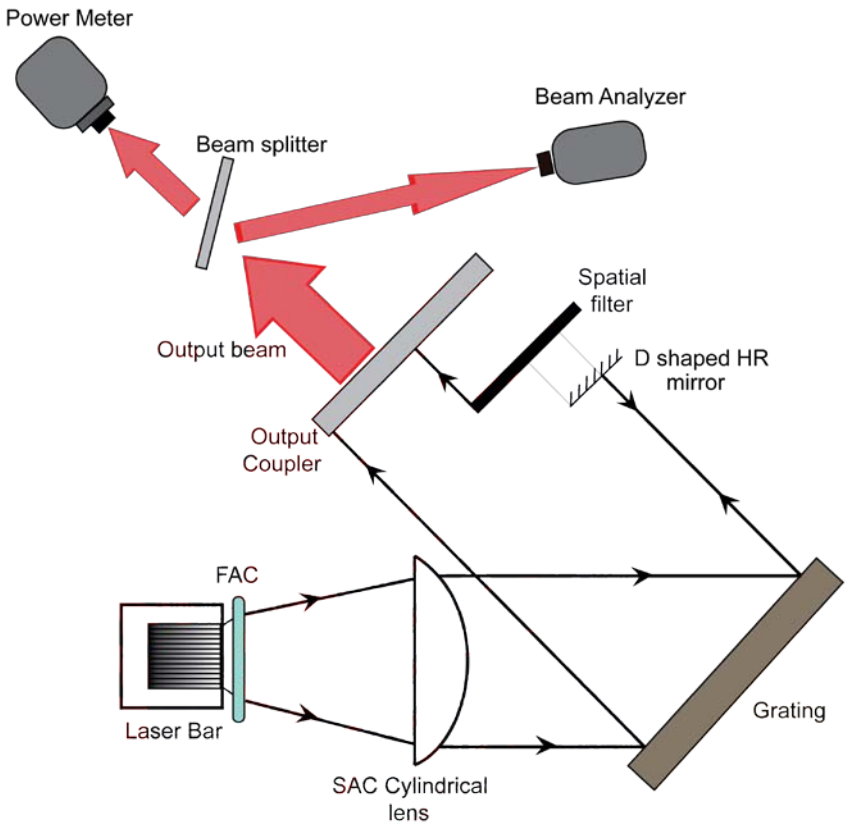


*Fig. 5.2. The experimental setup of OASBC. The SAC lens is a Fourier lens which superimposes the light from different emitters on the grating. The diffracted light is fed back using the output coupler and in addition to this, a few spatial modes from the bi lobed far field of the laser bar is also fed back to the laser using the high reflective mirror.*

In this configuration, the reflection grating is placed on the Fourier plane of the slow axis collimation lens and slow axis collimation lens makes the light from different emitters superimpose on the reflection grating. The angle of incidence of the beam onto the grating was approximately 52°. The first order diffracted beam is fed back into the laser using the output coupler as in a SBC setup. In addition to this, as the broad area laser bar produces a twin lobed intensity profile in the far field, the high reflective sharp edged mirror selects a few spatial modes from one of the two lobes and feeds them back into the laser. Thereby selectively suppressing the lower order spatial modes and amplifying the higher order modes [22]. Thus a single lobed emission of the broad area laser bar with a good beam quality has been achieved. The spatial filter helps filtering any residual side peaks in the emission.

The single lobed emission could be stabilized by properly selecting the feedback angle of the high reflective mirror. This twin feedback configuration helps improving the slow axis beam quality of the broad area diode laser bar. In ordinary SBC, the beam quality of the output beam cannot be better than that of a single emitter beam quality while this in this technique, the beam quality of the combined beam can be improved even further, i.e., to a quality exceeding the beam quality of a single emitter. The experimental results observed using this configuration follows.

### 4.3.2 Output power and beam quality

The broad area diode laser bar produced 9 W of output power at an operating current of 30 A. The slope efficiency was measured to be 0.38 W/A with a threshold current of approximately 5 A. The laser temperature was stabilized at 20°C using a thermo-electric temperature controller. Figure 5.3 shows the light current characteristics of the broad area diode laser bar in both the free running mode and the off-axis external cavity mode. The low power emission in the free running mode is due to the good antireflection coating on the laser front facet. A similar laser bar with a standard antireflection coating produced over 22 W at the same input current level. The beam propagation parameters of the output were measured using a Nanoscan beam profiler (*Photon Inc.).*

The $M^2$ values of the external cavity laser along the slow and the fast axes were measured to be 6.4 and 1.9 respectively. Compared to the values

obtained with individual emitters on the same laser bar, an improvement of 5-6 times were observed in the slow axis beam quality thus making OASBC useful in achieving beam qualities better than that of single emitters. This proves to be a great advantage over regular spectral beam combining. Figure 5.4 shows the caustic of the output beam along the slow axis and the beam profile at the focus of a 100 mm achromatic lens. A slight astigmatism could be noted in the figure. The $1/e^2$ values of the beam widths have been measured throughout the experiments.

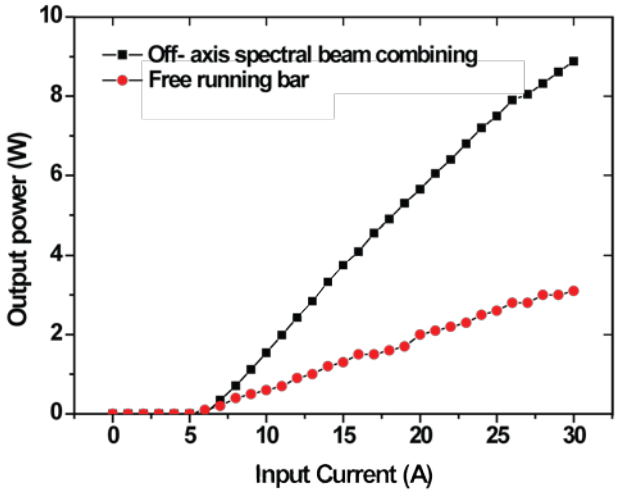


*Fig. 5.3. Light current characteristics of the broad area diode laser bar. Laser temperature stabilized at T= 20°C.*

Further investigations on the off-axis spectral beam combining by Jensen et al., [74] proves that compared to ordinary spectral beam combining, the beam quality of the combined beam depends less critically on the position of the dispersive element in the setup. In SBC, the dispersive element must be placed on the Fourier plane to ensure a perfect overlap of the light from individual emitters. However, in this approach using the off-axis mirror, dispersive element could be displaced by at least 50% of the focal length of the collimating lens away from the Fourier plane without compromising the performance of the external cavity. This opens up the possibility to build even more compact off-axis systems than before.

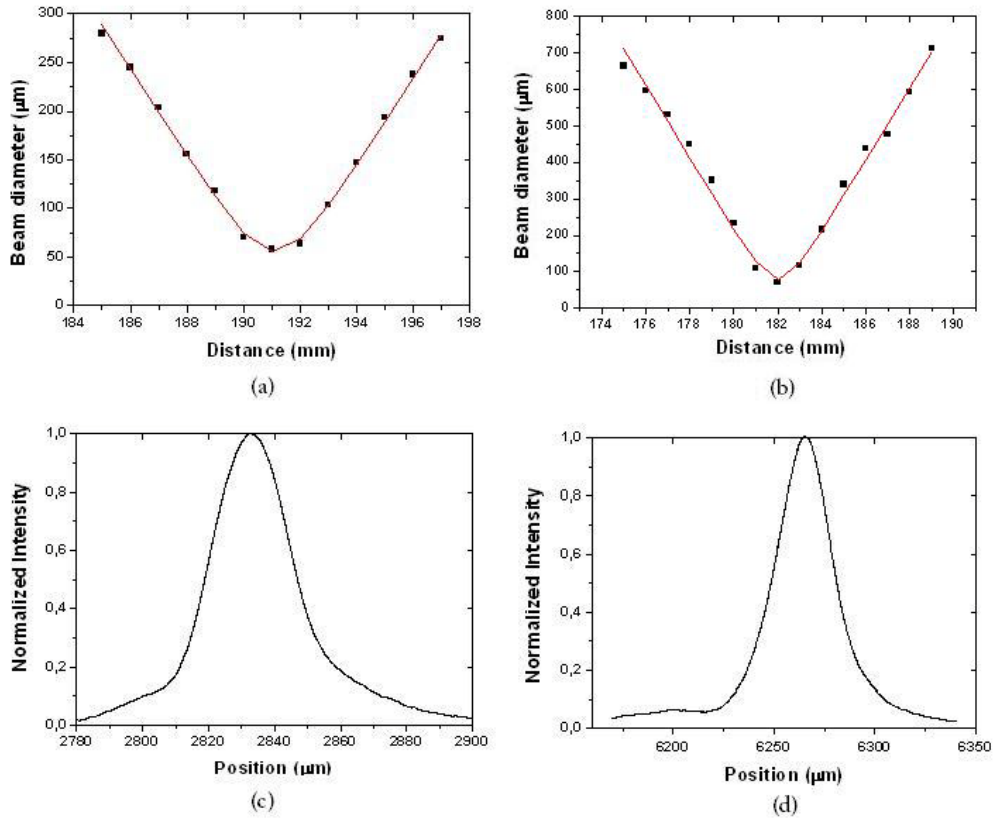


*Fig. 5.4. (a) Caustic of the output beam along the fast axis. (b) Caustic of the output beam along the slow axis. (c) Fast axis beam profile at the focus of a 100 mm achromatic lens. (d) ) Slow axis beam profile at the focus of a 100 mm achromatic lens*

### 4.3.3 Spatial brightness

A brief description on the spatial brightness is given in section 2.5.1. The improvement in the spatial brightness of the broad area diode laser bar in the OASBC experiment is quite noticeable. At 30 A in the free running mode, the 19 emitter laser bar with a standard anti- reflection coating displayed a spatial brightness of 2.3 MW/cm$^2$-str. This value is quite low even though the output power is as high as 22 W. This is due to a bad beam quality along the slow axis. The calculation of the spatial brightness has been done based on the equation 2.19. In the off-axis external cavity mode, the good anti reflection coated laser bar displays a spatial brightness of 79 MW/cm$^2$-str. To the best of my

knowledge, this represents the highest spatial brightness ever achieved from a broad area diode laser bar.

### 4.3.4 Spectral behaviour

The off-axis external cavity laser has been characterized in terms of spectral behaviour as well. As in general spectral beam combining, the wavelength spectrum of the output beam consists of 12 equally spaced main peaks which correspond to the emitters on the bar. Figure 5.5 shows the wavelength spectrum of the output beam.

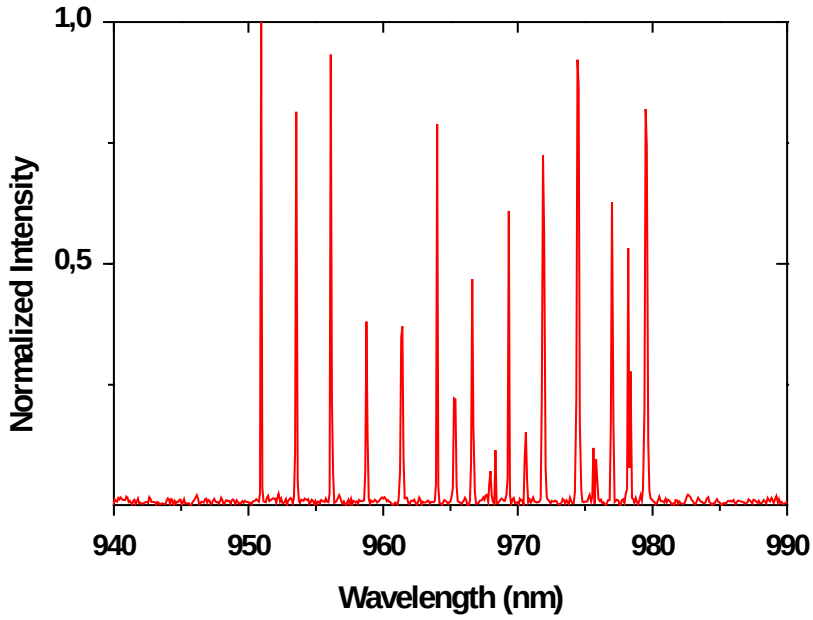


*Fig. 5.5. Wavelength spectrum of the output beam. T=20°C.*

The external cavity has been designed for a wavelength separation of 2.56 nm between the emitters. This value is quite close to the experimentally observed value of 2.67 nm. However, a few side peaks were also observed in the spectrum which could possibly due to slight misalignments of the system which could lead to an imperfect overlap of the beams from all the emitters on

the grating surface. The output wavelengths were found to be in the range from 950 nm to 980 nm with a centre wavelength of approximately 965 nm.

### 4.3.5 Discussion

A high power near infra red external cavity broad area diode laser bar which exceeds a single emitter beam quality has been demonstrated in this work. The high brightness of such a laser system could be very interesting for certain applications such as cutting or marking of certain polymers. Experiments were also made to optimize the system performance by changing the feedback strength of the setup. Figure 5.6(a) shows the variation in the output power with respect to the output coupler reflectivity and Fig 5.6(b) shows the change in the beam quality of the system with respect to the output coupler reflectivity.

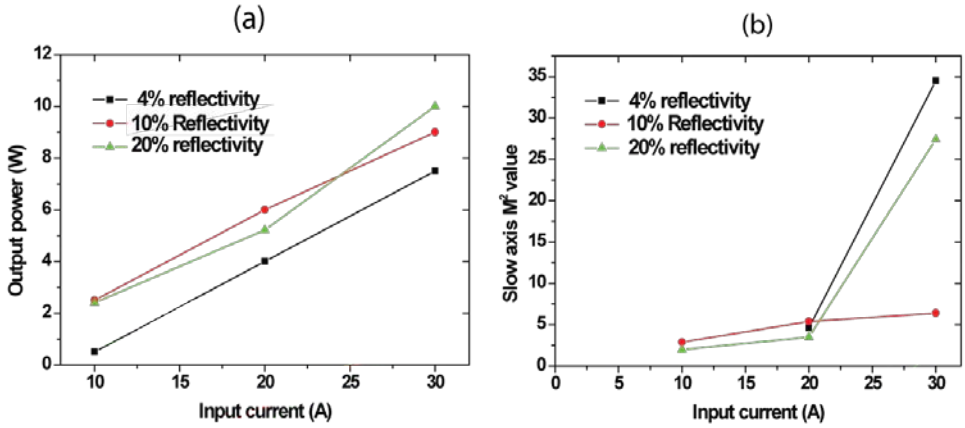


*Fig. 5.6. (a) Change in the output power with the output coupler reflectivity at different current levels. (b) Change in the slow axis beam quality with the output coupler reflectivity at different current levels.*

Output couplers of different reflectivity ranging from 4- 20% has been used for this purpose. With each value of reflectivity, there was a considerable change the output power and beam quality of the output beam. The system shows the best performance with the output coupler of 10% reflectivity. The beam quality of the output beam from the setup with different output coupler reflectivity tends to be comparable at currents up to 20 A. Above that level, a steady degradation in the beam quality was observed.

To summarize the results, 9 W of optical output power has been obtained from a 12 emitter broad area diode laser array in an off axis spectral beam combining cavity: The beam quality factors was measured to be 1.9 and 6.4 along the fast and slow axis respectively. The system delivers a high spatial brightness of 79 MW/cm$^2$-str. Results related to this experiment has been reported in article **3** in the appendix. As mentioned in the earlier sections, moderate power level diode lasers with spatial brightness of the order of several tens of MW/cm$^2$-str are interesting when it comes to material processing in polymers [9]. Experiments were performed using the output beam to see how the focused laser light interacts with certain polymer materials, aluminium and solder. More details about these tests are given along with the discussion towards the end of this thesis.

# CHAPTER 5

# TALBOT EXTERNAL CAVITY

## 5.1 Motivation

So far, incoherent beam combining techniques have been discussed in this thesis. The output beam consisted of several spectral peaks which may not be desirable for wavelength specific applications. In that context, passive phase locking is of great interest. Coherent operation of a 12 emitter gain guided tapered diode laser bar has been achieved by passive phase locking using Talbot effect which lead to 2.45 W of coherent wavelength narrowed emission. This is the first time ever to my best knowledge, such a technique has been applied on a gain guided tapered diode laser.

## 5.2 Talbot effect

Talbot effect [75] is a pure diffractive phenomenon which was observed in 1836 by Henry Fox Talbot. It results in the self imaging of an infinite optical field source at integer distances termed as Talbot distance determined by the spatial extend or the period of the field and the wavelength of the light. It was Lord Raleigh who showed that Talbot effect is a natural consequence of Fresnel diffraction and the Talbot distance could be calculated as [76]

$$Z_T = \frac{2p^2}{\lambda}, \qquad 5.1$$

where $Z_T$ is the Talbot distance, $p$ is the period of the optical field and $\lambda$ is the wavelength of the light. The images formed due to this effect vary both in amplitude and in phase. Moreover, these images could also occur at fractional Talbot distances $Z_T/n$. At a half Talbot distance from the source, for the fundamental mode ($n$ =1), the optical field distribution maintains its phase but shows a shift in the lateral position by a factor of half the period. The highest mode ($n = N$) where $N$ is the number of emitters would reproduce the same intensity pattern as the source with the exact lateral positions. Thus there is

some inherent mode selectivity in this phenomenon which could be useful in the coherent combining of laser arrays.

In an external cavity diode laser bar based on Talbot effect, the mode selectivity could be used for the operation of the laser bar in an in phase ($n$ =1) mode or an out of phase ($n = N$) mode by employing an angular feedback element placed at the Talbot distances. The feedback element could be a mirror or even a wavelength selective element such as a volume Bragg grating. In a cavity of round trip distance equal to half the Talbot distance, the in phase fundamental mode produces similar images to that of the source but with a lateral shit of $d/2$. Here, $d$ is the pitch of the laser bar (the centre to centre spacing). Hence the feedback element would image it back into the laser which results in the superimposing these images on to the space between the emitter facets. This would result in very high cavity losses. But by tilting the feedback element by an angle of $\alpha = \lambda/2d$, we can select the in phase mode. Thus the angular selectivity of the cavity helps in the propagation of either the out of phase or the in phase mode at a time. Figure 5.1 shows the self imaging of the in phase and the out of phase modes at different fractional Talbot distances.

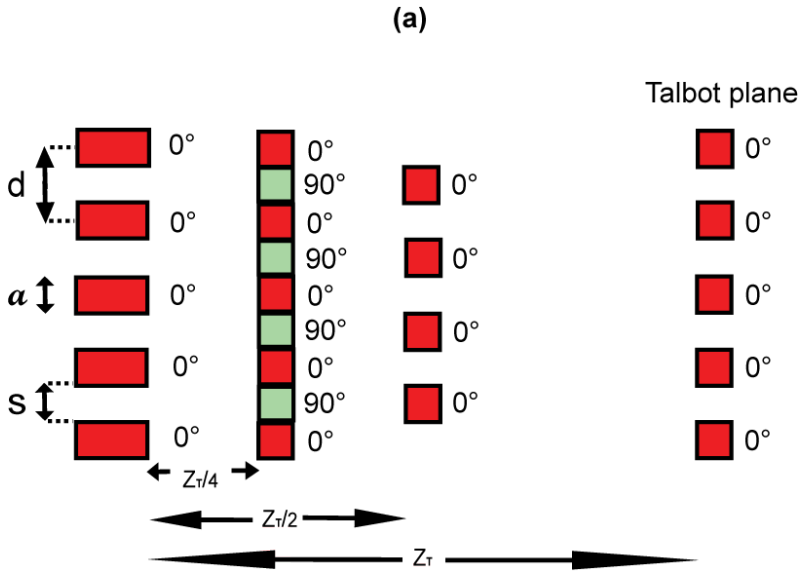

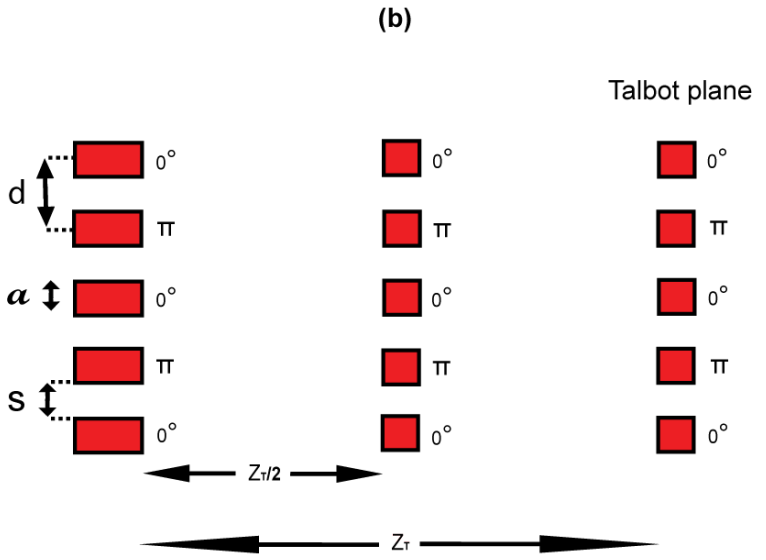


*Fig. 5. 1. Self imaging of modes in the fractional Talbot planes. (a) In phase mode. (b) out of phase mode. Red rectangles on the left side show a periodic optical field. The self imaging at different distances from the source is represented by the squares on the right side. Green square represents the image with a phase shift. For the in phase mode, at a quarter Talbot distance, the intensity pattern doubles the frequency with the adjacent peaks having a phase shift of 90°.*

Coherent operation of diode laser arrays in the Talbot cavity mode has been demonstrated by several research groups. In 2008, Liu et al [77] demonstrated 5.3 W of coherent optical power with a narrow line width of 0.1 nm from a broad area diode laser array in a V- shaped Talbot cavity. In 2010, they further improved their broad area diode laser array system using a feedback loop closed off-axis external Talbot cavity [78] which resulted in an optical output of 12.8 W with a line width of 0.07 nm. Huang et al [79] has demonstrated 7.2 W of CW power from a setup using an array of 10 slab coupled optical waveguide emitters with a mirror as the feedback element. Paboeuf et al [59] demonstrated coherent combining of an index guided tapered diode laser bar in a VBG based Talbot cavity setup with an output power of 1.7 W with a line width of 0.1 nm. Recent developments in the VBG technology have driven the researchers to employ these devices in the external cavity setups due to their wavelength selective nature. Narrow line width coherent emission could be possible using such setups.

## 5.3 Talbot cavity operation of a gain guided tapered diode laser bar

Gain guided tapered diode laser bars provides output powers of the order of several watts. Hence, the coherent operation of such a device in a Talbot cavity would be quite interesting. The tapered diode laser bar used in these experiments consists of 12 tapered emitters with a pitch spacing of 500 microns. The fill factor corresponds to 30%. This is also similar to the laser bar used in the spectral beam combining and spectral narrowing experiments described in chapter 4 and 7 respectively. A large pitch is due to the factors related to the heat management in high power laser bars. The front facet anti-reflection coating has a rest reflectivity of 0.1% and the laser bar is collimated on the fast axis with a cylindrical micro lens and custom collimated along the slow axis using 12 individual cylindrical micro lenses. As the laser bar showed a large smile, a phase plate based wave front correction has been done which compensates the smile and bow-tie effect observed along the fast axis. The smile observed on the laser bar amounts to 4.0 m.rad peak to valley, corresponding to 2.4 micron mechanical smile of bar. With the wave front correction, this value reduced to 0.9 m.rad peak to valley which corresponds to less than 0.6 microns of mechanical smile. The laser bar emits 8 W at an operating current of 25 A in the free running mode. The spectral width of the emission amounts to more than 5.5 nm. The laser has been temperature stabilized at 20°C using a thermo-electric temperature controller. The divergence of the smile corrected laser bar was 12 m.rad along the slow axis and 4 m.rad along the fast axis. The laser displayed an individual emitter $M^2$ value less than 2 along both the axes.

## 5.4 Experimental setup

The Talbot cavity length depends on the emitter pitch of the laser bar as explained by the equation 6.1. Hence in this case the Talbot distance was calculated as $Z_T$ = 520 mm. Considering the round-trip of the light beam in the cavity, A cavity length of $Z_T/4$= 130 mm is realized. This is due to the fact that, at the half Talbot plane, one could achieve a good selectivity between the in phase and the out of phase modes as evident from the figure 5.1.For the sake of the wavelength selectivity of the whole system, a VBG is used as the feedback mirror. The reflectivity of the VBG is 25% around 981 nm and it has a

bandwidth of 0.2 nm. The cavity length is much longer in this setup compared to the experiments described in [59]. This is due to an increased pitch length of the gain guided tapered diode laser bar. Thus the Talbot cavity consists of the smile corrected collimated tapered diode laser bar and the VBG as the feedback mirror. Figure 5.2 shows the experimental setup of the Talbot cavity.

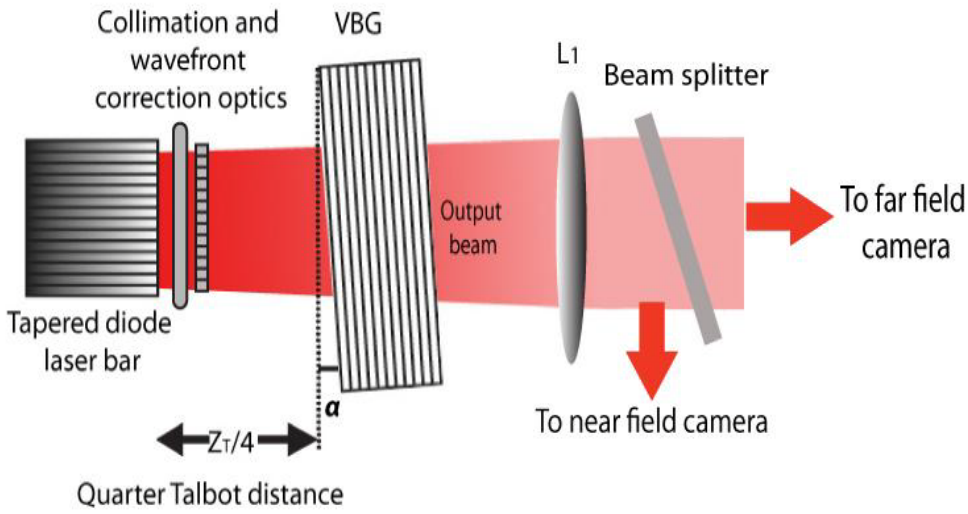


*Fig. 5.2. Schematic setup of the Talbot external cavity.*

The VBG has been mounted on a mirror mount and the coherent operation of the laser bar could be achieved by aligning the feedback in to the laser by rotating the VBG along the fast and slow axis which results in the phase locking between the emitters on the laser bar. The wave front correction done on the laser bar helps improving the coupling between the emitters by the external cavity feedback. By adjusting the angle of the feedback, one can achieve an in phase or out of phase super-mode emission from the laser bar.

### 5.5 Experimental results

Coherent phase-locked emission could be obtained from the Talbot external cavity. The far field of the output beam consists of an in phase super mode as shown in figure 6.3. It consists of a single high intensity peak surrounded by symmetrical side peaks. This is obtained by tilting the VBG at an angle of $\alpha$ =

$\lambda/2d$. When the angle $\alpha = 0°$, the out of phase mode could be observed in the far field profile which corresponds to two central peaks of equal intensity. The far field exhibits a narrow angular profile with a fewer number of peaks compared to the results demonstrated by Pabouef et al in [59]. This is due to a higher fill factor in the gain guided tapered diode laser bar compared to the index guided bar used in their experiments.

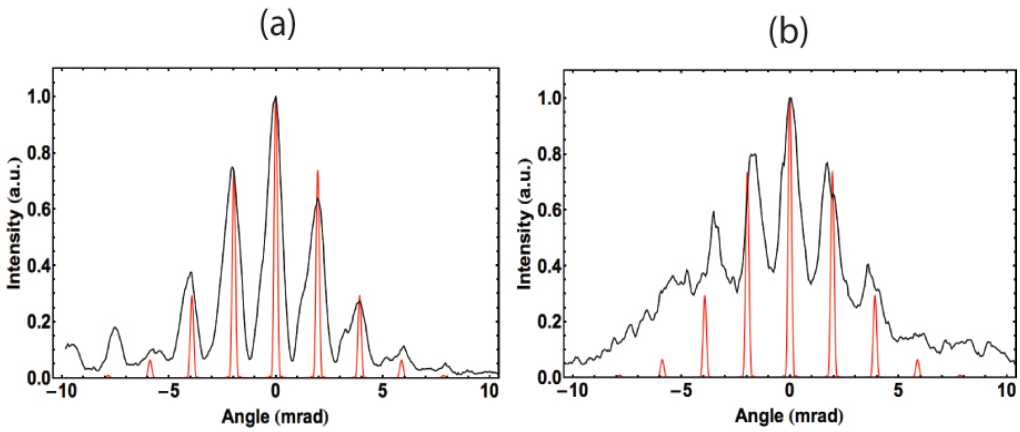


*Fig. 5.3. Far field profiles of the Talbot cavity output beam in the in phase mode of operation. (a) I= 5.5 A (laser threshold). (b) I= 15 A. The black curves show the experimental data and the red curve shows the numerical data.*

The diffraction limited red peaks in the far field profile correspond to the numerical simulations of this cavity. The thickness of the peaks is considerably lower compared to the experimental profiles. In the numerical simulations, the thermal effects, spatial hole burning etc. were not considered. These phenomena are responsible in the distortion of the phase in the laser which in turns broadens the far field peaks. The width of the numerical peaks corresponds to $2\lambda/Nd$. At 15 A, the experimental width of the peaks corresponds to ~ 1.2 m.rad. Above 20 A, the phase locking of the laser bar was not possible any more.

The $M^2$ value of an individual emitter on the laser bar is given by,

$$M^2_{em} = \frac{\Delta\theta}{\lambda}\pi w, \tag{5.2}$$

where $\Delta\theta$ is the $1/e^2$ half width of the far field profile, $\lambda$ is the operating wavelength and $w$ is the spatial extend of the laser bar. The $M^2$ value of the entire laser bar could be written as,

$$M^2_{coh} = \frac{2\delta\theta}{\lambda} Np\,, \tag{5.3}$$

where $\delta\theta$ is the full width of the far field peak at half maximum, $N$ is the number of emitters on the laser bar and p is the pitch spacing of the emitters on the bar. $\lambda/Np$ represents the diffraction limit. The calculated values of the beam quality parameters of both the individual emitters and the entire bar based of eqn. 5.2 and 5.3 are given in table 5.1. At 15 A with an output power of 2.45 W, the laser bar displays a slow axis $M^2$ which is almost 7 times the diffraction limit.

At the threshold current, the peaks in the far field show a good visibility whereas the visibility drops considerably at higher currents as evident from figure 6.3. This is due to the competition with the free running contribution of the tapered diode laser bar. Even though the laser has an anti-reflection coating of 0.1% reflectivity, it seems sufficient to support a high free running contribution at higher operation currents. If one could provide an anti-reflection coating which is significantly better than this, the visibility of the peaks at higher currents could be improved. The coherence of the laser is related to the fringe visibility in the far field profile by the simple equation,

$$V = \frac{(I_{max} - I_{min})}{(I_{max} + I_{min})}\,, \tag{5.4}$$

where $V$ is the visibility, $I_{max}$ is the maximum intensity of the peak and $I_{min}$ is the minimum intensity of the peak. The coherence of the laser decreases rapidly with the decrease in the visibility. A numerical calculation of the dependence of the coherence on the visibility is shown in figure 5.4. Experimentally obtained values of the fringe visibility of the far field profile and coherence of the output beam at different current levels is given in table 5.1. The light current characteristics of the laser bar in the free running mode and the VBG Talbot cavity mode is shown in figure 5.5. The laser bar in the Talbot cavity produced 2.45 W at an operating current of 15 A.

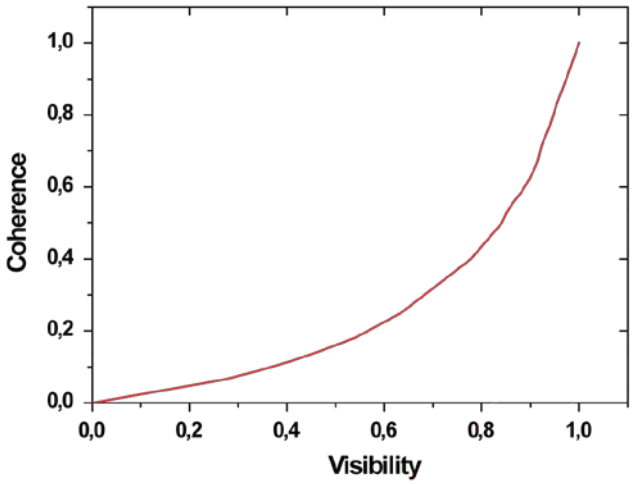


*Fig. 5.4. Variation in the coherence with respect to the fringe visibility in the Talbot cavity. A rather steep drop in the coherence could be noted with the reduction I the fringe visibility of the far field profile.*

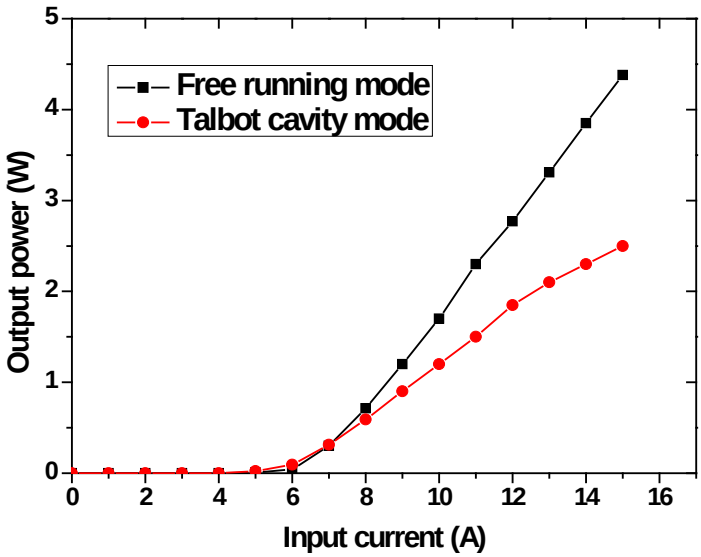


*Fig. 5.5. Light-current characteristics of the tapered diode laser bar in the free running and Talbot cavity modes.*

## 5.6 Discussion

At the threshold current levels, the total coherence was measured to be 62.5% which degraded to just 18% at a current level of 15 A. The gain guided tapered laser bar with a pitch of 500 microns leads to a long cavity length compared to many of the works referred above. But the emitters deliver higher output power which is quite an interesting fact to consider. With an anti-reflection coating significantly better than 0.1% reflective, it should be possible to suppress the free running contribution from the laser bar and hence to improve the coherence of the output beam at higher current levels. A detailed experimental and numerical analysis of tapered diode laser arrays in VBG Talbot cavities has been submitted by Lucas-Leclin et al. to JOSA-B. The article is titled "Volume Bragg grating external cavities for the passive phase locking of high-brightness diode laser arrays: a theoretical and experimental study". This has been listed as article **4** in the appendix. Recently, Paboeuf et al [80] reported a technique based on the coherent superposition of the light from 10 tapered diode emitters on a bar using a Dammann grating. This method opened up new possibilities to obtain majority of the output power from a Talbot cavity into a single lobed output beam which could be much easier to be coupled to an optical fibre for instance.

The experimental results regarding the fringe visibility, coherence etc. of the laser bar in the Talbot external cavity obtained from this experiment has been given in the following table.

| Wavelength (nm) | Current (A) | Reflectivity | Output power (W) | Fringe visibility | Coherence | $M^2_{em}$ | $M^2_{coh}$ |
|---|---|---|---|---|---|---|---|
| 980.5 | 5.5 | 25% | 0.12 | 90% | 62.5% | 2.11 | 5.26 |
| 980.5 | 12 | 25% | 1.60 | 65% | 27% | 2.05 | 5.20 |
| 980.5 | 15 | 25% | 2.45 | 54% | 18% | 2.18 | 6.85 |

*Table 5.1 Experimental results from the VBG based Talbot external cavity.*

Coherent combining using passive phase-locking technique such as a Talbot cavity is quite interesting in a context where high power narrow

wavelength emission is required. Beam combining techniques described in chapter 3 and 4 i.e., spectral beam combining, off- axis spectral beam combining respectively has an inherent drawback which is the wavelength spread of the combined output beam. When it comes to applications such as spin exchange optical pumping, non-linear frequency conversion (second harmonic generation) etc, which demand highly coherent narrow line width laser sources, these techniques fails to meet the requirements. On the other hand, passive phase locking offers a good solution to this problem. Compared to active phase locking which is commonly used in fibre lasers, a passive setup includes less complexities and no electronic control loops. Thus, Talbot cavities in combination with wavelength selective volume Bragg gratings could be considered as a promising technique for the generation of moderately high coherent power outputs with good spectral stability.

# CHAPTER 6

# WAVELENGTH STABILIZATION OF DIODE LASERS

## 6.1 Motivation

Broad line width emission of high power diode laser bars limits their usage for wavelength specific applications. Hence, there is a great need for the wavelength stabilization and spectral narrowing of these devices. As discussed in the previous chapters in this thesis, new generation tapered diode lasers are interesting devices due to their ability to deliver high output powers with good beam quality and reliability. To tailor a tapered diode laser emission for wavelength specific applications, spectral narrowing of a gain guided tapered diode laser has been demonstrated for the first time ever to my best knowledge. External cavities based on Littman Metcalf configuration and a VBG has been discussed in detailed with both leading to efficient line width reduction of the emission. 8W of optical power with a spectral line width of 40 pm has been obtained from a Littman Metcalf cavity where as 5 W with a line width of 0.2 nm has been obtained from a VBG cavity. This promises compact and efficient high power narrow line width diode laser systems in the future.

## 6.2 Schemes for spectral narrowing

High power broad area diode laser bars and tapered diode laser bars usually emit with a line width of a few nanometres. Even though such an emission is generally sufficient for applications such as solid state or fibre laser pumping, the broad line width leads to a lot of energy expenditure. Moreover, for certain applications; for example pumping of alkali vapour lasers [46], spin exchange optical pumping [81] etc., a very high spectral brightness is desirable. i.e., high power emissions with line widths of a few tens of picometres are necessary. A 70% increase in the efficiency of pumping has been noted using frequency narrowed pump source over regular laser diodes [46] [82] [83]. Free running laser bars with very less wavelength selectivity would prove useless in such scenarios. Even though one can always depend on solid state lasers in such a

situation, their bulky nature and relatively higher costs makes them less desirable. Moreover, solid state lasers available today are always limited to a few wavelengths. Hence, a wavelength stabilized diode laser source could be an excellent candidate for such an application. It can deliver the required amount of output power at a comparatively lesser costs.

There are different schemes for the spectral narrowing/stabilization of the diode lasers. The most typical way towards it is to build an external cavity which involves a wavelength selective element and to apply feedback from the diffracted beam. A Littrow cavity, Littman Metcalf cavity or a volume Bragg grating cavity could be used for this purpose. The first two makes use of a reflective grating while the last one makes use of a volume Bragg grating as the name indicates.

### 6.2.1 Littrow cavity

This is a simple external cavity which includes a laser diode, collimation optics and a reflective diffraction grating which serves as the wavelength selective element and as the end mirror which provides the feedback. The first order diffracted beam is fed back to the laser diode. The wavelength tuning is achieved by rotating the diffraction grating. In this configuration, the direction of the output beam would be changing with respect to the wavelength tuning as the grating is rotated. Figure 6.1 shows the schematic diagram of a Littrow external cavity.

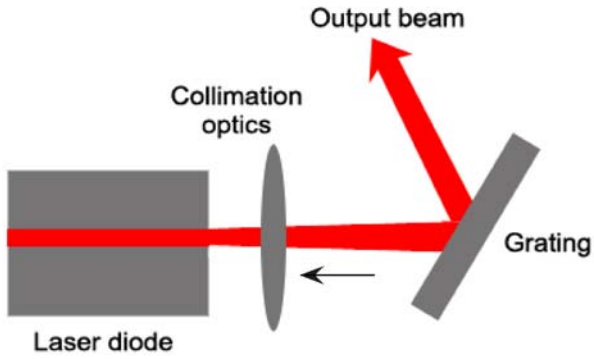


*Fig. 6.1. Schematic diagram of a Littrow external cavity. Black arrow shows the feedback.*

Liu et al [84] achieved 12.5 W of optical output power with a line width of 0.1 nm using a broad are diode laser array in a compound Littrow external cavity. Zhu et al [85] obtained 115 W of output power with a line width of 0.4 nm using a commercial stack of diode laser arrays in a Littrow cavity. Zhdanov et al [44] reported 10 W with a narrow line width less than 20 pm at 852 nm using a diode laser array in a Littrow cavity with a holographic grating.

### 6.2.2 Littman Metcalf cavity

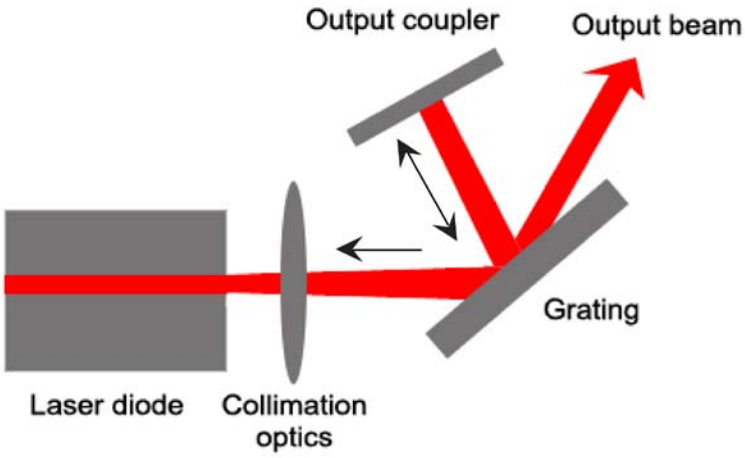


*Fig. 6.2. Schematic diagram of a Littman Metcalf cavity. Black arrows shows the direction of the feedback.*

A Littman Metcalf cavity [86] [87] consists of the diode laser, collimation optics, a reflective diffraction grating and an output coupler mirror which provides the feedback. In this geometry, the grating is usually fixed and the wavelength tuning is achieved by rotating the output coupler. This geometry allows the double incidence of the laser beam before it is fed back to the laser thereby enhancing the spectral selectivity of the system. Hence, narrower wavelengths could be obtained from this configuration compared to the Littrow geometry. Figure 6.2 shows a Littman Metcalf external cavity. In both Littrow and Littman Metcalf configuration, the grating equation is generally stated as,

$$m\lambda = d(\sin\alpha \pm \sin\beta), \tag{6.1}$$

Where *m* is the order of diffraction, *d* is the line spacing of the grating, $\alpha$ is the incident angle on the grating, $\beta$ is the diffraction angle and $\lambda$ is the operating wavelength. In the Littrow configuration, as the angle of incidence and the angle of diffraction are equal, equation 6.1 can be re-written as,

$$\sin\alpha = \frac{\lambda}{2d}, \tag{6.2}$$

The wavelength resolutions of a Littrow and Littman Metcalf external cavity are given by equations 6.3 and 6.4 respectively [88].

$$\Delta\lambda_{Littrow} = \frac{\lambda^2}{\pi L_g}, \tag{6.3}$$

$$\Delta\lambda_{Littman} = \frac{\lambda^2}{2\pi L_g}, \tag{6.4}$$

where $\lambda$ is the wavelength of operation, $L_g = 2\omega tan\beta$ is the filled depth of the grating which is a projection of the illuminated area of the grating on to the optical axis of the cavity. $\omega$ is the beam waist and $\beta$ is the angle of diffraction.

### 6.2.3 Volume Bragg grating cavity

A volume Bragg grating (VBG) [89] is a wavelength selective transparent device with a periodic variation in the refractive index. It reflects the light in a certain bandwidth when the Bragg condition is fulfilled. The condition is given by the equation

$$\frac{2\pi}{d} = 2\frac{2\pi n}{\lambda}\cos\theta, \tag{6.5}$$

where *d* is the grating period, *n* is the refractive index of the medium, $\theta$ the propagation angle in the medium relative to the grating normal and $\lambda$ the wavelength of the light. The other wavelengths are not affected by the grating except for some side lobes in the reflection spectrum which are generally quite weak. Figure 6.3 show the diagram of a laser diode in a VBG cavity.

Volume Bragg grating helps building very simple and compact cavities of length of the order of a few millimetres. But the whole setup is somewhat rigid in terms of wavelength tenability as VBGs are designed to be reflective around a certain wavelength. Hence the laser operates at the Bragg wavelength and is not tuneable as in a Littrow or Littman cavity. In the following section of this thesis, I would discuss in detail about the spectral narrowing of a tapered diode laser bar using a Littman Metcalf cavity and a VBG cavity.

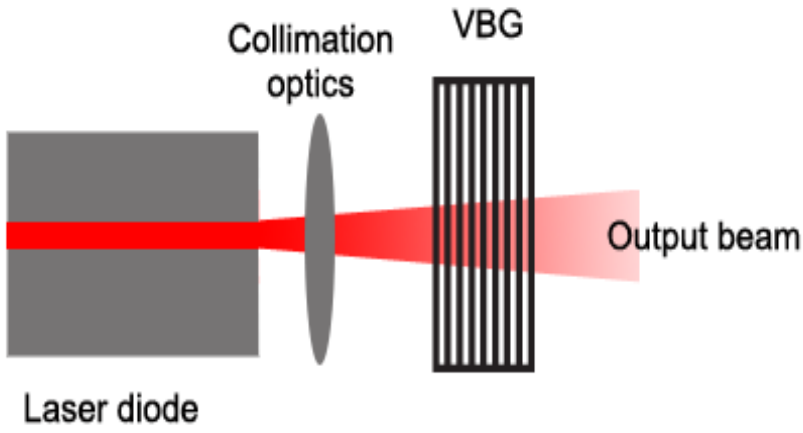


*Fig. 6.3. Schematic diagram of a VBG external cavity.*

### 6.3 Spectral narrowing of a gain guided tapered diode laser bar

Gain guided tapered diode laser bars are interesting devices that gives relatively high output powers [57] with good beam quality compared to broad area bars. Hence the narrow line width emission from a tapered bar would be interesting in applications such as spin exchange optical pumping. This section of this thesis is dedicated to the experiments performed with a gain guided tapered diode laser bar in order to limit the line width of the emission. A tapered diode laser bar which is similar to the one discussed in section 3.1 has been used in the following experiments.

One of the main factors that limit the line width of the emission from laser bars are the smile associated with the bar geometry. A smile could be

defined as the curvature observed on the linear laser array caused by the manufacturing process. The smile can cause a broadening in the line width of the laser bar. This broadening $\delta\lambda$ is quantified as [90],

$$\frac{\delta\lambda}{\lambda} = \frac{x \cot\theta}{M f_c}, \tag{6.5}$$

where $x$ is the amount of smile, $\lambda$ is the wavelength of the emission, $M$ is the magnification factor of the telescopic lens system, $\theta$ is the angle between the optical axis and the grating normal, $f_c$ is the focal length of the second lens in the telescopic system. Thus using a large focal length lens to increase the magnification factor would reduce the resultant line width of emission. This is due to the reduction in the effective angles due to smile and due to the reduction of the angular spread of the emission at the grating.

This common technique to compensate or reduce the effect of the smile has been used by several research groups around the world. [90] Chann et al produced 14 W of output power with a narrow line width of 50 GHz using an external cavity with a magnifying telescope. [53] Gopinath et al used a combination of GRIN lens and a large magnification telescope for the reduction of smile in the spectral beam combining experiments. In another context, Talbot et al [91] reduced the effective smile in a large smile laser array by tilting the cylindrical lens used in the telescope. This led to a line width reduction from 2 to 0.15 nm. Another interesting approach to the smile reduction is by the use of phase plates. This refractive plate corrects the optical path difference of the beams from different emitters in the direction of the fast axis. Monjardin et al [92] corrected the fast axis beam errors on a 11 bar diode laser stack. A similar approach has been made in the experiment described in this section. The wave front errors on the tapered diode laser bar have been corrected using a custom made phase plate (*powerphotonic*, UK). This compensates the smile that was observed on the bar.

A volume Bragg grating is another straight forward solution for high power narrow wavelength emissions. This could also help in scaling down the external cavity dimensions and reduce the complexity of the setup as it normally involves no cylindrical optics or wave plates. Several research groups

have demonstrated efficient line width reduction of high power diode laser arrays using a VBG external cavity. Considering the prior art, in 2006, Meng et al. [93] demonstrated 13.5 W of spectrally narrowed optical power with a line width of 14 pm. In 2008, Gourevitch et al. [94] displayed 30 W of output power with a narrow line width of 20 pm using a diode laser bar incorporated into an external cavity with a volume Bragg grating. In 2009, Liu et al. [78] reported 12.8 W of output power with a narrow line width of 70 pm from a V- shaped Talbot cavity. In the coming section, an attempt toward the narrow line width operation of the gain guided tapered diode laser bar in a VBG cavity has been described.

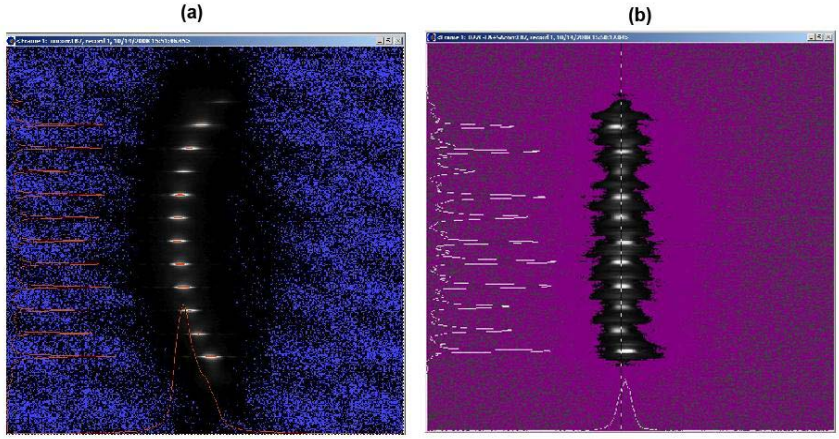


*Fig.6.4. Near field images of the tapered diode laser bar at 10 A. (a) without wave front correction phase plate. (b) with wave front correction phase plate.*

The figure 6.4 shows the near field photograph of the emitters on the laser bar before and after the wave front correction. These phase plates are both custom made and commercially available these days. The compensation of a prominent smile could be observed in the figure. The smile observed on the laser bar amounts to 4.0 m.rad peak to valley, corresponding to 2.4 micron mechanical smile of bar. With the wave front correction, this value reduced to 0.9 m.rad peak to valley which corresponds to less than 0.6 microns of mechanical smile. The tapered diode laser bar has also been collimated along the fast axis using a cylindrical micro lens with a numerical aperture of 0.8 and a focal length of 600 microns and along the slow axis using individual cylindrical micro lenses. This compensates the intrinsic astigmatism in the laser

bar. The phase plate has been attached to the collimation optics. At all currents, only 11 out of 12 emitters on the laser bar were lasing. At 30 A of operating current, the line width of the laser emission was measured to be around 5.5 nm. This custom collimated, wave front error corrected laser bar has been used in two different wavelength narrowing schemes in the experiments. i.e.,

- Littman Metcalf cavity and
- VBG cavity.

### 6.3.1 Experimental setup for Littman Metcalf configuration

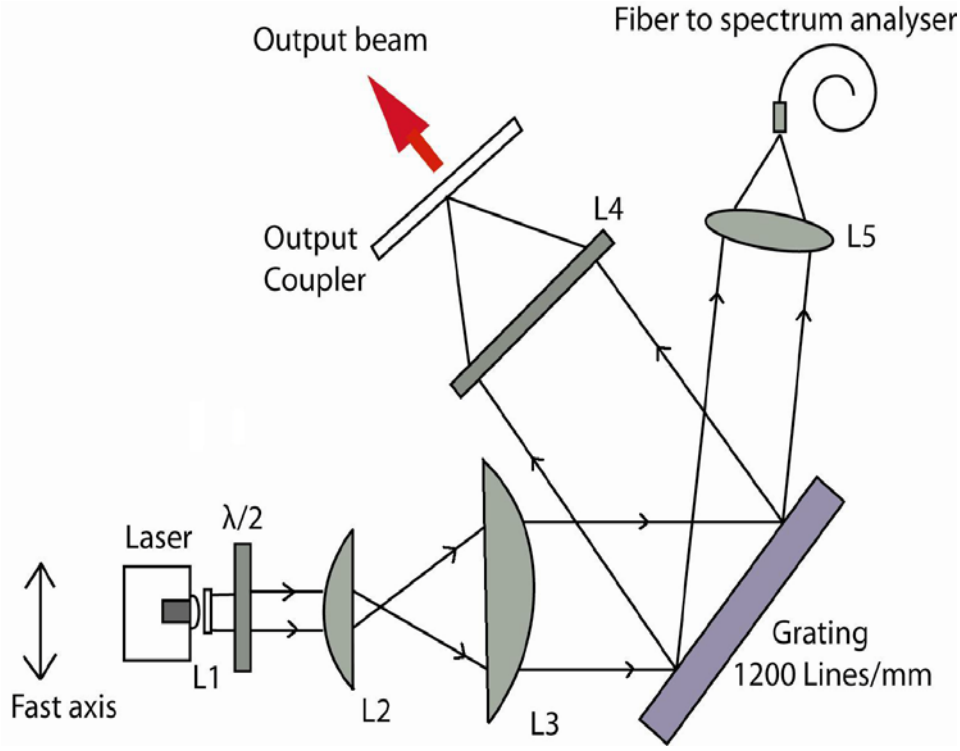


*Fig.6.5. A schematic diagram of the experimental setup of the Littman Metcalf configuration for the spectral narrowing of the tapered diode laser bar.*

The Littman Metcalf cavity adapted in this experiment consists of the laser bar, a combination of the collimation and wave front correction optics, a half wave plate to adjust the polarization of the beam and maximize the diffraction efficiency along the first order, a telescopic system for the magnification of the

laser beam in the fast axis ($L_1$= 15 mm and $L_2$=100 mm in focal length), a reflective diffraction grating with 1200 lines/mm and 85% diffractive efficiency in the first order, a 40 mm cylindrical slow axis focusing lens $L_4$ and a 10% reflective output coupler that feeds the diffracted light back into the laser. Figure 6.5 shows the schematic diagram of the experimental setup.

### 6.3.2 Output power

The free running laser bar produced 12.7 W of output power at 30 A of operating current. In the Littman Metcalf cavity at the same operating current, the laser produces 8 W of output power. The external cavity has an efficiency of 63% compared to the free running laser bar. Figure 6.6 shows the comparison of the light current characteristics of the laser bar in the free running mode and the external cavity mode.

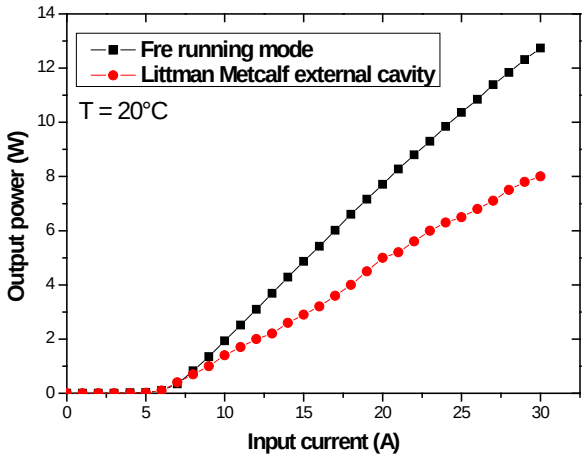


*Fig. 6.6. The light current characteristics of the laser bar in the free running and Littman Metcalf external cavity modes.*

### 6.3.3 Spectral properties

The tapered diode laser bar displayed a broad line width of 5.5 nm while operated at 30 A of input current. In the external cavity mode, this could be narrowed down to 40 pm at FWHM. This results in an improvement of the

spectral brightness by a factor of 86. The figure 6.7 shows the wavelength spectrum of the laser bar in the free running and Littman Metcalf cavity modes.

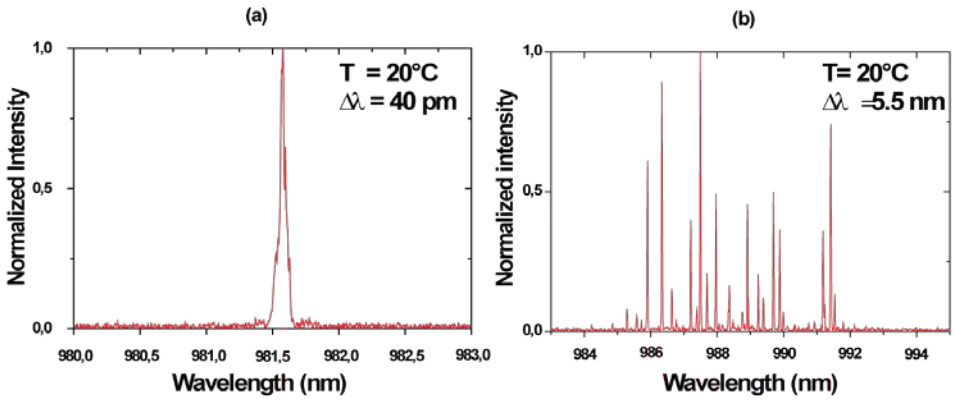


*Fig. 6.7. Wavelength spectra of the output beam (a) Littman Metcalf cavity mode. (b) Free running mode.*

The output beam was tuneable over a span of 16 nm by rotating the diffraction grating. Outside this range, the laser cavity could not sustain the feedback required for the operation of the laser and hence the output starts to get dominated by the self lasing components. Figure 6.8 shows the wavelength tuning of the laser bar.

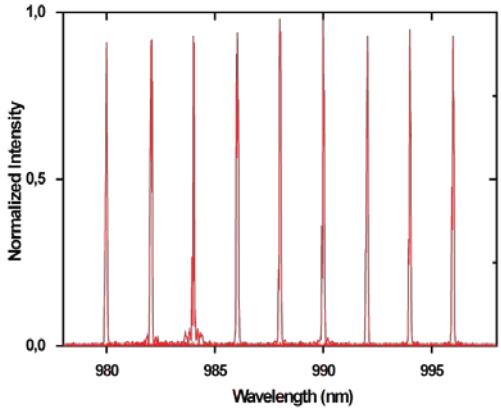


*Fig. 6.8. Wavelength tuning of the tapered diode laser bar at I= 30 A and T= 20° C.*

Tuning range of 16 nm is well below the gain bandwidth of this laser, and a similar laser bar could emit with a wavelength spread of 44 nm in the spectral beam combining experiments mentioned in section 3.1. This could possibly due to the fact that, in a Littman Metcalf cavity, the feedback is applied to the fast axis which is much smaller in terms of aperture size and so it requires precise alignment for sustaining an efficient feedback compared to the spectral beam combining which is done along the slow axis of the laser bar. In this range of 16 nm the laser output power never went below 95% of the highest output power. The spectral width of the output beam varied between 40- 60 pm while tuning in this range.

### 6.3.4 Experimental setup for the VBG cavity

A much more compact system for the spectral narrowing of the tapered diode laser bar was designed based on a VBG external cavity. The cavity measured less than 10 mm in length. The experimental setup is shown in figure 6.9.

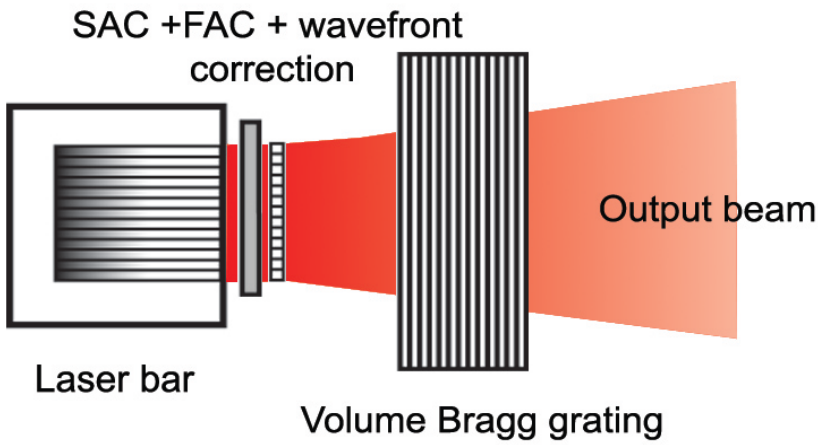


*Fig. 6.9. Experimental setup of the VBG cavity.*

The external cavity consists of the custom collimated, wave front error corrected tapered diode laser bar and the volume Bragg grating placed close to the laser bar. The VBG has been mounted on a mirror mount. The reflectivity of the VBG is 25% around 981 nm. The bandwidth is 0.2 nm. Once the grating has been placed close to the laser bar, the VBG has been rotated both along the fast and the slow axis in order to achieve a perfect wavelength locking in the laser emission. The laser bar has been maintained at a constant temperature of 17°C using a thermo-electric temperature controller. A part of the laser output was sent to an optical spectrum analyzer (resolution of 50 pm) for characterization. Moreover, another part of the beam was sent to a spectrometer and has been viewed using a solid state camera (*COHU*) in order to get a space resolved spectral image of the laser which helps in the cavity alignment.

### 6.3.5 Output power

Figure 6.10 shows the light current characteristics of the laser bar both in the free running and VBG cavity mode. At a current of 20 A, the VBG cavity produced 5 W of output power. Above this current, the self lasing acquired strength and the VBG cavity could not enforce a perfect wavelength locking. The cavity has a total efficiency of 65% compared to the free running mode.

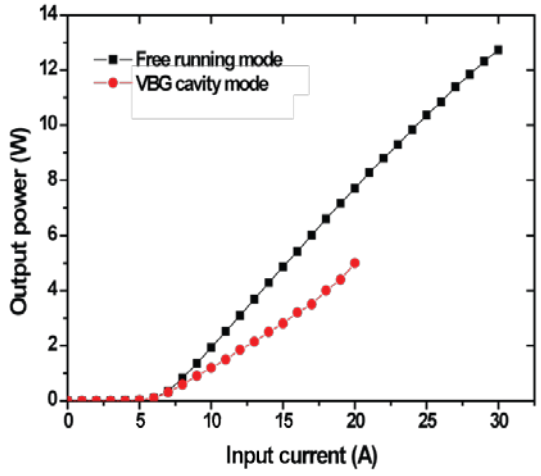


*Fig. 6.10. Light current characteristics of the laser bar in the free running and VBG cavity mode.*

### 6.3.6 Spectral behaviour

An efficient spectral narrowing could be obtained using the VBG cavity. The line width of the emission has been narrowed from over 5.5 nm to 0.2 nm FWHM at 20 A of operating current. This is partially limited by the bandwidth of the VBG. The main limitation of such a system is the limited tunability of the wavelength. The spatially resolved spectral images of the laser emitters are shown in figure 6.11.

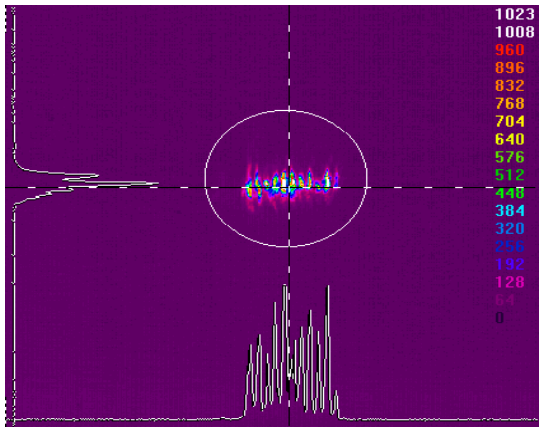


*Fig. 6.11. Spatially resolved spectral image of the tapered diode laser bar at I= 20 A and T= 17°C. (Not to scale)*

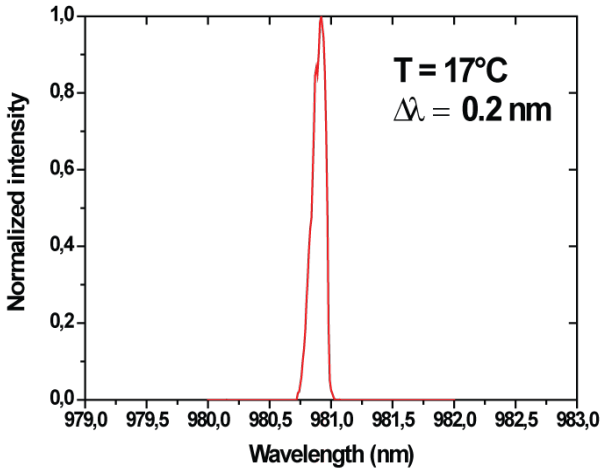


*Fig. 6.12. Wavelength spectra of the output beam from VBG cavity.*

The wavelength spectrum of the output beam from the VBG cavity is shown in the figure 6.12. The VBG cavity led to an improvement in the spectral brightness by a factor of 18 compared to the free running mode.

### 6.4 Discussion

Both of the above described schemes are quite useful in the line width reduction of diode laser bars. But they have their own inherent advantages and disadvantages. The Littman Metcalf configuration offers a two pass system which significantly improves the wavelength selectivity of the external cavity. The output laser beam is also wavelength tuneable over a range of several nanometres which is definitely interesting. Also the efficiency of the external cavity was found to be comparable to that has been achieved using regular broad area diode laser bars in external cavities [95]. But the whole system consists of a number of optical elements such as lenses, grating, half wave plate and the feedback mirror. The alignment of each component can be very critical and this system is quite sensitive to mechanical vibrations. The VBG cavity on the other hand offers a quite compact setup for the line width reduction. Fewer numbers of optical elements in the cavity makes this configuration a small size easy to align setup. But the wavelength of emission is not flexible and is dependent on the Bragg wavelength of the grating.

The Littman Metcalf setup could also be made without the beam expander lens combination which makes the cavity simpler in terms of the number of optical components. Experiments were made without the beam expander and the line width of the output beam could not be reduced below 100 pm at the same operating current level of 30 A. Efforts were also made to optimize the magnification factor, $M$ of the lens combination. Cavities with $M$ = 2.5, 4 and 6.6 were tested with the latter giving the best performance. Beyond that level of magnification, the line width starts increasing. A cavity with $M$ = 10 gave a line width of 150 pm. The strength of feedback is also an important factor that determines an efficient wavelength locking. Output couplers with different values for reflectivity (3- 15%) were tested with the 10% one giving the best results. Above 10%, even though the spectral locking was good enough; the output power levels dropped below 8 W due to the increase in the

cavity losses. Below 10% reflectivity, the system could not provide enough feedback to maintain the locking of the emitters.

Tapered diode lasers are designed to emit at high power levels and their front facet coatings are optimized to support and amplify even the slightest output from the ridge section. The laser bar used in this experiment is also a similar case. In the VBG cavity, while operated at a current level above 20 A, the laser bar started supporting the emission in the free running mode and the effect of the feedback from the cavity was overpowered by it. Anything above 25 A, the majority of lasing was in the free running mode. This is a major limitation in achieving good wavelength locking and spectral narrowing in a VBG cavity at high power levels. In the future, if it is possible to provide very good front facet anti-reflection coatings for such laser bars, it could help restricting their free running tendency at higher current levels.

In both cases, the smile correction performed on the laser bar has proved to be a very important factor in limiting the line width. A high optical power emission at 980 nm is also interesting for pumping Erbium doped fibre lasers [96] [97]. These systems could also be extended to other wavelengths of interest. In the future, it could lead to simple and compact laser systems with high output power and narrow emission line width suitable for wavelength specific applications. Results from this experiment has been reported in the article **5** referred in the appendix.

# CHAPTER 7

# APPLICATIONS

## 7.1 Applications of high power diode laser systems

The diode lasers have been used in material processing since 1991 [98]. Due to their high power efficiencies, long life time and low maintenance cost, over the years they became more and more interesting for these applications. Today, diode lasers are used for many applications which were earlier performed using Nd:YAG or $CO_2$ lasers. Even though they suffer from astigmatism (which could be corrected using two cylindrical lenses), when it comes to applications such as surface treatment of materials, it serves as a boon so that no further beam integration is necessary to create a rectangular beam profile. Moreover, due to their compact size and use of standard interfaces, diode lasers are easy to be integrated in to the production lines and machines.

Majority of the high power diode laser material processing applications are related to soldering, hardening [99], marking [100] [101], cutting, drilling [102] [103] etc. Laser soldering was first performed by Polijanczuk et al [98] back in 1991. Laser soldering has the advantage of selective heating of the target sport and thereby reducing the thermal damage of the surrounding areas of the sample. As a laser beam could be focused down to a spot several microns wide, it helps in soldering connectors which are extremely small ~ 200 microns. Due to the low focusability of high power diode laser beams, the cutting and drilling on metals in the past did not yield results as good as other laser sources. But the technology is evolving and better solutions are expected in the near future [104]. Applications such as welding of polymers and metal foils [105], bending of glass and ceramics [106], sintering of metal powders [107] [108] has also been of interest.

Comparing the diode laser systems described in this thesis to other state of the art technologies, fiber lasers [109] can deliver much higher output powers with excellent beam qualities [110]. Beam combining an array of fiber layers

has lead to several hundreds of Watts [56]. They offer good beam qualities, even better than Nd:YAG lasers whose beam quality degrades due to thermal lensing [111] [112] at high power levels. In order to reach a comparable power level, several laser diode bars or single emitters needed to be combined which may lead to much more complex setups. However, if we consider applications with a moderately high power level system with a power level in the range of several watts or tens of watts, then using an expensive fiber laser system with such high output power levels would be inappropriate and very less cost effective. Whereas in case of gas and solid state laser systems, their bulky nature, low power efficiencies, high price tags and maintenance issues makes them less interesting as a reliable solution. Another aspect within the comparison of these laser types are the emission wavelengths. Due to their material compositions, diode lasers offer a wider range of wavelengths [113], which might provide advantages for certain applications. Therefore these lasers enable new applications not accessible using laser emissions based on atomic transitions. Furthermore, these applications may benefit from the possibility of power scaling using diode lasers.

On the other hand, for applications such as key hole drilling, even though the wavelength range that high power diode lasers offers are more absorptive than Nd:YAG or $CO_2$ lasers, limitations in power densities and low focusibility still acts as constraints [9]. High power diode laser systems in effect have disadvantages such as poor focusibility and lower lens to sample work distance, astigmatism which leads to different material processing characteristics along the slow and the fast axis, lower power densities compared to other technologies such as solid state, fiber and gas lasers, colour dependent absorbance of the laser beam and inability for Q switching. A comparison of different types of industrial laser systems used in material processing has been shown in the table 7.1 [40].

The 980 nm high power emission from the off-axis spectral beam combining setup has been used to cut certain polymer materials. The experimental results and the details regarding the tests conducted are given below. The sample materials tested were:

- Expanded polystyrene (EPS) Sheets ( both usual ones and black painted ones)
- Aluminium sheets 4 mm thick
- Acrylic polymer Sheets
    - *Makrolon 099* 3mm thick,
    - *Riacryl SE 1011* 3mm thick,
    - *Makrolon 130* 3mm thick,
    - *Riacryl black 799* 3mm thick.
- Solder

The astigmatism present in the output beam was compensated using two cylindrical lenses and the output beam from the external cavity laser was focused on to the test samples using a 35 mm achromatic lens which formed a (30×30) $\mu m^2$ spot on the samples. The test results are,

- **EPS Sheets:**
    - Less affected by the laser light which could possibly due to lack of absorption in the white surface.
    - When painted black, the sheets could be easily cut with the current laser output as the light absorption in the material is increased.
    - No significant difference was noted while using sheets of two different densities.
- **Aluminium:**
    - No significant change when exposed to the radiation.
    - It clearly seems that it requires a higher power density to cut through.
- **RIAS Polymer sheets:**
    - *Riacryl (black) 799* could be easily cut though and it produces lot of smoke.

- *Makrolon 130 polycarbonate plates (white)* could also be cut; but this material is producing significant amount of smoke and soot.
- *Makrolon 099 polycarbonate plates (transparent)* and *Riacryl SE 1011 (grey)* seem to be less effected by the radiation while the former being better but giving out a lot of soot.

- **Solder**
  - Solder could be melted effectively. This could open up the possibility of using this laser beam for precision soldering.

On conclusion, the polycarbonate materials are producing more soot while exposed to the laser light. The acrylic ones are producing no soot at all. The near infra red light is sensitive to the colour of the sample to be processed. Light coloured samples reflect more light and could not be cut properly while the laser beam made a smooth cut through the dark coloured polymer samples. This could also be seen as one of the disadvantages of laser being used for material processing. Figure 7.1 shows the photograph of some of the materials cut using the laser system.

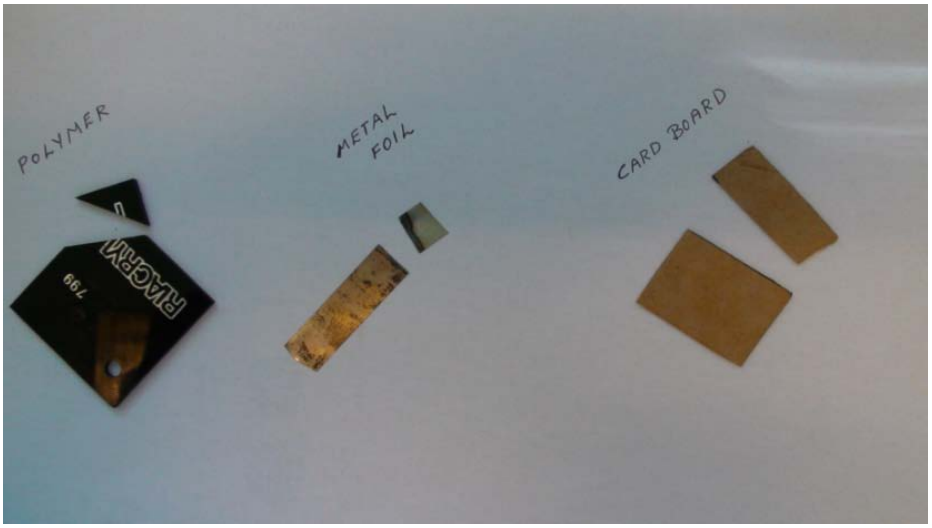


*Fig. 7.1. Photograph of some materials cut using the laser beam.*

| | **High power diode lasers** | **Diode Pumped Solid State lasers** | **Fiber lasers** | **$CO_2$ lasers** |
|---|---|---|---|---|
| **Wavelength (nm)** | 0,98 | 1,06 | 1,07 | 10,6 |
| **Power Range** | 10 W to 10 kW | 100 W to a few kW | 100 W to 10's of kW | 100 W to 10's of kW |
| **Physical Size** | Very Small | Large | Medium | Large |
| **Electrical Efficiency** | 40% | 15% | 25% | 10% |
| **Maintenance Interval** | 2 years | 1 year | 2 years | 6 months |
| **Initial Capital Cost** | Low | High | High | Medium |
| **Cost of Ownership** | $23/hour | $53/hour | $43/hour | $49/hour |

*Table. 7.1 Comparison of material processing lasers* [19].

# CHAPTER 8

# CONCLUSION

Owing to the application potential of near infra red high power diode laser systems with good beam qualities and narrow spectral line widths, several external cavity setups aimed at the improvement of the beam quality and spectral properties have been presented. In chapter 3, a 12 emitter gain guided tapered diode laser bar operating around 980 nm has been used in a spectral beam combining external cavity using a reflective diffraction grating to improve the beam quality of the entire bar to a level that matches the beam quality of a single emitter on it. This is the first time to my knowledge, a gain guided tapered diode laser bar has been used for spectral beam combining. The slow axis beam propagation parameter of the entire bar in the beam combined was measured to be 5.3 with 9 W of optical output power. High power DBR-tapered diode single emitters has also been used in the spectral beam combining mode with a volume Bragg grating which yielded 16 W of output power at 1060 nm with a slow axis $M^2$ value of 3.3. This approach also portrays the advantages and flexibility of the experimental setup of spectral beam combining using single emitters which could be impossible with laser arrays or bars. In these days of ever increasing power levels from single emitters, this mode of spectral beam combining has its own significance.

In chapter 4, another approach has been made towards the improvement of the spatial coherence properties of a broad area diode laser bar. An off-axis spectral beam combining configuration of a 980 nm BA laser bar has been demonstrated. The output power from 12 emitters in this setup was 9 W with a slow axis $M^2$ value of 6.4 while the individual emitters displayed a slow axis $M^2$ value of 30- 35 at the same operating current levels. This approach overcomes an inherent limitation of general spectral beam combining and improves the beam propagation factors of the combined beam to a value much below that of the individual emitters. The system displayed a high spatial brightness of 79 MW/cm$^2$-str which was to my knowledge, the highest brightness from a broad area diode laser system at the time of the publication.

Talbot cavity setup of the gain guided tapered diode laser bar has been depicted in chapter 5. This dealt with the passive phase locking of the 12 emitters on the bar making use of the diffractive phenomenon termed as Talbot effect. The phase locked laser bar produced 2.45 W of optical output power in the in phase mode at a current of 15 A. However due to the free running contribution from the laser, a good phase locking could not be obtained above this current level which was quite evident from the decreasing fringe visibility in the far field patter of the output beam.

In a first ever attempt towards the spectral narrowing of the emission from a gain guided tapered diode laser bar, both Littman Metcalf and a volume Bragg external cavity has been explained in detail. Narrow line width operation down to 40 pm with 8 W of near infra red optical power has been demonstrated using a Littman cavity. On the other hand, 5 W of optical power was obtained from a VBG cavity with line widths not exceeding 0.2 nm. The smile correction performed on the tapered diode laser bar has been of great importance in limiting the line widths.

The work done with broad area bar, tapered diode bar and tapered diode single emitters towards the improvement of spatial coherence could be useful in the context of material processing applications which requires moderate power level compact laser systems with good beam qualities. The spectral narrowing along with the smile reduction techniques if extended to other wavelengths of interest could be useful for applications that demand narrow line width high power emissions. Improvements could be made in the future on factors like good quality anti reflection coatings on the front facets of the laser bars to avoid free running contributions, using laser bars with no failed emitters etc. Moreover, industrial applications demand compact and rugged laser systems which pose some instrument design challenges. So far these systems have been only been demonstrated in a laboratory environment. Some level of engineering challenge is anticipated to convert these bench tops experimental setups into prototypes. The outcomes of the experiments are sometimes limited by our lack of access to some other equally good or better technologies. This is always a challenge in this competitive world of scientific research. But I hope these issues can only improve as time goes on.

# LIST OF ACRONYMS

| | |
|---|---|
| AR | Anti-reflection |
| AlGaAs | Aluminum Gallium Arsenide |
| BAL | Broad area laser |
| BPP | Beam propagation parameter |
| CCP | Conduction cooled package |
| COMD | Catastrophic optical mirror damage |
| CuW | Copper Tungsten |
| cw | continuous wave |
| DBR | Distributed Bragg reflectors |
| EDCL | External cavity diode laser |
| FWHM | Full width half maximum |
| GaAlInAs | Gallium Aluminum Indium Arsenide |
| GaAs | Gallium Arsenide |
| InGaAs | Indium Gallium Arsenide |
| LED | Light emitting diode |
| Nd:YAG | Neodymium Yttrium Aluminum Garnet |
| OASBC | Off-axis spectral beam combining |
| OSA | Optical spectrum analyzer |
| RW | Ridge waveguide |
| SBC | Spectral beam combining |
| SCOWL | Slab coupled optical wave guide laser |
| $SiO_2$ | Silicon dioxide |
| VBG | Volume Bragg grating |

# APPENDIX

**Journal articles**

1. D. Vijayakumar, O.B. Jensen, R. Ostendorf, T. Westphalen, and B. Thestrup, "Spectral beam combining of a 980 nm tapered diode laser bar," Opt. Express **18**, 893-898 (2010). DOI: 10.1364/OE.18.000893 http://www.opticsinfobase.org/oe/abstract.cfm?URI=oe-18-2-893

   Status: *Published.*

2. A. Müller, D. Vijayakumar, O. B. Jensen, K-H. Hasler, B. Sumpf, G. Erbert, P. E. Andersen, and P. M. Petersen' "16 W output power by high-efficient spectral beam combining of DBR-tapered diode lasers".

   Status: *Submitted to Optics Express.*

3. D. Vijayakumar, O. B. Jensen, and B. Thestrup, "980 nm high brightness external cavity broad area diode laser bar," Opt. Express **17**, 5684-5690 (2009). DOI: 10.1364/OE.17.005684 http://www.opticsinfobase.org/oe/abstract.cfm?URI=oe-17-7-5684

   Status: *Published.*

4. D. Pabœuf, D. Vijayakumar, O. B. Jensen, B. Thestrup, J. Lim, S. Sujecki, E. Larkins, G. Lucas-Leclin, and P Georges, "Volume Bragg grating external cavities for the passive phase-locking of high-brightness diode laser arrays: a theoretical and experimental study".

   Status: *Submitted to Journal of the Optical Society of America B.*

5. D. Vijayakumar, O. B. Jensen, J. Barrientos-Barria, D. Pabœuf, G. Lucas-Leclin, B. Thestrup, and P. M. Petersen, "Narrow line width operation of a 980 nm gain guided tapered diode laser bar".

   Status: *Accepted for publication in Optics Express.*

**Conference Proceedings**

1. D. Vijayakumar, G. Lucas-Leclin, O. B. Jensen, and B. Thestrup, "Spectral narrowing of a 980 nm tapered diode laser bar", Poster ac-

cepted for High-Power Diode Laser Technology and Applications IX, SPIE Photonics west 2011.

2. D. Vijayakumar, O. B. Jensen, B. Thestrup, "Wavelength beam combining of a 980-nm tapered diode laser bar in an external cavity," Proceedings of SPIE Vol. 7720, 77201U (2010).

3. D. Vijayakumar, , O. B. Jensen, , B. Thestrup, “High brightness external cavity broad area diode laser bar using off-axis spectral beam combining,” The European Conference on Lasers and Electro-Optics (CLEO_E), 2009. CLEO/Europe and EQEC 2009 Conference Digest (ISBN: 978-1-4244-4080-1) (paper id: CB_P31), 2009, IEEE conference proceedings.

4. D. Vijayakumar, O. B. Jensen, B. Thestrup, “High power NIR laser bar with improved beam quality,” Presented at: European Semiconductor Laser Workshop 2008, Eindhoven, The Netherlands.

**Book Chapter**

1. D. Vijayakumar, “The laser has potential applications in all walks of life,” part of: Beyond optical horizons, today and tomorrow with photonics, pages: 188 pages: 267, 2009, DTU Fotonik, Kgs. Lyngby.

# BIBLIOGRAPHY


[1] P.A. Crump, M. Grimshaw, J. Wang, W. Dong, S. Zhang, S. Das, J. Farmer, M. DeVito, L. S. Meng, and J. K. Brasseur, CLEO/QELS, Technical digest, paper JWB24.

[2] M. Kanskar, T. Earles, T. J. Goodnough, E. Stiers, D. Botez, and L. J. Mawst, Electron. Lett., **41**, 245-247 (2005).

[3] M. T. Knapczyk, J. H. Jacob, H. Eppich, A. K. Chin, K. D. F. Lang, J. T. Vignati, R. H. Chin, SPIE Photonics West 2011, Paper 7918-14.

[4] N. I. Katsavets, V. A. Buchenkov, M. O. Iskandarov, A. A. Nikitichev, É. G. Sokolov, and A. L. Ter-Martirosyan, Tech. Phy. Lett., **34**, 46-47 (2008).

[5] www.dilas.com

[6] http://www.lightwaveelectronics.com

[7] L. Fan, C. Cao, G. Thaler, D. Nonnemacher, F. Lapinski, I. Ai, B. Caliva, S. Das, L. Zeng, R. Walker, M. McElhinney, P. Thiagarajan, SPIE Photonics West 2011, Paper 7918-4.

[8] L. Bao, J. Wang, M. A. Devito, P. O. Leisher, D. Xu, M. Grimshaw, W. Dong, X. Guan, S. Zhang, C. Bai, J. G. Bai, D. Wise, R. J. Martinsen, SPIE Photonics West 2011, Paper 7918-5.

[9] L. Li, Opt. Laser. Eng., **34**, 231-253 (2000).

[10] C. H. Henry, IEEE J. Quantum Electron., **18**, 259-264 (1982).

[11] V. Krause, ECLAT'92 Proceedings, Gottingen, 1992.

[12] T. H. Maiman, Nature, **187**, 493–494 (1960).

[13] Hall R. N, G. E Fenner, J. D Kingsley, T. J Soltys, and R. O Carlson, Phy. Rev. Lett., **9**, 366-368 (1962).

[14] Nathan M. I, W. P. Dumke, G. Burns, F. H. Hill, and G. Lasher. App. Phys. Lett., **1,** 62-64 (1962).

[15] Holonyak. N. and S. F Bevacqua. App. Phys. Lett., **1**, 82-83 (1962).

[16] P. Unger, in *High Power Diode Lasers: Fundamentals Technology, Applications*, 78 ed., R. Diehl, ed., (Springer-Verlag, Berlin, Germany, 2000).

[17] G.H.B Thompson, Optoelectronics, **4**, 257-319 (1972).

[18] K. J Paschke, S. Einfeldt, A. Ginolas, K. Häusler, P. Ressel, B. Sumpf, H. Wenzel, and G. Erbert, CLEO/QELS 2008 Conference digest p.CMN4 (2008).

[19] P. Crump, M. Grimshaw, J. Wang, W. Dong, S. Zhang, S. Das, J. Farmer, and M. DeVito, Proc. of SPIE, **5711**, (2005).

[20] L. Lang, J. J. Lim, S. Sujecki and E. C. Larkins, Opt. Quant. Electron., **40**, 51097-1102 (2008).

[21] B. Thestrup, M. Chi, and P. M Petersen, Proc. of SPIE, **5336,** 38-44 (2004).

[22] S. Wolff, Rodionov, A. Sherstobitov, V.E. Fouckhardt, H. IEEE J. Quantum Electron. **39,** 448 - 458 (2003).

[23] G. Hunziker and C. Harder, Appl. Opt., **34**, 6118-6122 (1995).

[24] G. Beister, F. Bugge. G. Erbert, J. Maege, P. Ressel, J. Sebastian, A. Thies, H. Wenzel, Electron. Lett., **34**, 778- 779 (1998).

[25] M. T. Kelemen, F. Rinner, J. Rogg, N. Wiedmann, R. Kiefer, M. Walther, M. Mikulla, G. Weimann, Proc. of SPIE, **4648,** 233-243 (2002).

[26] B. Sumpf, P. Adamiec, M. Zorn, P. Froese; J. Fricke, P. Ressel, H. Wenzel, M. Weyers, G. Erbert, and G. Tränkle, Proc. of SPIE, **6876**, 68760M (2008).

[27] S. Sujecki, L. Borruel, J. Wykes, P. Moreno, B. Sumpf, P. Sewell, H. Wenzel, T.M. Benson, G. Erbert, I. Esquivias, E.C. Larkins, Selected Topics in IEEE. J. Quantum Electron., **9**, 823 - 834 (2003).

[28] J. P. Donnelly, J. N. Walpole, S. H. Groves, R. J. Bailey, L. J. Missaggia, A. Napoleone, R. E. Reeder, and C. C. Cook, IEEE Photon. Technol. Lett., **10**, 1377–1379 (1998).

[29] S. Mariojouls, S. Margott, A. Schmitt, M. Mikulla, J. Braunstein, G.Weimann, F. Lozes, and S. Bonnefont, Proc. SPIE **3944**, 395–406 (2000).

[30] L. Goldberg, M. R. Surette, and D. Mehuys, Appl. Phys. Lett., **62**, 2304 –2306 (1993).

[31] A. Egan, C. Z. Ning, J. V. Moloney, R. A. Indik, M. W. Wright, D. J. Bossert, and J. G.McInerney, IEEE J. Quantum Electron., **34**, 166–170 (1998).

[32] B. Sumpf, K.-H. Hasler, P. Adamiec, F. Bugge, J. Fricke, P. Ressel, H. Wenzel, G. Erbert, G. Tränkle, Proc. of SPIE, **7230** (2009).

[33] O. B. Jensen, P. E. Andersen, B. Sumpf, K-H Hasler, G. Erbert, and P. M. Petersen, Opt. Express, **17**, 6532-6539 (2009).

[34] J-M Verdiell and R. Frey, IEEE J. Quantum Electron., **26,** 270- 279 (1990).

[35] A.C. Fey-den Boer, H.C.W. Beijerinck, and K.A.H. van Leeuwen, App. Phys. B, **64,** 415-417 (1997).

[36] B. Koehler, J. Biesenbach, T. Brand, M. Haag, S. Huke, A. Noeske, G. Seibold, M. Behringer, J. Luft, Proc. of SPIE, **5711,** 73-84 **(2005).**

[37] J. M. Verdiell, H. Rajbenbach, and J. P. Huignard, J. App. Phys. **66,** 1466- 1468 (1989).

[38] J-M Verdiell and R. Frey, IEEE J. Quantum Electron., **26,** 270- 279 (1990).

[39] D. Vijayakumar, O. B. Jensen, and B. Thestrup, Opt. Express, **17,** 5684-5690 (2009).

[40] www.coherent.com

[41] G. P Agrawal and N. K Dutta, *Semiconductor lasers, Second edition* Van Nostrand Reinhold, New York 1993.

[42] T. Numai, ed., *Fundamentals of semiconductor lasers* (Springer series in optical sciences, 93) Springer NewYork 2004.

[43] A. E Siegman, Proc. of SPIE, **1224**, 11-14 (1990).

[44] B.V. Zhdanov, T. Ehrenreich, and R.J. Knize, Electron. Lett., **43,** 221-222 (2000).

[45] I. A. Nelson, B. Chann, and T. G. Walker, App. Phys. Lett., **76**, 1356-1358 (2000).

[46] R. H. Page, R. J. Beach, V. K. Kanz, and W. F. Krupke, Optics Lett., **31**, 353-355 (2006).

[47] G. D. Boyd and D. A. Kleinman, J. Appl. Phys., **39**, 3597 (1968).

[48] R. L. Sutherland, *Handbook of Nonlinear Optics*, 2nd edition, Marcel Dekker, New York (2003).

[49] V. Daneu, A. Sanchez, T. Y. Fan, H. K. Choi, G. W. Turner, and C. C. Cook, Optics Lett., **25**, 405-407 (2000).

[50] C.C Cook and T. Y Fan, OSA Trends in Optics and Photonics, **26**, 163–166 (1999).

[51] S. Klingebiel, F. Röser, B. Ortaç, J. Limpert, and A. Tünnermann, J. Opt. Soc. Am. B, **24**, 1716-1720 (2007).

[52] B. Chann, A. K. Goyal, T. Y. Fan, and A. Sanchez-Rubio, Optics Lett., **31**, 1253-1255 (2006).

[53] J. T. Gopinath, B. Chann, T. Y. Fan, and A. Sanchez, Opt. Express, **16**, 9405-9410 (2008).

[54] R. K. Huang, B. Chann, L. J. Missaggia, J. P. Donnelly, C. T. Harris, G. W. Turner, A. K. Goyal, T. Y. Fan, and A. Sanchez-Rubio, IEEE Photon. Tech. Lett., **19**, 209- 211 (2007).

[55] A. Jechow, V. Raab, and R. Menzel, Appl. Opt., **45**, 3545-3547 (2006).

[56] O. Andrusyak , V. Smirnov, G. Venus, V. Rotar, and L. Glebov, IEEE Sel. Top. Quantum Electron., **15**, 344- 353 (2009).

[57] C. Scholz, K. Boucke, R. Poprawe, M. T. Kelemen, J. Weber, M. Mikulla, and G. Weimann, Proc. of SPIE, **6104**, 61040G.1– 61040G.8 (2006).

[58] P. Adamiec, B. Sumpf, I. Rüdiger, J. Fricke, K. H. Hasler, P. Ressel, H. Wenzel, M. Zorn, G. Erbert, and G. Tränkle, Optics Lett., **34**, 2456–2458 (2009).

[59] D. Paboeuf, G. Lucas-Leclin, P. Georges, N. Michel, M. Krakowski, J. Lim, S. Sujecki, and E. Larkins,, Appl. Phys. Lett., **93**, 211102 (2008).

[60] A. Sevian, O. Andrusyak, I. Ciapurin, V. Smirnov, G. Venus, and L. Glebov, Optics Lett., **33**, (2008).

[61] T. H. Loftus, A. Liu, P. R. Hoffman, A. M. Thomas, M. Norsen, R. Royse, and E. Honea, Optics Lett., **32**, 349-351 (2007).

[62] C. Wirth, O. Schmidt, I. Tsybin, T. Schreiber, T. Peschel, F. Brückner, T. Clausnitzer, J. Limpert, R. Eberhardt, A. Tünnermann, M. Gowin, E. ten Have, K. Ludewigt, and M. Jung, Opt. Express, **17**, 1178-1183 (2009).

[63] Z. Sheng-bao, Z. Shang-hong,C. Xing-chun,W. Zhuo-liang, S. Lei, Opt. Laser Tech., **42,** 308–312 (2010).

[64] I. V. Ciapurin, L. B. Glebov, L. N. Glebova, V. I. Smirnov, and E. V. Rotari, Proc. of SPIE, **4974**, 209-219 (2003).

[65] H. Po, J. D. Cao, B. M. Laliberte, R. A. Minns, R. F. Robinson, B. H. Rockney, R. R. Tricca, and Y. H. Zhang, Electron. Lett., **29**, 1500-1501 (1993).

[66] Y. Zheng, X. Gao, H. Miyajima, and H. Kan, J. Appl. Phys., **95**, 6489-6491 (2004).

[67] N. Stelmakh, IEEE Photon. Tech. let., **19**, 1392-1394(2007).

[68] F. Wang, A. Hermerschmidt, and H. J Eichler, Opt. Commun., **209**, 391-395 (2002).

[69] R.J. Lang, A.G. Larsson, J.G Cody, IEEE J. Quantum Electron., **27** 312-320 (1991).

[70] J. P. Hohimer, and A. Owyoung, IEEE J. Quant. Electron., **23**, 765-774 (1987).

[71] G. R. Hadley, J. P. Hohimer, and A. Owyoung, Appl. Phys. Lett. **49**, 684- 685 (1986).

[72] M. Chi, B. Thestrup, and P. M. Petersen Optics Lett., **30**, 1147-1149 (2005).

[73] O. B. Jensen, B. Thestrup, P. E. Andersen, and P. M. Petersen, Appl. Phys. B, **83**, 225- 228 (2006).

[74] O. B. Jensen, B. N. Thestrup P. M. Petersen, Opt Comm., **82**, 2898-2900 (2009).

[75] H. F. Talbot, Philos. Mag., **9**, 401-407 (1836).

[76] Lord Rayleigh, Philos. Mag., **11**, 196-205 (1881).

[77] B. Liu, Y. Liu, and Y. Braiman, Opt. Express, **16**, 20935-20942 (2008).

[78] B. Liu, Y. Liu, and Y. Braiman, Opt. Express **18**, 7361-7368 (2010).

[79] R. K. Huang, B. Chann, L. J. Missaggia, S. J. August, M. K. Connors, G. W. Turner, A. Sanchez-Rubio, J. P. Donnelly, J. L. Hostetler, C. Miester, and F. Dorsch, CLEO/QELS (2009).

[80] D. Paboeuf, F. Emaury, S. de Rossi, R. Mercier, G. Lucas-Leclin, and P. Georges, Optics Lett., **35**, 1515-1517 (2010).

[81] T. G. Walker and W. Happer, Rev. Mod. Phys., **69**, 629–642 (1997).

[82] Y. Wang, T. Kasamatsu, Y. Zheng, H. Miyajima, H. Fukuoka, S. Matsuoka, M. Niigaki, H. Kubomura, T. Hiruma, and H. Kan, Appl. Phys. Lett., **88**, 141112–141114 (2006).

[83] B. V. Zhdanov, T. Ehrenreich, and R. J. Knize, Opt. Commun., **260**, 696–698 (2006).

[84] B. Liu, Y. Liu, and Y. Braiman, Appl. Opt., **48**, 365-370 (2009).

[85] H. Zhu, I. C. Ruset, and F. W. Hersman, Optics Lett., **30**, 1342-1344 (2005).

[86] M. G. Littman and H. J. Metcalf, Appl. Opt., **17**, 2224-2227 (1978).

[87] K. Liu and M. G. Littman, Optics Lett., **6,** 117-118 (1981).

[88] C. Ye, in Tunable external cavity diode lasers, Chapter 4, World Scientific Publishing Company Pte. Ltd.

[89] G. B. Venus, A. Sevian, V. I. Smirnov, and L. B. Glebov, Optics Lett., **31**, 1453-1455 (2006).

[90] B. Chann, I. Nelson, and T. G. Walker, Optics Lett., **25**, 1352-1354 (2000).

[91] C. L. Talbot, M. E. J. Frese, D. Eang, I. Brereton, N. R. Heckenberg, and H. Rubinsztein – Dunlop, Appl. Opt., **44**, 6264–6268 (2005).

[92] J. F. Monjardin, K. M. Nowak, H. J. Baker, and D. R. Hall, Opt. Express, **14**, 8178–8183 (2006).

[93] L. S. Meng, B. Nizamov, P. Madasamy, J. K. Brasseur, T. Henshaw, and D. K. Neumann, Opt. Express, **14**, 10469-10474 (2006).

[94] A. Gourevitch, G. Venus, V. Smirnov, D. A. Hostutler, and L. Glebov Optics. Lett., **33**, 702-704 (2008).

[95] E. Babcock, B. Chann, I. A. Nelson, and T. G. Walker, Appl. Opt., **44**, 3098-3104 (2005).

[96] W. L. Barnes, P. R. Morkel, L. Reekie, and D. N. Payne Optics Lett., **14**, 1002-1004 (1989).

[97] M. Dubinskiia, V. Ter-Mikirtychevb, J. Zhanga, and I. Kudryashovc, Proc. of SPIE, **6952**, 695205 1-10, (2008).

[98] A.V Polijanczuk and D. G Whitehead, Proceedings of IEE: Advances in Interconnection Technology, **82**, 1-3 (1991).

[99] W. Chen, C. S. Roychoudhuri, C. M. Banas, Opt Eng., **33**, 3662-3669. (1994).

[100] L. Li, J. Lawrence, J. T, Spencer, Proc. of SPIE, **3097**, 600-11 (1997).

[101] S. V Ponnaluri and P. A Molian, ICALEO'98 Proceedings, **85G**, 103-110 (1998).

[102] H. K Tönshoff, A. Berndt, M. Strürmer, D. Golla, J. Schumacher, J. De Phys. IV, **4**, C4-59-63 (1994).

[103] L. Li, J. Lawrence and J. T Spencer, ICALEO'96 Proceedings, **81E**, 38-47. (1996).

[104] www.laserline.de

[105] W. Schulz, and R. Poprawe, IEEE J. Sel. Top. Quantum Electron., **6**, 696-705 (2000).

[106] D. Wu, Q. Zhang, G. Ma, Y. Guo, and D. Guo, Opt. Lasers Eng., **48**, 405-410 (2010).

[107] C. Roychoudhuri, Proc. of SPIE, **3274**, 162-170 (1998).

[108] H. Shabir, B. Lal, and M. Rafat, Ceram. Int., **36**, 365-369 (2010).

[109] E. Snitzer, J. App. Phys., **32**, 36-39 (1961).

[110] D. J. Richardson, J. Nilsson, and W. A. Clarkson, J. Opt. Soc. Am. B, **27,** B63-91 (2010).

[111] W. Koechner, Appl. Opt., **9**, 2548-2553 (1970).

[112] T. Kimura and K. Otsuka, IEEE J. Quantum Electron., **QE-7**, 403- 407 (1971).

[113] M. Behringer, "High-Power Diode Laser Technology and Characteristics," in *High Power Diode Lasers: Technology and Applications*, F. Bachmann, P. Loosen, and R. Poprawe, ed. Springer, Berlin, (2007).

# ACKNOWLEDGMENT

I would like to thank numerous personalities who either directly or indirectly contributed towards the success of my doctoral studies at the Technical University of Denmark. First of all, I would like to thank my supervisors Dr. Ole Bjarlin Jensen, Dr. Birgitte Thestrup and Dr. Paul Michael Petersen for being perfectly organized when it comes to my studies and for giving the right guidance and advices to their student. The working atmosphere at DTU Fotonik was quite friendly and the casual discussions we had in our offices have always helped pushing my work towards progress during times of intellectual crisis. Special thanks to Ole Bjarlin Jensen for bearing me, entertaining me and enlightening me whenever I showed up in his room with my doubts or ideas which I collected from last night's dreams. I would also like to sincerely thank all my colleagues at DTU Fotonik.

Haynes Cheng is a wonderful friend and a great office mate with a good deal of knowledge in optics and a great sense of humour. We shared the same office and most burdens of PhD students. It was great to work with him. I am grateful to Dr. Gaëlle Lucas-Leclin and Dr. David Pabouef for the interesting collaboration we carried out. The time I spent with them gave me a great exposure towards a new area of expertise and the working atmosphere in a foreign research institute. I also extend my sincere thanks to Andre Müller, PhD student, DTU Fotonik with whom I collaborated for a brief while which turned out to be quite productive.

Thanks to Dr. Ralf Ostendorf of Fraunhofer Institute for Applied Solid State Physics IAF for providing us with the lasers and Thomas Westphalen from Fraunhofer Institute for Laser Technology, Germany for mounting the collimating lens on the laser bars. Experimental works are hardly successful without the aid form a qualified laboratory technician. Peter Jensen of DTU Fotonik was of great help with his prompt and precise engineering skills. Moreover, he gave good company during department parties.

I am also using this opportunity to thank my dear parents who raised me, loved me, supported me and above all, trusted me throughout my life. I believe this thesis is a dream comes true for them.

Last, but not least, I would like to thank my dear wife Nimi who inspired me, motivated me and helped me deal with even the toughest times in my life. Thank you Ikroo, you are the best!!

Deepak Vijayakumar

Roskilde, 31/December/2010